# AN EXPERIMENTAL INVESTIGATION OF FORCED CONVECTIVE HEAT TRANSFER TO A FLUID IN THE REGION OF ITS CRITICAL POINT

Thesis by

Edward Gerald Hauptmann

In Partial Fulfillment of the Requirements

For the Degree of

Doctor of Philosophy

California Institute of Technology

Pasadena, California

1966

(Submitted December 7, 1965)

# ACKNOWLEDGEMENTS

During all stages of the present study, the Author has benefited greatly from the advice and guidance of Professor R. H. Sabersky, to whom he expresses his deep gratitude. Sincere thanks are also extended to Professor A. J. Acosta, for many stimulating discussions, and to Professors D. A. Morelli and B. Auksmann for their assistance in the design of the apparatus.

Support for this research was provided by a National Science Foundation Grant, and financial assistance offered the Author by a Shell Companies Foundation Fellowship, and by California Institute of Technology Graduate Teaching Assistantships. The Author is grateful for this assistance.

Special thanks are due to Mr. D. Laird, to Mr. F. McDonald, to Mr. C. Eastvedt, and to Mr. F. T. Linton of the California Institute of Technology staff for their co-operation. Additional thanks are extended to Miss K. Balderson for preparing the Figures.

Finally, the Author wishes to thank his wife, who in addition to providing an atmosphere of encouragement and understanding, patiently transformed his scribbling into a final typed draft. Without her assistance this work could not have been completed.

# ABSTRACT

Experimental results are presented for forced convective heat transfer from a heated flat plate in carbon dioxide near the thermodynamic critical point. The heated plate was in a horizontal position and most measurements were made in the fully turbulent downstream portion, with the heated surface facing both up and down.

The bulk conditions of the carbon dioxide were varied from below the pseudocritical temperature ("liquid-like" region) to above the pseudocritical temperature ("vapor-like" region), and in some instances the bulk and wall temperatures were on either side of the pseudocritical temperature. Some limited observations on the effect of free stream velocity were made, and experiments were also conducted below the critical pressure in order to obtain a comparison with boiling.

One of the principal objectives was to observe the nature of the heated boundary layer. High speed movie films were taken using a color schlieren apparatus, modified to obtain semi-focusing effects. Although the experimentally determined heat transfer coefficient became high whenever the wall temperature approached the pseudocritical, no significant change in the gross nature of the flow field could be observed. A few exploratory hot wire measure-

ments of the velocity fluctuations near the plate were also made, and they confirmed that no significant increase in turbulence was associated with the regions of high heat transfer coefficients.

On the basis of the results it is concluded that the high heat transfer coefficients observed were due to the large values of thermodynamic and transport properties occurring near the critical point, and not because of the occurrence of a "pseudo-boiling" phenomena. It is further concluded that the "pseudo-boiling" phenomena does not occur with this particular heater geometry or in the range of parameters investigated, although it may in others.

Because of the similarity of fully turbulent boundary layers to turbulent pipe flow, it is felt these conclusion may be extended to cover the latter case as well.

Photographic materials on pages 171-175 are essential and will not reproduce clearly on Xerox copies. Photographic copies should be ordered.

# TABLE OF CONTENTS

Contents continued

Contents continued

# LIST OF TABLES

# LIST OF FIGURES

Figures continued

Figures continued

Figures continued

Figures continued

Figures continued

Figures continued

# I. INTRODUCTION

In several modern applications of natural and forced flow heat exchangers, the demands for large heat transfer and mass flow rates have forced the bulk conditions of the fluid into regions near the thermodynamic critical point. Current large thrust liquid propellant rocket engines with regenerative cooling of the nozzle area generally have combustion chamber pressures greater than 500 psig, surpassing the critical pressure of most common hydrocarbon propellants. A steam generator installation soon to be completed for a public utility company in the southeastern United States is expected to produce steam pressures in the vicinity of 3,800 psig, some 600 psig above the critical pressure of water.

Designers of such heat transfer equipment have been faced with rather unique and complex problems. Near the critical state, very large changes in thermodynamic and transport properties may occur with changing fluid temperature and pressure, and accurate prediction of heat transfer characteristics becomes a complicated if not impossible procedure. In addition, very little is known about the basic mechanism of heat and momentum transport in fluids in the vicinity of the critical point. Nevertheless, near-critical

fluids are attractive heat transfer media because of the very large heat transfer rates that can be obtained using relatively small temperature differences.

The critical point itself may be defined as the pressure and temperature at which no distinction can be made between the liquid and vapor phase of a fluid. If the pressure of a fluid is above its critical value, a constant pressure heating process brings about a continuous change from a very dense state resembling a liquid to a lighter state resembling a gas. If the temperature of the fluid is above its critical value, a constant temperature compression or expansion process can likewise only bring about a continuous change in properties. This implies that no distinct interface can occur between liquid and vapor at the critical point, and so surface tension ceases to exist. Boiling and condensation can not occur in fluids above their critical pressure and temperatures, hence the critical point can also be considered as the limiting pressure and temperature at which these phenomena may still exist. Experimental measurements indicate that precisely speaking, the critical point is not a single or unique value of pressure, temperature and density, but that this phenomenon occurs in a small region of bulk states, perhaps 0.002% of the critical values. Temperature and pressure

differences normally occurring in engineering processes are usually much larger than the range of this critical region, so that for most purposes it is usually considered to be a unique point. Table 1 gives the critical values of some fluids having current interest for engineering usage.

It is usually convenient to term fluids with pressures above the critical as supercritical, those with pressures below as subcritical. At a specified pressure in a subcritical fluid there is a distinct temperature (saturation temperature) at which change takes place from liquid to vapor. Supercritical fluids have no such unique temperature, but there is usually a well defined temperature at which the rate of change of thermodynamic or transport properties from the denser to lighter state will have a maximum. This temperature is called the pseudocritical temperature, and depends upon the pressure of the fluid. Individual properties have their maximum rate of change at different temperatures, but the variation between them is slight close to the critical point. In this study the pseudocritical temperature will be considered to be the location of the maximum rate of change of enthalpy at constant pressure, or equivalently, the location of the maximum specific heat at constant pressure. Supercritical fluids below the pseudocritical temperature

are called liquid-like, those with temperatures above are called vapor-like. While this terminology is by no means unique, it appears to be most prevalent in the literature. Figure 1 summarises these definitions graphically.

The use of supercritical fluids as coolant and power generating media in cases as cited above required the knowledge of their heat transfer and pressure drop characteristics. Early investigations of heat transfer to supercritical fluids attempted to provide this information through suitable experiments. During these investigations unusual behavior of the experimental equipment and erratic heat transfer results were sometimes observed. Distribution of temperature and heat transfer coefficients throughout the apparatus would sometimes exhibit sharp peaks, and overall heat transfer coefficients were much larger than those occurring in fluids further removed from the critical point. Some experimenters observed large pressure and flow oscillations as well as intense noise generation in the experimental apparatus. Several theoretical investigations attempted to incorporate the large property variations occurring in supercritical fluids into the basic equations governing shear stress and heat transfer, and thereby predict heat transfer results. When the bulk states considered were sufficiently far

removed from the critical or when heat transfer rates were low, reasonably good agreement could be obtained. However at states closer to the critical wide discrepancies would occur. These theoretical calculations also fail to predict the unusual distributions in temperature along the heated surfaces.

The unusual behavior of experimental apparatus, and the discrepancy between theoretically predicted and experimentally observed results has led some observers to suggest that the basic mechanism of heat transfer to supercritical fluids must be different than that of single phase fluids far removed from the critical point. Since noises, pressure pulsations and sharp increases in heat transfer frequently occur in forced-flow boiling, it has been hypothesized that under certain conditions the supercritical heat transfer mechanism may be similar to subcritical, or boiling heat transfer. One hypothesis states that although only a single phase can exist under equilibrium conditions in a supercritical fluid, large heat transfer rates may produce a non-equilibrium situation so that two "phases" may coexist transiently. If a pocket of liquid-like fluid were brought into contact with a heated wall, a small addition of heat would cause it to "explode" into something more like a vapor. A second hypothesis presumes that the fluid adjacent to a very hot

wall will have overall properties much like a vapor, while the relatively cool free stream the fluid would be more like a liquid. The "interface" between these regions may become unstable under certain conditions of flow rates and property variation so that disturbances would cause it to become wavy and finally break, much like the breaking of ocean waves. The resulting motion of liquid and vapor regions might produce a situation very similar to ordinary boiling.

The "pseudo-boiling" hypotheses described above have formed the basis of divergent opinions about the mechanism of heat transfer to supercritical fluids. Many experiments have now been performed in a variety of fluids, heater geometries, bulk conditions, heat transfer rates and fluid flow conditions. By examining the trend of their results, or by comparision with analysis when available, experimenters have concluded that the hypothesis either is or is not valid. Conclusions on this basis leave much to be desired however, as in at least in one case either the supposition of conventional or boiling like mechanisms will predict heat transfer rates that compare equally well with experimental results. Further experiments are necessary in order to establish the basic mechanism of heat transfer to supercritical fluids.

In some recent experiments in free convective heat transfer to supercritical carbon dioxide, attempts were made to actually visualize the flow field around the heating surface, and thereby gain information on the type of phenomena occurring during heat transfer to supercritical fluids. Under some conditions, the flow field was observed to be completely conventional, that is, the flow was of a type which is observed during free convective heat transfer to ordinary fluids. In some instances however, this flow pattern was observed to abruptly change to one more similar to that occurring in boiling heat transfer, and measurements of heat transfer rates show a sharp increase coincident with the onset of this second type of flow. These experiments have definitely shown that at least for one particular geometry, with certain bulk conditions and heat transfer rates, a second mechanism of heat transfer similar to boiling can occur during free convection in supercritical fluids.

The purpose of the present investigation was the study of forced convection heat transfer to supercritical fluids. The primary objective was to determine the basic mechanism for heat transfer and obtain quantitative information that might be applicable for design purposes as well. Since the possibility of an unusual mode of heat transfer exists, it was felt that direct observation of the

heated surface, in a manner similar to the free convection experiment described above, would be of great value in identifying such a mechanism. It was hoped that by comparing the observed flow fields in several circumstances of heat transfer, flow rate and bulk conditions, while making direct measurements of these quantities, some definite ideas about the transport mechanisms could be obtained.

An apparatus was designed and constructed for circulating supercritical carbon dioxide past a heated surface. The apparatus has many features of an ordinary low-speed wind tunnel, except that special provisions had to be made to contain the fluid near its critical state. Direct observation and photography of the heated boundary layer was also a principal consideration of the design. Flexibility was retained in all features of the design so that several different types of experiments could also be performed after slight modification.

The optical records and limited measurements of heat transfer in this type of experiment would admittedly have little quantitative value for actual prediction of supercritical heat transfer rates. It was hoped however that they would help in the selection of realistic models of the heat transfer mechanism to be used in

theoretical predictions of heat transfer rates. Further, more detailed measurements of velocity and temperature, their fluctuations and correlations are still needed in order to fully understand the phenomena occurring.

# II. REVIEW OF PREVIOUS STUDIES IN SUPERCRITICAL FLUIDS

In the past three decades, a significant amount of research has been devoted to heat transfer in supercritical fluids. As was mentioned in Chapter 1, experimental and analytical studies have been made for various heater geometries, fluid bulk states, heat transfer rates and fluid flow conditions. For the purposes of the present discussion, it is convenient to make only the following distinction: experimental studies in both free and forced convection; analytical studies in both free and forced convection. Although the present study is primarily concerned with forced convection, it is felt that some of the observations in free convection experiments, because of their basic nature, may shed light on the corresponding forced flow problem. For this reason the free convection studies will also be included in this review.

## A. Experimental Investigations

Perhaps one of the earliest investigations of heat transfer to supercritical fluids was that of Schmidt, Eckert and Grigull (1).* Schmidt suggested that because of the rather large specific heat and coefficient of expansion near the critical point, significant increases in heat transfer rates may occur. Their experimental apparatus consisted of a natural convection loop filled with ammonia, heated in one vertical section and correspondingly cooled in another. Their results were presented in terms of an "apparent thermal conductivity", defined as the thermal conductivity required to transfer an equivalent amount of heat at the same temperature difference through a material having the same cross sectional area and length as the loop. This apparent conductivity was observed to grow very large near the critical point, perhaps as much as 100 times that of water at 60°C. Fluctuations in both pressure and temperature were observed when the pressure was near its critical value. Later studies by Schmidt (2) in a closed vertical tube showed that the apparent thermal conductivity could be as much as 4,000 times that of

---

* Numbers in brackets refer to references.

copper. By inclining the apparatus, Hahne (3) found that the apparent thermal conductivity could be further increased to almost 10,000 times that of copper! These high values of apparent thermal conductivity were reached only in narrow ranges of bulk temperature however, and slight displacements from this critical range would cause the apparent conductivity to decrease rapidly. Nevertheless this type of set-up has been used successfully for internal cooling of gas turbine blades (4). A natural convection loop filled with Freon-12 was also studied by Boggs and Holman (5). They observed pressure fluctuations and intense vibrations of the apparatus as the fluid approached the critical region, but were able to successfully correlate heat transfer and flow rate measurements when removed from this region. Similar observations were made in water by Van Putte and Grosh (6) and in Freon-114 by Harden and Boggs (7). A numerical analysis of the stability of such a loop with respect to pressure oscillations was given by Harden (8) in terms of enthalpy-density plots. Experimental verification of this stability criterion was given by Walker and Harden (9), using several different fluids.

The problem of free convective heat transfer to quiescent, quasi-infinite fluids near their critical point has also been the subject of recent experiments. Eckert and Simon (10) were able

to make extremely precise measurements of the temperature field around a vertical flat plate in $CO_2$ by use of interferometry techniques. Their experiment was necessarily restricted to small temperature differences (0.001-0.01°C.) in order to keep the flow laminar, and thus closely approximated a constant-property condition. Both the thermal conductivity and heat transfer coefficient attained large values near the critical point, and also exhibited dependence on the heat transfer rate. Fritsch and Grosh (11) performed experiments with a similar heater geometry in water. The flow about the plate was also laminar, with temperature differences between the heated plate and bulk fluid of about 20°F. The temperatures were measured with thermocouples. Heat transfer coefficients were largest when the bulk temperatures were near the pseudo-critical, but still compared favorably with an analytical prediction of Fritsch and Grosh (12). On the basis of this agreement they concluded that the heat transfer mechanism near the critical point was unchanged from that of ordinary fluids, and that the large heat transfer rates previously reported could be accounted for by consideration of the property variations. Similar conclusions for low temperature differences were reached by Brodowicz and Bialokoz (13) during turbulent natural convection from a vertical

plate in Freon-12, and by Larson and Schoenhals (14) in supercritical water. Somewhat larger temperature differences (approximately 100°F.) were obtained by Doughty and Drake (15) during free convection to Freon-12 from a horizontal cylinder. They observed that the heat transfer coefficient grew large as the fluid approached the critical state, but remarked that this increase was limited to a small region of state conditions. Bonilla and Sigel (16) measured heat transfer from a horizontal flat plate to a pool of n-pentane both below and above the critical pressure, with bulk temperatures 200-300°F. below the critical. They found that even with large temperature differences their results could be correlated favorably using familiar dimensionless groups. When the temperature differences became large enough for the wall temperature to surpass the critical, a "limiting phenomenon" was observed to affect the heat transfer, and the heat transfer coefficient became essentially constant.

In all of the above mentioned investigations, conclusions about the heat transfer mechanism were formed by studying the trend of experimental data, rather than by direct observation of the heated flow fields. Some of the first direct observations of a heated surface in a supercritical fluid were performed by Griffith

and Sabersky (17) on a heated horizontal cylinder in Freon-114A. "Bubble-like" flow was observed around the wire, but did not correspond to any large increases in heat transfer rate such as those at the onset of nucleate boiling. Nevertheless they concluded that "bubble-like" flows can exist in some cases. Holt (18) photographed the heated surface of a vertical plate in water at large temperature differences (up to 1000°F.) but concluded that no "boiling-like" mechanism was present. Graham et al (19) observed a heated horizontal flat strip in liquid hydrogen at a range of pressures and accelerations, and reported that the flow field during heat transfer in the supercritical region was quite similar to boiling. In a recent experiment on a heated wire in $CO_2$, Knapp (20) obtained photographs which clearly show a secondary or "bubble-like" flow on the heated surface under some conditions. This "bubble-like" flow was coincident with a sharp increase in heat transfer rate. The flow around vertical and horizontal strips was also studied, but no indication of a "bubble-like" flow or increased heat transfer rate was observed for these cases. On the basis of these observations, he concluded that a secondary or "bubble-like" flow definitely could exist under certain conditions of heater geometry and bulk states, and may produce corresponding

increases in heat transfer rates. He further concluded that this secondary flow arose from a hydrodynamic instability of the usual laminar convection pattern. Yamagata et al (21) independently performed a very similar experiment and obtained results similar to (20).

Research on forced convective heat transfer to supercritical fluids was first stimulated by the requirement for more technical information about cooling of nuclear reactors. Some of the earliest studies were those of Chalfant (22), and Randall (23). These investigations were conducted with supercritical water flowing through electrically heated tubes at extremely high heat transfer and mass flow rates. Under certain conditions, "singing" or "whistle-like" noises would occur coincident with increases in the heat transfer coefficient. Goldmann (24) compared the data of (22) and (23) to an earlier analytical prediction (Goldmann (25)) and found good agreement for the regions in which "whistle" did not occur. Goldmann (26) further hypothesized that the heat transfer mechanism during "whistle" was similar to boiling at subcritical pressures. He visualized the heat transfer process as a sufficiently non-equilibrium phenomena so that two phases could actually coexist transiently. If by some mechanism a pocket of "liquid-like"

fluid was brought into contact with the heated surface it would "burst" into a "vapor-like" fluid, and the ensuing motion of high and low density pockets would supposedly resemble that occurring in normal boiling. Goldmann also proposed a second mechanism based on hydrodynamic stability arguments to account for the high heat transfer coefficients. He proposed that the interface between the liquid-like freestream fluid and the vapor-like fluid on the heated surface might become unstable under certain conditions of heat transfer rates and bulk fluid states. The "waves" on the interface would "break" much like ocean waves, thereby bringing the liquid-like fluid into contact with the heated surface and produce large heat transfer rates.

Hines and Wolf (27) also observed intense pressure fluctuations and "whistle" during turbulent forced convective heating of RP-1 and Diethylcyclohexane (hydrocarbon mixtures commonly used as liquid rocket propellants). In some cases the pressure fluctuations were severe enough to rupture the thin-walled heater tubes, and coincided with sharp increases in the heat transfer coefficient. They hypothesized that because of the rapid change in viscosity near the critical region, the boundary layer could become unstable and thereby trigger the pressure fluctuations and resultant

increases in heat transfer. Pressure oscillations during heat transfer to supercritical fluids were also observed by Thurston (28) in liquid hydrogen and Cornelius and Parker (29) in Freon-114. Thurston believed his oscillations due to different acoustic modes within the experimental apparatus, but Cornelius and Parker also found a mode whose frequency was much lower than expected from an acoustic mode. They concluded this unusual mode was triggered by the onset of a "boiling-like" phenomena.

Forced convective heat transfer without the occurrence of unusual pressure pulsations or noises has also been frequently reported. Dean and Thompson (30) studied the forced convective heat transfer to liquid nitrogen in annular flow, comparing their results to boiling in the same apparatus. The heat transfer coefficients for a supercritical fluid were larger than those of stable film boiling. Powell (31) observed that during flow of supercritical nitrogen, oxygen and hydrogen respectively below their critical temperatures, the heat transfer coefficient showed a minimum as the wall temperatures approached the critical. However, Bringer and Smith (32) found that during turbulent forced convection heating of $CO_2$ in a round tube, the heat transfer coefficient was a maximum near the critical point, in contrast to the results of

Powell. The occurrence of a maximum heat transfer coefficient during turbulent forced convection near the critical point was also observed by Dickinson and Welch (33) using water, Del Bene and Barger (34) using Freon-12, Koppel (35) in $CO_2$ and Petukhov et al (36) in $CO_2$. Similar trends were also reported by Armand et al (37), and Miropolsky and Shitzman (38) in water, and Szetela (39) in hydrogen. The occurrence of a maximum heat transfer coefficient when the wall temperature approaches the critical region seems to be well substantiated in view of the above mentioned investigations.

Measurements of the actual velocity and temperature profiles occurring during turbulent forced convection to $CO_2$ in a vertical tube were made by Wood and Smith (40). They showed that in some instances the maximum velocity in the tube does not occur at the tube centerline, but at some point between the center and wall. Temperature profiles showed no unusual trends, but density profiles inferred from the temperature showed sharp discontinuities across the tube. Large increases in the heat transfer coefficient were also measured when the fluid bulk temperature approached the pseudo-critical. They concluded these results were due to a "two resistance concept, which considers the thermal conductivity near the wall and the heat capacity some distance from the wall", but also thought

that very near the critical point the phenomenon could be treated as an extension of boiling.

In normal constant property forced convective heat transfer it is often convenient to express heat transfer and fluid flow relationships in terms of dimensionless groups such as the Nusselt, Prandtl and Reynolds numbers. In some cases these techniques have also been applied successfully to supercritical fluids. By suitable selection of temperatures at which to evaluate properties. Domin (41) was able to satisfactorily express his data for heat transfer to supercritical water in terms of these quantities. Shitzman (42) had previously presented a similar correlation for experiments in water, oxygen and $CO_2$. Further dimensionless groups accounting for property variations were proposed by Petukhov et al (36), and by Swenson, Kakarala and Carver (43). Petukhov et al were able to derive a generalized correlation scheme applying to supercritical water and $CO_2$, while Swenson et al successfully applied their correlations to experiments in water.

The previously mentioned hypothesis about the analogy between supercritical and boiling heat transfer was exploited in a novel correlation scheme proposed by Hendricks et al (44). By

assuming a supercritical fluid to be composed of a certain fraction of "light" and "heavy" species, heat transfer results could be correlated with the Martinelli parameter, which is a coefficient accounting for shear stresses at the wall and phase boundaries in two-phase flow. The authors concluded that the favorable correlation of experimental data supported the hypothesis of "boiling" in supercritical fluids.

It should be pointed out that correlation techniques, while extremely useful for engineering purposes, have limited value for determining the actual mechanism of heat transfer to supercritical fluids. Hess and Kunz (45) used the data of Hendricks et al and proposed a correlation scheme based on conventional forced convection parameters. They showed that both conventional and two-phase fluid approaches would correlate the same data equally well ! It is apparent that a successful correlation can be made by judicious choice of fluid properties and flow model, but the actual transport mechanism may well be veiled with such a technique.

## B. Analytical Investigations

Attempts at analytically predicting heat transfer to supercritical fluids have been severely restricted by two facts; the severe property variations with temperature and pressure near the critical point; the lack of a complete understanding of the basic heat transfer mechanism. The first of these effects, that of property variations, can be circumvented by the choice of problem in some cases. One example of this is the case of laminar flow heat transfer at fairly low temperature differences. Since the temperature differences are low, the constant property case may be closely approximated, and hence analytical solutions may be obtained by series expansions in some suitable parameter about the constant property case. Another instance is when the basic flows yield to similarity type solutions. Fritsch and Grosh (12) considered the case of laminar free convection from a vertical flat plate. By assuming that only density and specific heat varied significantly in the critical region, they were able to reduce the boundary layer equations using a conventional similarity transformation. The resulting equations were numerically integrated on an electronic computer for specific bulk states and temperature

differences. The results compared favorably with experiments (11). Brodowicz and Bialokoz (13) performed a similar computation but included variations in viscosity and thermal conductivity as well. For the case of turbulent free convection the problem is complicated by the fact that no quantitative values of the velocity and temperature profiles are available. Larson and Schoenhals (14) used approximate integral methods with assumed velocity, temperature and enthalpy profiles to compute turbulent free convection from a vertical plate in water. Fairly good agreement with experiment was obtained for lower temperature differences, but wide deviation occured as temperature differences were increased. They concluded that this discrepancy was due to lack of accurate knowledge of values of the Prandtl number in the critical region.

Analyses of forced convective heat transfer to supercritical fluids are limited by the same complications as in free convection. Koppel and Smith (46) considered the laminar forced convection of supercritical carbon dioxide in a vertical tube. By neglecting radial velocity and introducing a modified temperature potential, they were able to numerically integrate the equations of conservation of mass, momentum and energy. Results for the axial variation of heat transfer coefficient were presented for specific bulk states,

flow rates and heat transfer rates. Turbulent forced convection problems are additionally complicated by a lack of information on turbulent transport of heat and momentum even in constant property flows. In what has become the most cited analytical work in variable-property turbulent heat transfer, Deissler (47) assumed certain analytical forms of the turbulent eddy diffusivity for turbulent heat and momentum transfer in order to integrate expressions for shear stress and heat flux. Specific results for supercritical water were presented in terms of Nusselt and Reynolds numbers, with an additional heat flux parameter $\beta$ . Good agreement with experimental results was achieved, for moderate property variations, but discrepancies as large as 50% occurred when the bulk fluid and wall temperature straddled the pseudocritical. Goldmann (25) proposed an alternate scheme of integrating the shear stress and heat flux expressions which gave better agreement with experiments, even when straddle occurred (reference (24) ). Hsu and Smith (18) modified Deissler's approach to account for radial momentum transport and buoyancy effects during turbulent flow through vertical tubes. Specific results were computed for $CO_2$, and compared well with the data of Bringer and Smith (32). The velocity and temperature profiles were also computed. These

computations showed that the velocity could have a maximum at a location other than the centerline of the tube, and this phenomenon was later verified by the experiments of Wood and Smith (40). Hess and Kunz (45) modified a variable property method proposed by Wiederecht and Sonnemann and applied it to supercritical hydrogen. The calculated values of shear stress and heat flux agreed well with data, and an engineering correlation scheme was proposed. They further investigated the change in Nusselt number along the length of the tube and found good agreement even at points where the data showed sharp peaks in heat transfer coefficient. On the basis of this agreement they concluded that the sharp changes in heat transfer coefficient could be explained by accounting for property variations, and that no hypothesis about pseudo-boiling was required.

# III. CHARACTERISTICS OF FLUIDS NEAR THE CRITICAL POINT

## A. Thermodynamic Properties

In Chapter I it was mentioned that fluids near the thermodynamic critical point are characterized by their extreme variations in thermodynamic and transport properties. In order to determine how these property variations may affect heat transfer processes, and to define the range over which they may be significant for engineering applications, a brief examination of these properties will now be given.

The thermodynamic properties most pertinent to heat transfer processes are density, volumetric coefficient of expansion, and specific heat at constant pressure. The product of specific heat and density determines the ability of a volume of fluid to absorb heat, while the coefficient of expansion determines whether body forces can significantly affect the motion of the fluid.

At subcritical pressures the fluid may be in either its liquid or vapor phase, their densities varying slightly with temperature and pressure. At the saturation temperature and pressure, the density may have any value from the pure liquid to pure vapor

values. A graph of density versus temperature at constant pressure such as Figure 2 shows a step change in density at the saturation temperature and pressure. As the pressure is increased the saturated liquid and vapor densities approach each other, becoming equal at the critical point. At the critical pressure the density versus temperature curve has a vertical tangent when the critical temperature is reached, but it is smooth and shows no discontinuities. Above the critical pressure the density also varies smoothly, but its rate of change with temperature may become quite large at the pseudocritical temperature. As an example Figure 2 shows that the density of $CO_2$ at 1,100 psia can change by a factor of 8 when the temperature changes from 80°F. to 160°F. With increasing pressures the density change becomes less pronounced and eventually approaches the density-temperature relationship of a perfect gas.

The volumetric coefficient of expansion is proportional to the negative of the slope of the density-temperature curve at constant pressure, that is

$$\beta = -\frac{1}{\rho} \left.\frac{\partial \rho}{\partial T}\right|_p$$

The description of density variation given above points out that a subcritical saturated fluid may change density discontinuously from

the liquid to vapor phase. Thus in a manner of speaking $\beta$ can be considered infinite when liquid and vapor coexist, although it is finite in the individual pure phases. As the pressure increases the coexistence region diminishes and exists only in a limiting sense at the critical point. Hence $\beta$ becomes infinite precisely at the critical point. At pressures above the critical $\beta$ can have large although finite values, for example $CO_2$ at 1,100 psia and 90°F. has $\beta = 0.5°F.^{-1}$, about 250 times larger than air at standard temperature and pressure. Such large values of $\beta$ may give rise to large buoyancy forces, so that free convection effects become important even in a predominately forced convection problem. This can be visualized in the case of forced convection heating of a supercritical fluid with the bulk temperature sufficiently removed from the critical, and the heating surface temperature near the critical. Next to the heated wall the flow would be of a mixed free and forced convection type, and thus would affect the normal forced convection heat transfer results.

The specific heat at constant pressure varies in a manner similar to that of the volumetric coefficient of expansion. Adding a small amount of heat to a subcritical liquid at constant pressure changes the temperature slightly, so that $c_p$ has a finite value.

However in a saturated condition the liquid is able to absorb the entire latent heat of vaporization without change in pressure or temperature, thus $c_p$ is infinite in the coexistence region. Since the critical point can be considered as a limiting value of the coexistence line, $c_p$ is also infinite right at the critical point. The variation of $c_p$ is conveniently described by studying the slope of a constant pressure curve in an enthalpy-temperature graph. Since

$$c_p = T \frac{\partial S}{\partial T}\bigg|_p = \frac{\partial h}{\partial T}\bigg|_p$$

the specific heat is equal to the slope of this curve. Figure 3 shows a plot of enthalpy versus temperature for $CO_2$, which has a behavior typical of fluids in the critical region. Below the critical pressure the specific heat is infinite in the coexistence region as described above. At supercritical pressures the specific heat remains finite, but may take on large values in particular cases. For example at 1,100 psia and 90°F., $c_p = 15$ BTU $(lb_m °F.)^{-1}$, about 75 times larger than air at S. T. P. The very large values of $c_p$ can be expected to significantly affect heat transfer processes, since only a small change in temperature is required to absorb a large amount of heat. Large increases in heat transfer coefficients may then be expected when

the bulk fluid or wall temperature is near the pseudocritical temperature.

It should be pointed out that while both the coefficient of expansion and the specific heat assume large values near the critical point, the actual range over which this occurs may be very small. Figure 3 shows that although the specific heat of $CO_2$ at 1,100 psia is large when the temperature is between 89 to 92°F., it drops very rapidly outside this range. Hence the effect of large values of $c_p$ and $\beta$ may not be fully realized in a practical application unless either the wall or bulk temperatures can be accurately maintained within this small region. However in a broad region around the critical point these properties may still be larger than those of normal fluids, so that some improvement in heat transfer might still occur.

Thermodynamic properties such as specific heat at constant volume and latent heat of vaporization can also influence heat transfer rates. However, they are not expected to produce any unusual effects near the critical point since their values do not differ markedly from those of normal fluids.

## B. Transport Properties

Forced convection heat transfer processes are also influenced by the momentum and thermal transport properties of the fluid, that is, by the coefficient of absolute viscosity and the thermal conductivity. Except for a small region extremely close to the critical point, the thermal conductivity and viscosity exhibit similar dependence on temperature and pressure around the critical point.

In a subcritical liquid, the viscosity and thermal conductivity decrease smoothly as the temperature is increased at constant pressure. At the saturation temperature they may vary from the pure liquid to the pure vapor values. Increasing the temperature of the pure vapor causes these properties to decrease further, until minimum values are attained. Further increases in temperature cause increases in viscosity and thermal conductivity, with the fluid then behaving as a perfect gas. At pressures far above the critical, the viscosity and thermal conductivity change smoothly from liquid-like to vapor-like values as the temperature increases. However at pressures and temperatures only slightly above the critical values, the thermal conductivity exhibits extremely large peaks while the viscosity drops rapidly with increasing temperature.

This behavior is shown for $CO_2$ in Figures 4 and 5.

The occurrence of a sharp peak in the thermal conductivity has been actively discussed by workers in this field. In practice it is extremely difficult to prevent the occurrence of free convection within the thermal conductivity measuring apparatus, and some workers hold the view that the sharp peaks observed are actually due to the onset of such convection patterns (49). In an experiment carefully designed to prevent such convection, Michels et al (50) still observed large peaks in thermal conductivity, and it has now become generally accepted that this is the true behavior in the critical region. A recent review of the transport properties of $CO_2$ in the critical region was given by Sengers (51).

The very large values of thermal conductivity could be expected to produce large heat transfer coefficients, since large amounts of heat could be conducted with only small temperature differences. However as in the case of the specific heat, the occurrence of large thermal conductivity is restricted to a narrow range in temperature and pressure so that in practice the very large heat transfer rates may not be achieved. Nevertheless the sharp variation in $c_p$ with temperature may still have a significant influence on heat transfer.

The rapid drop in viscosity near the critical region may also affect heat transfer through changes in the basic convection pattern. Changes in viscosity with temperature can influence the curvature in the velocity profile of a flowing fluid, thereby affecting its stability. Near the critical point the changes in viscosity may conceivably be large enough to make the primary flow unstable, so that a completely different type of motion may result.

C. Additional Properties

In constant-property flows, heat transfer results are significantly influenced by changes in the Prandtl number, defined as the ratio of viscous to thermal diffusivities of the fluid $\mu c_p/k$.

In the critical region both $c_p$ and $k$ change rapidly, and the Prandtl number attains very large values close to the critical point. Figure 6 shows that the Prandtl number of $CO_2$ can be as large as 27 in the critical region. Heat transfer to such a fluid would produce large variations in Prandtl number, with corresponding changes in the relative importance of momentum and thermal transport.

Compressibility effects can also affect heat transfer and shear stresses. Fluids may be considered incompressible whenever the flow velocity is much less than sonic velocity (52). The speed of sound (at zero frequency) is usually given as

$$c = V\sqrt{-\frac{c_p}{c_v}\frac{\partial p}{\partial V}\Big|_T}$$

At the critical point $c_p$ becomes infinite while $(\partial p/\partial V)_T$ goes to zero, so that this expression for sonic velocity is indeterminate. However this expression may be transformed so that the

limiting value for c at the critical point is given by

$$c = V \left.\frac{\partial p}{\partial T}\right|_V \sqrt{\frac{T}{c_v}}$$

Hence c has a non-zero, finite value near the critical point. Carbon dioxide has a minimum sonic velocity of about 520 feet per second near the critical point (53), so that for most engineering heat transfer applications it can be considered as incompressible.

Summarizing this description of near critical fluids, it may be said that the unusual variation of fluid properties might be expected to produce significant changes in heat transfer. In addition the heat transfer processes will not only depend upon the actual value of the fluid properties, but on their rate of change with pressure and temperature as well. Thus heat transfer coefficients can be affected by the heat transfer rate itself. It is well to note however, that the actual range of bulk states in which these changes occur is extremely small, so that the very high heat transfer rates may be hard to achieve in practice despite the high heat transfer coefficients.

# IV. EXPERIMENTAL APPARATUS

## A. General Features

Selection and design of the components of the apparatus were governed by the basic experimental objectives; to provide a means for measurement of heat transfer rates, flow rates and heated surface temperatures in a supercritical fluid, while allowing for direct visualization of the heated surface and heated flow field.

Previous forced convection studies have been performed in situations such as flow through pipes and annuli. Visualization of the flow next to the heater surface is difficult in these geometries because of their curvature and the blurring effect of the bulk field. On the other hand a flat plate geometry in a uniform flow has essentially the same type of turbulent boundary layer velocity and temperature profiles as fully developed turbulent pipe flow, and direct observation is not hindered by the factors mentioned above. Since visual observation was to be a principal concern of this experiment, a flat plate geometry was chosen for the heated surface. In addition, a large amount of work has been carried out both experimentally and analytically on heat transfer from flat plates with constant property fluids, so that some comparison could be

made with fluids near the critical point.

Two basic flow producing schemes are commonly used in forced convection studies, a closed circulation loop and a "blow-down" system. "Blow-down" schemes are principally used where high mass flow rates or low turbulence levels are required. Only moderate flow rates were contemplated for these experiments however, so that the circulating loop system was chosen. It was felt that satisfactory flow conditions could be produced in a loop with proper selection of the pump and turbulence damping screens.

The general features of the apparatus are schematically indicated in Figure 7. The fluid is circulated through the loop by a centrifugal pump driven at constant speed with an A. C. motor. The fluid flow rate in the test section is controlled by a series of valves and a simple by-pass system. The heated flat plate is located at mid-height in a glass walled rectangular channel, with the plane of the heated surface horizontal. The rectangular channel itself is located inside a long horizontal cylindrical vessel which has two glass viewing ports. The rectangular channel may be moved within the vessel so that the entire heated length of the flat plate can be observed. The fluid flows into the cylindrical vessel at a low speed and passes through flow straightening and turbulence

damping devices. It then passes through a contracting transition section, entering the rectangular channel and passing over the heated flat plate. The field also passes simple heating and cooling devices located in other parts of the circuit for maintaining system temperature. A free piston hydraulic accumulator connected to a nitrogen reservoir is used to control system pressure. Flow rates are measured using an ASME standard venturi section. An optical bench, with provision for mounting of lenses, lamps and cameras, is located with its axis normal to the flow direction and parallel to the plane of the flat plate. The optical system may be used as either a shadowgraph or schlieren device. The present study was performed with a specially modified schlieren scheme, described more completely in Section E of this Chapter.

The flat plate is made of glass with a thin electrically conducting film fired on to one surface. A direct current, controlled by a series of air cooled resistors, is dissipated in the surface film of the plate and thereby transmitted to the fluid. Plate temperatures are measured with thermocouples located in small holes drilled through the plate and inserted flush with the heated surface. The thermocouples are cemented into position, the upper portion of the small hole being filled with cement and smoothed off so as to

minimize disturbances to the flow field.

Carbon dioxide (critical pressure 1071 psia, critical temperature 87.8°F.) was selected as a working fluid. The selection of carbon dioxide was made for several reasons; it is readily obtained in high purities, its thermodynamic and transport properties have been well established in the critical region, it is chemically stable, non-toxic, non-corrosive and non-flammable. The critical state, although requiring moderately high pressure apparatus, is easily reached in the laboratory. It was felt that previous experiments performed in $CO_2$ may also afford some comparison with the present study. The various components of the apparatus are described in more detail in the following sections.

B. Design and Construction

The main pressure vessel in which the heated test section is contained is a precision-bore steel cylinder 45" long with 3" inner diameter. A 2" diameter hole was drilled normal to the cylinder axis at approximately mid-length in order to provide an optical path through the apparatus. A collar for passing over the outside of the cylinder was made by boring a hole through one side of a 5" by 5" by 7" steel block. A second hole was bored through the square side of the block, thereby forming the optical path when aligned with the hole in the cylinder. Crown borosilicate glass discs 2.5" in diameter and 1.25" thick were inserted into a mating shoulder inside the collar before installation over the cylinder, and served as the viewing ports. The ends of the cylinder were fitted with steel caps that were tied together with two tie plates. Tube fittings were connected to each end to deliver and return the working fluid. The clearances between the glass porthole and collar, cylinder and collar, and end cap and collar were sealed with neoprene "O"-ring gaskets. One of the end caps was fitted with sealed gland assemblies for passing power cables and thermocouple leads out of the apparatus. An overall view of the assembly mounted in position is

shown in Figure 8. The design features of the apparatus described above resulted in great ease of assembly, maintenance and alignment. The entire apparatus, designed to withstand pressures of 2,000 psia and temperatures of 200°F., could be completely assembled in minutes.

After fabrication, the apparatus was assembled and tested in a hydraulic test stand at 2,000 psia for 24 hours with no leaks being detected. It was then dismantled, thoroughly degreased and plated with a layer of cadmium. The apparatus was then mounted and connected to the various components of the loop with 1" diameter stainless steel tubing. After checking the entire assembly for leaks, the apparatus was cleaned with Cineclene, a commercial degreasing agent.

The rectangular channel in which the heated plate was situated, shown in Figure 9, was machined from aluminum and inserted in a cylindrical carriage having clearance fit with the long precision-bore pressure vessel. The entire carriage slides smoothly within the larger cylinder, and a keyway along the top provides proper alignment. The carriage was pulled along the cylinder by 0.035" diameter steel wire which passed through both end caps. The position of the carriage could thus be changed during

a test run. The upstream end of the carriage contained a contracting transition section from the circular cylinder to the rectangular test channel. The transition section was cast from Cerrobend, a low melting temperature lead alloy, and was smoothly finished and aligned to provide a uniform entering flow believed to be free of secondary motions. The downstream end of the carriage served as a terminal board for power and thermocouple leads which passed through the end caps. Figure 10 shows a sectioned sketch of the cylindrical vessel and test carriage, and a photograph of the test carriage is shown in Figure 9.

The pump used to circulate the carbon dioxide was a 4 vane centrifugal pump operating at 3,600 RPM and producing about 30 feet of head in the working fluid at a flow rate of 30 lb./sec. The drive shaft was sealed with a rotating carbon-face seal installed by the pump supplier. The pump and driving motor were mounted as a unit and connected to the apparatus with flexible high pressure hoses. In this way a minimum of vibration was transmitted to the test section.

## C. Controls and Instrumentation

The pressure within the apparatus was maintained by a free-piston hydraulic accumulator with one side of the accumulator connected to the apparatus, the other to a nitrogen supply reservoir. The pressure on the nitrogen side was controlled by a pressure regulator and vent, the total volume of the nitrogen system being about 3 times that of the apparatus. Because of the large nitrogen to $CO_2$ volume ratio, large changes in the $CO_2$ bulk temperature could be accomodated without substantial pressure change. By slight venting or addition of nitrogen, the $CO_2$ pressure could be easily controlled to within 1 psia. The pressure within the cylindrical pressure vessel was measured with a Heise bourdon tube gauge, calibrated against a dead-weight tester and accurate to 0.1% of the full scale reading. The pressure within the pressure vessel actually varies from upstream to downstream end, but the difference between ends is slight (see Appendix F). The pressure readings only served to indicate the bulk fluid conditions and are not actually used for computational purposes, so that simply measuring the pressure at the downstream end of the vessel was felt to be sufficient.

The system temperature was controlled by passing the fluid through either heated or cooled lengths of piping. The heater was formed by wrapping electrical heating tape around a 3 foot length of the main flow loop. The heating rate in the tape was controlled with a variable A. C. transformer. The cooled section was a 4 foot length of straight tubing in the main flow loop. An annulus was fashioned around the tubing, and ice water from an ice bath circulated through the annular jacket. By adjusting either the ice water flow or the power to the heater, the system temperature could be maintained to 0.3°F. in a range from 60°F. to 120°F.

All temperature measurements were made using iron-constantan thermocouples, calibrated against an ASTM precision thermometer. A probe for measuring freestream fluid temperature approaching the heated plate was made by butt-welding 0.005" diameter iron and constantan wires. This probe was located slightly in front of and below the leading edge of the plate. Surface temperatures of the flat plate were measured with Aeropak sheathed thermocouple assemblies. These assemblies are 0.004" diameter wires insulated from each other by magnesium oxide and encased in a 0.025" outer diameter stainless steel sheath. The hot junction was attached to the inner surface of the sheath tip and the entire

sheath assembly was mounted in a 0.026" diameter hole drilled completely through the glass plate. The tip of the sheath was flush with the heated surface, and the portion of the hole not occupied by the sheath was filled with epoxy cement and smoothed off. The hot junction is insulated both electrically and thermally from the heat-generating film and as such does not measure its temperature directly. However it does measure the temperature of the fluid adjacent to the thermocouple tip, which differs only slightly from the heated surface temperature nearby. An estimate of the error involved with this technique is presented in Appendix F.

The plate and freestream thermocouple leads were passed out of the pressure vessel by a Conax transducer gland, and a cold junction was formed by connecting them to individual copper leads. The cold junctions were coated with electrically insulating varnish and inserted into a distilled water-ice bath. The copper leads were connected to a selector switch which permitted measurement of either individual thermocouples, or the difference between plate and freestream thermocouples. The thermocouple E. M. F's were measured with a Leeds and Northrop thermocouple potentiometer, Model 8686, or a Hewlett-Packard Model 425A microvolt-ammeter.

A venturi tube inserted in the main flow loop was used to deter-

mine the freestream fluid velocity approaching the flat plate. The venturi geometry conformed with ASME standards for this type of meter (54). It has an upstream diameter of 0.875", a diameter ratio of 0.5, and a discharge coefficient of 0.971 over the entire velocity range used in this investigation. It was installed with about 50 tube diameters of straight run preceding the upstream pressure tap. Pressure differences between the upstream and throat sections were measured with a Barton Model 200 differential pressure meter. A thermocouple for measuring bulk fluid temperature was located about 1.5" downstream of the diffuser.

Heat transfer rates from the flat plate were determined by measuring the power dissipated in the conducting surface film. A simple circuit, shown in Figure 7, was arranged to vary the dissipation in the plate by adjusting a large bank of air cooled resistors. Current was taken from a 120 volt D.C. main, passed through the dropping resistors and into the heated film. The maximum power dissipated in the plate in the present investigation was about 1 kilowatt. A Weston Model 281 ammeter-voltmeter combination was used to measure power to the plate at higher power levels, each meter having an accuracy of about 1% of full scale reading. Lower power levels were measured using a Weston Model 310 precision

wattmeter with 0.25% accuracy at full scale.

D. Features of the Flat Plate and Flow Channel

A Corning pyrex glass plate, 1" wide, 10 1/2" long and 1/8" thick served as the flat plate test section. A metallic oxide film was fired on to one side of the plate, forming an integral conducting surface that was smooth, hard, and would not flake off. The resistivity of the film was uniform to within 3%, so that the heat transfer rate was approximately constant over the plate surface.

Power was transmitted to the film by two narrow conducting strips that ran along both of the 10 1/2" long plate edges. The conducting strips were painted on with aluminum conducting paint, and were about 1/4" wide, leaving a 1/2" wide strip of dissipating film in the middle of the plate. Copper conductors were attached to both strips at the downstream end of the plate. The current passed along the length of the plate through the conducting strips, and across the width through the dissipating film. The leading edge of the plate was formed by attaching a small metal tip having a circular arc profile to the upstream edge. This tip had a sharp leading edge and joined smoothly with the heated surface. The unheated length of the plate due to the tip was about 1/4". Two thermocouples for measuring the surface temperature were located in the center of the

heated film, 3.25" and 7.25" from the leading edge respectively. The flat plate was located at approximately mid-height in a rectangular channel 1.06" wide, 1.75" high and 12.5" long, shown in Figure 9. Two side walls of the channel were glass, and the heated plate was attached to one of them with a small angle bracket at the middle of the plate. The small gap between the glass side walls and plate edges was sealed with RTV 5, a flexible silicone rubber cement. The plate was thus free to move due to thermal expansion, and could sustain a heated surface temperature of 500°F. without cracking.

The plate was not parallel to the upper and lower channel surfaces, but was inclined at about 0.8° to them. The inclination was such that a stagnation point occurred on the heated side of the plate, just downstream of the sharp edge. This insured the existence of a laminar boundary layer starting on the plate. A shadowgraph picture of the leading edge flow is shown in Figure 11. In this photograph the streamlines were made visible by a small heated wire inserted in front of the plate. The thermal wake of the wire follows the fluid streamlines, which can then be recorded by the shadowgraph method.

Boundary layer growth along the plate plus the plate inclination caused a "blocking" effect within the channel. This resulted in about a 12% change in freestream velocity along the plate (see Appendix F).

Freestream turbulence levels are known to affect heat transfer rates and boundary layer stability (55), so that considerable attention was given to the nature of the flow approaching the plate. The fluid entering the cylindrical pressure vessel first passed through a 4" long porous matrix made from copper wood pads packed together. This matrix served to dissipate the energy in the larger turbulent eddies and partially reduce pressure fluctuations produced by the pump. The fluid then entered a 6" long 1/8" cell size honeycomb section, which removed swirl components from the main flow. A final section of 4 fine-mesh screens, selected on the basis of measurements by Dryden and Schubauer (56), served to further reduce the turbulence level. The entire set of straighteners and screens was located about 8" upstream of the converging transition section. The result of the turbulence damping screens was a freestream turbulence level of from 0.25% to 0.35%, considered sufficiently low for this investigation.

## E. Optical Bench

In this investigation a semi-focusing color schlieren method was used to photograph the heated boundary layer. Schlieren methods produce an image that depends on the gradient in refractive index (or equivalently, the gradient in density and temperature) occurring along the optical path. Because of the extreme property variations near the critical point, significant density gradients may also exist along the optical path outside of the heated boundary layer. Thus a conventional schlieren system may give rise to significant "optical noise" when used in the vicinity of the critical point. A semi-focusing scheme devised by Kantrowitz and Trimpi (57) was further modified to produce color images, and allowed "focusing" of the schlieren image from the heated boundary layer alone. The semi-focusing scheme relies on multiple source-knife edge combinations, arranged so that pencils of light traverse the test section oblique to the optical axis. A brief description of the optical principles involved in this technique is given in Appendix D. Figure 12 shows supercritical $CO_2$ flowing over a heated object when viewed with the conventional and semi-focusing techniques.

The principal elements of the optical bench are shown in Figure 13. The bench itself was machined from a 7 foot long, 3" deep I-beam section, and provided a rigid base for mounting of optical components. Micrometer adjustments were provided for the lens, source and filter holders so that the optical axis could be accurately positioned. The so-called schlieren lenses were a pair of 178 mm. focal length f/2.5 Aero-Ektars. These are astigmatic lenses, corrected for spherical and chromatic aberration and made from highest quality optical glass. The astigmatism is not required in conventional schlieren systems, but is necessary for the semi-focusing system because of the off-axis light sources.

The key element of the semi-focusing scheme is the multiple source plate and matching cut-off. Two types of source geometry were used; a single horizontal row of uniformly spaced small circles, and a single horizontal thin slit. The knife-edge normally used in black and white schlieren systems was discarded in favor of color filters for two reasons; poor performance in large range systems (see Appendix D), and inability to distinguish boundaries of heated opaque objects in the optical path. The filter corresponding to the row of circular sources was a matching row of

green dots surrounded by a concentric yellow ring and located on a red background. This produced an unheated flow that appeared green. Subsequent heating of the boundary layer caused the schlieren image to change from green to yellow to red in the heated regions.

The color filter and source were made by first pasting a row of yellow dots having small green centers on a 3 foot square sheet of red paper. A sheet of tracing linen was placed on top and a row of black dots made to coincide with the green. The black dots and colored paper were then photographed together, and the resulting negatives used as filters after being reduced to the desired size. The horizontal slit source was made by simply photographing an accurately drawn uniform black line on a large white sheet. A reduced negative was then used for the source. The matching color filter was made by mounting thin strips of various color Wratten filters on a glass plate following North (58). The actual spacing and size of the light sources was not critical, and several sizes and color arrangements were tried until optimum performance was obtained. However in order to provide the semi-focusing effect the maximum obliquity of the light rays

to the optical axis was kept as large as possible. The largest obliquity used in this investigation was about 6°.

The images formed were recorded with two lamp-camera combinations. Still photographs were taken using a Speed Graphic camera with a Polaroid back. A Strobex Model 122 electronic flash lamp was used for the light source. Flash duration was about 25 microseconds for the flash intensities used. Motion pictures were taken with a Fastex WF 3 16 mm. high speed camera, having a terminal framing speed of about 8,000 frames per second. A tungsten filament lamp connected to a regulated D. C. power supply was used for a light source.

## F. Hot Wire Anemometer

Measurements of the turbulent velocity fluctuations in the approaching flow as well as next to the heated plate were made using a Shapiro and Edwards Model 60B constant-temperature hot wire set. The hot wire probe forms one leg of a Wheatstone bridge, and a feedback loop maintains the wire surface at a desired temperature by adjusting the instantaneous current passing through the probe. A more complete description of this and other hot wire techniques may be found in Kovasznay (59).

The fluctuations in the wire current are actually a measure of fluctuations in velocity and temperature in the neighbourhood of the probe, and a strict interpretation of their separate magnitudes is extremely complicated, if not impossible. For purposes of this study however, it will be sufficient to simply term their combined effect as the "turbulence level" near the probe. Appendix E gives a brief discussion on the feasibility of such an interpretation for the present study.

Quantitative measurements of the wire current fluctuations were made with a Hewlett-Packard Model 400D root mean square vacuum tube voltmeter. An actual trace of the instantaneous wire

current fluctuation was obtained with a Type 551 Tectronix Dual Beam Oscilloscope, fitted with a Polaroid camera. These traces served to indicate whether the fluctuations were composed of any predominant frequencies.

The probe used to measure turbulence in the approaching flow was located at the centerline of the rectangular channel about 1/2" upstream of the leading edge of the plate. The probe was a tungsten wire, 0.0004" in diameter and about 1/4" in length. It was removed from the channel during the flat plate heat transfer studies.

Turbulence levels near the heated surface were recorded with a probe fixed at a height of approximately 0.010" above the plate and located about 1/4" downstream of the back plate thermocouple (7.50" from the leading edge). The probe was made by soldering a 0.0004" diameter by 0.010" long platinum wire to two copper needles, using soldering techniques described in (59). The probe can be seen mounted in the channel in Figure 9. A color schlieren photograph of the heated wake from the wire is shown in Figure 14.

# V. EXPERIMENTAL PROCEDURE

## A. Initial Preparation

After the apparatus had been pressure tested, dismantled, cleaned and reassembled as described in Chapter IV, it was carefully aligned so that the upper and lower rectangular channel surfaces were horizontal. The lamp on the optical bench was turned on, and the bench adjusted so that the optical axis was parallel to the heated flat plate. The apparatus was then connected to the $CO_2$ and nitrogen supply cylinders. The $CO_2$ cylinder held the fluid in a saturated state corresponding to room temperature, and was fitted with an internal siphon for liquid withdrawl. Prior to filling the apparatus with $CO_2$, the entire system was evacuated and then purged with $CO_2$ at about 300 psia. When it was felt that purging was complete, the system was again evacuated and the purging cycle repeated several times until all air was expelled from the apparatus. Liquid $CO_2$ was then withdrawn from the supply cylinder and allowed to fill the apparatus, including the $CO_2$ side of the free-piston accumulator. The $CO_2$ supply valve was then closed, and the pressure on the nitrogen side of the accumu-

lator adjusted so that the $CO_2$ was near the desired test pressure. The main fluid circulation pump was turned on, and either the ice-water flow in the cooler or power dissipation in the heating tapes was adjusted in order to regulate the $CO_2$ bulk temperature. Final adjustments of the temperature, pressure and flow rate brought the fluid to any predetermined test condition.

## B. Test Procedure

### 1. Heat Transfer Measurements

The experiments were performed with the relevant parameters being varied in two separate ways. The main portion of the test were conducted with the freestream velocity, temperature and pressure fixed while the plate surface temperature ( or equivalently the heat transfer rate) was varied. In this sequence of tests, the bulk properties were brought to their fixed values, the plate current was turned on and the variable resistors adjusted to provide the desired surface temperature. Measurements of the freestream pressure, temperature, flow rate, plate temperature, and heat transfer rate were made. The resistors were then re-adjusted to provide a different surface temperature and the readings were repeated. The freestream conditions were frequently checked between settings of surface temperature, and if significant deviations from the desired values occured the plate current was shut off and the bulk conditions were re-established.

The second, less extensive, set of tests were performed with the freestream pressure, velocity and plate heat transfer rate fixed while the freestream temperature was allowed to vary.

After the bulk fluid conditions were established and the resistors set to provide the desired plate current, readings of the freestream temperature, pressure, velocity, heat transfer rate and plate temperature were made as in the previous set of tests. The free-stream velocity, pressure and heat transfer rate then remained fixed while the freestream temperature was brought to a new value, and the same readings repeated.

All of the experiments described so far were performed with the heated surface facing upwards, that is, with gravity forces acting in a normal direction towards the heated surface. In order to gain some information about the effect of free convection on heat transfer rates, a few experiments were conducted with the heated surface facing downwards. To place the test plate into this position, the entire cylindrical pressure vessel was rotated 180° about its longitudinal axis. Thus the location of the flat plate in the rectangular channel and the approaching flow field was unchanged. The experiments with the plate in this position were performed at fixed freestream velocity, pressure and temperature while the plate surface temperature was allowed to vary. The results could thus be directly compared to some of experiments performed with the heated surface facing upwards.

2. Optical Bench Operation

High speed movies and still photographs were taken at several conditions of bulk temperature, pressure, velocity and heat transfer rate in order to determine the appearance of the heated boundary layer in the neighbourhood of the critical point. The bulk conditions for which it was deemed desirable to have photographs or movies were determined from the heat transfer measurements described in part B1 of this Chapter.

The bulk fluid conditions and heat transfer rates were first adjusted to reproduce the heated flow field to be photographed. The image of the flow field on the film plane of either the still or motion camera was adjusted for position, focus and color contrast. A light hood was then placed over the optical bench to screen all light from the camera except that from the optical bench itself. The pressure, temperature, heat transfer and flow rate were then recorded as the film was exposed. The motion pictures were taken at the maximum framing speed of the camera, about 8,000 frames per second, while the still photographs were taken with an exposure time of 25 microseconds. The high framing speed and short exposure times were found necessary in order to sufficiently slow down the motion of the image on the film plane.

3. Hot Wire Operation

Hot wire studies of the turbulence level in the heated boundary layer were made for a few cases of bulk conditions. The freestream pressure, temperature and velocity were held fixed while the plate temperature was varied, and turbulence measurements were taken at each value of plate temperature.

The hot wire was placed into position in the flow channel after the heat transfer rate measurements of part B1 were completed. The bulk temperature and pressure were brought to their desired values and the cold resistance of the hot wire probe measured. The hot wire set was then adjusted to maintain a hot resistance 10% higher than the cold resistance. This produced approximately a 115°F. temperature differential between the wire and the freestream fluid. Readings were made of the mean wire current, the root mean square fluctuation from the mean wire current, the freestream velocity and bulk conditions. Current was then passed through the plate, raising its surface temperature and creating a heated boundary layer so that the hot wire probe becomes situated in a higher bulk temperature flow. The new cold resistance of the probe was then measured, its hot resistance set to be

10% higher, and measurements of the new turbulence level recorded. Thus the temperature difference between the wire and the immediately surrounding fluid was constant for all turbulence readings.

An additional experiment was performed in order to determine the hot wire response at various bulk fluid temperatures. The plate current was shut off and the freestream fluid pressure and velocity maintained at the same values as in the turbulence measurements performed with heat transfer. The freestream fluid temperature was then slowly varied and the mean wire current and its fluctuation recorded. The hot wire probe was thus "calibrated" for the changing bulk fluid temperature effect.

C. Test Conditions

The test conditions were selected so that at supercritical pressures, the freestream and wall temperatures varied uniformly from below to above the pseudocritical temperature. Thus in some cases both wall and freestream temperature were below the pseudocritical, in others both were above, while in still others the wall and freestream temperature "straddled" the pseudocritical.

The series of tests having fixed freestream velocity, temperature and pressure were conducted at pressures of 1,100 and 1,200 psia, with bulk temperatures of 75, 85, 95, and 105°F. at each pressure. Freestream velocities of 1.5, 1.0, and 0.5 ft./sec. were investigated at temperatures of 75 and 85°F. for both 1,100 and 1,200 psia, while freestream velocities of 1.5 and 1.0 ft./sec. were studied at 95 and 105°F. for both 1,100 and 1,200 psia. Additional tests performed were; 1,100 psia at freestream temperatures of 75 and 85°F. with a velocity of 0.2 ft./sec.; 1,200 psia at 95°F. and 0.5 ft./sec., and 75°F. and 0.2 ft./sec.

In order to compare subcritical with supercritical heat transfer, tests were also conducted at freestream conditions of 1,050 psia and 75°F. with velocities of 1.5, 1.0, 0.5, and 0.2 ft./sec.

Measurements with the heated surface facing downwards were conducted with freestream conditions of 75°F. and 1.5 ft./sec. for both 1,100 and 1,050 psia.

The second sequence of tests at fixed pressure, velocity and heat transfer rate with varying freestream temperature were performed only at 1,100 psia and 1.5 ft./sec. The freestream temperature was varied from 60 to 110°F., with fixed heat transfer rates of 3,000, 4,400, 6,600 and 23,000 BTU/hr $ft^2$. The tests with the heated surface facing down covered the same conditions as above, but only heat transfer rates of 4,400 and 23,000 BTU/hr $ft^2$ were investigated.

High speed movies of the heated boundary layer were taken at pressures of 1,100 and 1,050 psia, with a freestream velocity of 1.5 ft./sec. About 20 different conditions of wall and freestream temperature were photographed, the wall temperature ranging from 80 to 400°F. and the freestream temperature from 75 to 125°F. Approximately the same conditions were also photographed with the heated plate facing downwards.

The hot wire studies were performed at freestream conditions of 75°F. and 1.5 ft./sec. for both 1,100 and 1,050 psia. The wall

temperature ranged approximately from 76 to 270°F. for both pressures. Turbulence levels with no heat transfer and varying bulk temperature were measured at 1,100 psia and 1.5 ft./sec., with a temperature range of 75 to 100°F.

# VI. EXPERIMENTAL RESULTS

## A. Heat Transfer Measurements

A turbulent boundary layer was observed to exist over the entire flat plate, except for a short laminar section near the leading edge. The actual point of transition on the plate was quite sensitive to bulk conditions and surface temperature, but for the test conditions reported here it was always within 2.0" of the leading edge. The transition point was easily detected by visual means, and can be seen in Figure 15. Both thermocouples employed for measuring surface temperature were always adjacent to a turbulent boundary layer, and thus lead to similar heat transfer results (except for a length-scaling factor due to their different locations). For the purposes of this investigation only the results of one thermocouple need be considered, and all references to plate temperature will be for the thermocouple located farthest downstream of the leading edge.

The results of heat transfer rate and surface temperature measurements at the downstream thermocouple are presented graphically in Figures 16 to 26. The heat transfer coefficients were also computed for these tests, and are displayed in Figures 27 to 39.

1. Heat Transfer Variation with Surface Temperature

The results of the heat transfer measurements taken with constant freestream and varying surface temperature were quite similar whenever the freestream temperature was below the pseudo-critical, that is, when the freestream fluid was in the liquid-like region. The heat transfer coefficient was observed to increase with increasing surface temperature, reaching a maximum when the surface temperature was very near the pseudocritical. Further increases in surface temperature above the pseudocritical resulted in a decreasing heat transfer coefficient. The actual magnitude of the peak heat transfer coefficient was observed to depend on free-stream pressure, temperature and velocity. Pressures nearest to the critical exhibited the highest heat transfer coefficients, while at any fixed pressure the heat transfer coefficients increased as the freestream temperature approached the pseudocritical. Increases in freestream velocity also produced increases in the heat transfer coefficient.

These features are shown graphically in Figures 27 to 35. At 1,100 psia and 85°F., the heat transfer coefficient rises sharply to a peak of 985 BTU/hr $ft^2$°F. at $T_w = 91$°F. with $V_o = 1.5$ ft./sec., then drops off rapidly to about one half this value as the surface

temperature increases to 100°F. above the freestream. At 1,100 psia and 75°F. however, the peak in heat transfer coefficient is not quite as sharp, and only reaches a maximum of 710 BTU/hr $ft^2$°F.

In a similar manner, at 1,200 psia and 95°F., the heat transfer coefficient increases to a peak of 1,060 BTU/hr $ft^2$°F., then drops rapidly to about one quarter of this value when the temperature difference increases to 270°F. At freestream temperatures of 85 and 75°F. however, the peak heat transfer coefficient is somewhat reduced, and the h versus $T_w$-$T_o$ curve is flatter.

It is important to note that although the heat transfer coefficient exhibits peak values, the actual heat transfer rate increased monotonically with increasing surface temperature. Figure 23 shows that at 1,200 psia and 95°F., the heat transfer rate increases uniformly with increasing surface temperature, reaching a value of 2,700 BTU/hr $ft^2$ when the surface is at the pseudocritical temperature. The heat transfer rate continues to increase smoothly with increasing surface temperature, although less rapidly, until a value of 77,000 BTU/hr $ft^2$ is reached at $T_w$-$T_o$ = 270°F.

At freestream temperatures above the pseudocritical, when the freestream fluid is in the vapor-like region, the experimental

results for constant freestream temperature and pressure were also similar to each other. As the surface temperature was increased the heat transfer coefficient decreased slowly, with no peaks appearing as in the case of liquid-like freestream fluid. The heat transfer coefficients were much lower than with liquid-like freestream fluids. Figures 29, 30, and 35 show that the heat transfer coefficient varies only slightly with freestream pressure and temperature. At 1,100 psia and 105°F., h decreases from 280 BTU/hr $ft^2$°F. at low temperature differences to about 130 BTU/hr $ft^2$°F. as the wall temperature approaches 400°F. The heat transfer rate increased monotonically with temperature difference as in the case of liquid-like freestream fluids. Figures 18, 19, and 24 show that virtually a linear relationship exists between log Q and log $(T_w - T_o)$ for all bulk conditions and freestream velocities when the fluid is in the vapor-like region.

With freestream fluids below the critical pressure, the familiar regimes of nucleate, partial and complete film boiling were identified. Figure 25 shows the heat transfer rate as a function of temperature difference at 1,050 psia and 75°F. Peak nucleate heat flux was about 18,500 BTU/hr $ft^2$, and temperature difference at the onset of stable film boiling was 152°F. for a freestream velocity

of 1.5 ft./sec. The heat transfer coefficient for this situation is shown in Figure 36. At the onset of nucleation, the heat transfer coefficient rises sharply to a peak value of 1,760 BTU/hr $ft^2$°F., then drops to one fifth this value at the onset of stable film boiling.

2. Heat Transfer Variation with Freestream Temperature

The heat transfer coefficient as a function of freestream temperature at 1,100 psia and a velocity of 1.5 ft./sec. is shown in Figure 38. For freestream temperatures below the pseudo-critical, the heat transfer coefficient was extremely dependent on heat transfer rate (or equivalently on surface temperature). Very large heat transfer coefficients were observed with the freestream slightly below the pseudocritical temperature, provided the heat transfer rate was adjusted so that the surface was just slightly above the pseudocritical temperature. Figure 38 shows that with a heat transfer rate of 6,600 BTU/hr $ft^2$ at $T_o = 75°F.$ ($T_w = 83.2°F.$), the heat transfer coefficient is 800 BTU/hr $ft^2°F.$ At $T_o = 86.3°F.$ the surface reaches the pseudocritical temperature, and the heat transfer coefficient rises to approximately 1,520 BTU/hr $ft^2°F.$ At $T_o = 88.4°F.$, the surface temperature is 92.4°F., and a peak heat transfer coefficient of 1,650 BTU/hr $ft^2°F.$ is reached.

If the freestream temperature was increased further, the fluid exceeded the pseudocritical temperature and entered the vapor-like region, and a sharp decrease in heat transfer coefficient occured. Figure 38 shows that as the freestream temperature increases from 89 to 91°F. the heat transfer coefficient drops by almost a factor

of 5.

Similar dependence on freestream temperature was observed at low heat transfer rates, although the variations are not as extreme. However at a heat transfer rate of 26,600 BTU/hr $ft^2$ the surface temperature was always well above the pseudocritical for the entire range of freestream temperatures investigated. No discernable peak in heat transfer coefficient occured, and heat transfer coefficients were considerably reduced from the lower heat transfer rate values.

3. Effect of Direction of Gravity

Experimental measurements of heat transfer rate and heat transfer coefficient as a function of temperature difference for the inverted plate are shown in Figures 20 and 31 at 1,100 psia and 75°F., with a freestream velocity of 1.5 ft./sec. Also shown in these Figures (dashed line) are the corresponding values for the heated surface facing upwards.

For surface temperatures below the pseudocritical temperature, the heat transfer coefficient was not significantly altered by inverting the plate. Thus as the surface temperature increased up to the pseudocritical, the heat transfer coefficient also rose, reaching a peak with the surface slightly below the pseudocritical temperature. However at surface temperatures above the pseudocritical, the heat transfer coefficient for the downward-facing heated surface dropped very rapidly, and at $T_w - T_o = 100°F.$ was only one half that of the corresponding upward facing surface.

The effect of freestream temperature on the heat transfer coefficient with the inverted surface may be seen in Figure 39. At a heat transfer rate of 4,400 BTU/hr $ft^2$ body forces do not affect the heat transfer coefficient for freestream temperatures below 84°F. Above 84°F. the surface temperature exceeds the pseudocritical,

and although the heat transfer coefficient continues to rise and reaches a peak, the peak is somewhat smaller than for the upward-facing surface. At a freestream temperature of 89°F., the peak heat transfer coefficient is 1,200 BTU/hr $ft^2$°F., compared with 1,600 BTU/hr $ft^2$°F. for the upward-facing surface. When the freestream temperature is increased above the pseudocritical, the heat transfer coefficient drops abruptly and is apparently unaffected by body forces. At a heat transfer rate of 26,600 BTU/hr $ft^2$, the surface temperature is above the pseudocritical for all freestream temperature shown, and the heat transfer coefficient is only about one half that of the upward-facing surface.

## B. Flow Field Observations

Single frames have been selected from each of the high speed movies taken of the heated flow field, and the most pertinent of these are reproduced in Figures 43 through 51. As stated in Chapter IV, Section E, green regions are to be interpreted qualitatively as the cold freestream fluid. Subsequent warmer regions are yellow and red, respectively. Extremely large changes in temperature deflect the light completely out of the field of the second schlieren lens, and thus appear black. The freestream fluid is moving from left to right, and the heated flat plate is the horizontal black band at the bottom of the photographs.

Figures 43 to 46 show the heated turbulent boundary layer at freestream conditions of 1,100 psia and 75°F. (liquid-like region), and a freestream velocity of 1.5 ft./sec. These Figures form a sequence in which the surface temperature is increasing, and the actual heat transfer measurements for the flow are those shown in Figure 27. At low heat transfer rates, the surface temperature is below the pseudocritical and the flow appears to be substantially that of a constant property fluid. As the surface temperature increases to 83.9°F. (Figure 44), a slight amount of fluid motion normal to the

heated surface begins to appear in the region close to the plate. By studying the time development of the flow with movies, it appears that short streams of warm fluid rise upwards and diffuse into the colder freestream fluid. However, except for these convection effects near the wall, the flow field still retains the basic characteristics of a turbulent forced convection flow field.

Figure 45 shows the flow field occurring near the peak heat transfer coefficient in Figure 27. The surface temperature is about 2°F. above the pseudocritical, so that the fluid near the plate is in the vapor-like region. The ratio of freestream to surface fluid density is approximately 2.5. In the outer portions of the boundary layer the flow does not exhibit any unusual effects and appears similar to normal turbulent forced convection. However, near the plate tiny black spots, indicating regions of rapid change in density, begin to appear. These "pockets" or clusters of different density fluid rise from the region next to the plate and rapidly diffuse into the colder upper portions of the boundary layer. If the surface temperature is increased to 135°F., these regions of differing density grow in size, as shown in Figure 46. Free convective motion becomes superimposed on the basic forced flow through a larger portion of the boundary layer. The edges of the density pockets are somewhat

blurred, indicating a gradual rather than sharp change across their boundaries. It should be noted that although significant mixing of the warmer "pockets" and cooler freestream fluid appears to occur in the upper regions of the boundary layer, the actual heat transfer coefficient recorded was considerably less than that for the more conventional flow shown in Figure 44.

The changes in flow field occurring with changing freestream temperature are shown in Figures 43, and 47 to 49 for a constant heat transfer rate of 6,600 BTU/hr $ft^2$. Figure 43 represents the flow field when both freestream and surface temperature are below the pseudocritical, and corresponds to the low heat transfer coefficient region at the left of the peak shown in Figure 38. The flow field resembles that of a constant property heated boundary layer, except for a small region next to the surface in which some free convection is also present (see page 77).

Figure 47 shows the flow field occurring when the freestream temperature was raised to 87.8°F., causing the heat transfer coefficient to reach its peak value. Although the ratio of freestream to surface density is about 2, property changes take place gradually through the boundary layer, as indicated by the lack of sharpness in the darker regions next to the surface. The entire boundary

layer is significantly affected by free convection, and vertical mixing between the freestream and surface region takes place freely. No appreciable "pockets" of different density fluid can be observed within the flow.

Increasing the freestream temperature further to 105.9°F. causes the heat transfer coefficient to drop sharply. The entire fluid is in the vapor-like region, with relatively slight property changes throughout the boundary layer. The flow field shown in Figure 48, is apparently quite similar to a normal constant property turbulent forced convection flow field.

An additional photograph with the freestream fluid in the vapor-like region, but at a larger temperature differential, is shown in Figure 49. The freestream temperature is 125°F. and the surface temperature 400°F., so that the freestream to surface density ratio is about 2.3. A few small "pockets" of hot fluid can be seen throughout the heated boundary layer, with some free convective motion superimposed on the basic forced flow.

Photographs of the flow field occurring in a subcritical fluid are shown in Figures 50 and 51. Figure 50 shows nucleate boiling at 1,050 psia and 75°F. Motion picture studies indicated that next to the heated surface very strong stirring action due to bubbles

occurring. Figure 51 shows the flow field during stable film boiling. The vapor film itself can not be seen, but large vapor clusters which break away and rise into the freestream fluid appear as the large black spots.

C. Hot Wire Measurements

The results of turbulence measurements at various temperature differences between the freestream fluid and heated surface are presented in Figures 40 to 42. The actual quantity representing the turbulence level was arbitrarily taken as four times the root mean square of the fluctuating part of the wire current divided by the mean steady wire current, in order to compare with usual measurements in homogeneous flows (see Appendix E).

Figure 40 shows that the turbulence level at 1,100 psia and 75°F. is relatively unchanged for surface temperatures up to the pseudocritical. As the surface temperature increases beyond the pseudocritical, the turbulence level begins to slowly increase until at a maximum temperature difference of 136°F. it is approximately 3 times the unheated plate level. No significant increase was noted when the surface temperature was at the pseudocritical, where the heat transfer coefficient reaches its peak. Oscilloscope records of the fluctuating components of the wire current are shown in Figures 52 to 54. At surface temperatures below the pseudocritical the fluctuations are virtually random in time, and no dominant turbulent eddy size can be detected in the flow. When the surface

temperature is sufficiently above the pseudocritical however, fluctuations of about 2-3 milliseconds duration can be recognized in the signal. Hence corresponding sizes of turbulent eddies must be contained in the flow in the region of the probe at the higher heat transfer rates.

Turbulence levels recorded in a subcritical fluid are shown in Figure 41. At the onset of nucleate boiling, a slight but definite increase in turbulence occurs. Turbulence levels remain constant until the onset of stable film boiling, after which increases in surface temperature are accompanied by a slow rise in the turbulence level. Oscilloscope records, shown in Figures 55 to 57, also indicate that fluctuations of approximately 2 milliseconds occur at high heat transfer rates, as for the supercritical fluid.

The effect of freestream temperature on the hot wire signal in a constant velocity flow with no plate heating is shown in Figure 42. Below the pseudocritical temperature the wire response is fairly insensitive to changes in freestream temperature. As the freestream temperature rises above the pseudocritical, the turbulence levels gradually decrease. The fact that no anomalous variations occur throughout the freestream temperature range means that wire current changes represent changes in freestream conditions only,

and that no unusual heat transfer phenomena occur on the wire itself.

# VII. DISCUSSION OF RESULTS

## A. Heat Transfer Mechanisms

The heat transfer results described in the previous Chapter indicate that heat transfer coefficients for fluids near the critical point are extremely dependent on freestream and surface temperature, and their relative location with respect to the pseudocritical temperature. In addition, the visual results show that somewhat different flow fields can occur at various heat transfer rates because of the large variation in fluid properties throughout the heated boundary layer.

The variation of heat transfer coefficient found to exist when freestream and surface temperature change throughout the critical region is quite similar to that found in several previous forced convection studies. For example in a liquid-like freestream fluid, a peak heat transfer coefficient was obtained when the surface temperature was near the pseudocritical. This type of peak was also found in reference (43). When the freestream temperature was increased while the heat transfer rate remained fixed, a peak in the heat transfer coefficient was obtained at a freestream temperature slightly below the pseudocritical. Wood and Smith (40) have also

observed this type of peak. The agreement between results of past and the present study tends to verify the occurrence of large peaks in heat transfer coefficient for fluids in the vicinity of the critical point. In addition this agreement also inspires confidence in the experimental approach and techniques used for the present investigation.

Comparing the photographs of the flow field occurring at the peak heat transfer coefficients with those where the fluid acted essentially as a constant property fluid, it can be seen that although differences exist in the detailed nature of the flow, the basic flow pattern resembles normal turbulent forced convection for all the regions investigated in this study. In particular, no significant break up of the normal forced convection pattern could be observed when the heat transfer coefficient reached its peak. The hot wire studies also showed that the turbulence levels occurring at the peak heat transfer coefficient were not significantly different from those occurring in normal turbulent flows. Thus both the photographs of the flow field and the hot wire studies seem to indicate that the sharp peaks in heat transfer coefficient recorded in this study are principally due to the large thermodynamic and transport properties of fluids in the critical region, and not because of the occurrence of any new or unusual heat transfer mechanism as has been proposed.

It should be stressed that although the basic heat transfer mechanism for flow of supercritical fluids over heated flat surfaces is similar to normal forced convection, this need not be the case for other heater geometries. In contrast to the present results, the experiments of Knapp (20) show that a discontinuous change in heat transfer rate may occur during natural convection from a heated wire under certain conditions, and is accompanied by a complete disruption of the flow pattern existing prior to the change. However in the present study no such change from the basic forced convection flow pattern was observed, and the heat transfer rate showed no abrupt increase or decrease under any circumstance. The investigation of this aspect was one of the main purposes of the present study.

Although normal forced convection seems to be the basic mechanism responsible for heat transfer in flat plate or pipe flows of supercritical fluids, the detailed nature of the turbulent flow patterns observed showed some variations with freestream and surface temperatures. These variations in flow patterns apparently played a secondary role in determining heat transfer, but nonetheless resulted in flow patterns which appeared slightly different from "normal" turbulence. A detailed discussion of the forced convection flow fields will be given in the following Sections.

B. Turbulent Forced Convection Flow Field

The photographs of the heated flow field taken at various conditions of freestream fluid and surface temperature seem to indicate that in some instances, secondary flows are superimposed on the basic turbulent flow pattern. As was shown in the foregoing Section, these secondary flows do not drastically affect the heat transfer results. Although detailed studies or comparisons of actual turbulent spectra or velocity fluctuation correlations were not performed, the flows can nonetheless be identified as slightly different from the type of turbulent flow field seen in a constant property fluid. The following comments are given for completeness, but they can, of course, only be qualitative in nature.

The condition for which the freestream fluid is in a liquid-like state will be considered first. Some free convection appears to be superimposed on the basic forced flow field near the heated surface when the surface temperature is in the vicinity of the pseudocritical temperature (Figure 44). The free convection has very little effect on the heat transfer coefficient and turbulence levels in the flow. Again it is stressed that although the heat transfer coefficient reaches a peak for surface temperatures near the pseudo-

critical temperature, the principal cause of the peak appears to be the large thermodynamic and transport properties of the fluid in this region, and not any change in the basic forced convection heat transfer mechanism.

When the surface temperature was increased above the pseudo-critical temperature in a liquid-like freestream fluid, small "pockets" or clusters of lower density, hotter fluid were observed in the vicinity of the heated surface (Figure 45). These "pockets" might be formed by turbulent temperature fluctuations occurring at the location in the heated boundary layer where the fluid temperature equals the pseudo-critical temperature. At this location, even small fluctuations in temperature may produce very large changes in fluid properties. These "pockets" of hot fluid diffuse rapidly into the freestream fluid and induce free convective effects and turbulent mixing at the location of this "interface" between the vapor-like fluid on the plate and the liquid-like freestream fluid. However the vapor-like fluid right on the surface is apparently undisturbed by the action of these "pockets", so that the heat transfer mechanism through the vapor-like layer is still a basic forced convection type of mechanism. Because of the poor thermal transport properties of the vapor-like fluid, the heat transfer coefficients are much lower than for surface temperatures

near the pseudocritical temperature.

The interpretation of the dark spots appearing in the photographs as "pockets" or clusters of hot fluid is given additional support by examining the oscilloscope traces of the wire current fluctuations in this region. As described in Chapter VI, a definite "time scale" in the fluctuations not present in normal turbulence can be detected, (see Figure 54). Estimating the time span of these fluctuations as from 2 to 3 milliseconds, and a freestream velocity in the region of the wire of approximately 1 ft./sec., the physical size of these fluctuations in the flow should be about 0.02 to 0.03 inches. The "pockets" appearing in the photographs of the flow field are actually of the same order of magnitude as this estimate.

The flow for which the freestream fluid is in a vapor-like state will be considered next. The properties now change gradually through the heated boundary layer, rather than abruptly as at the location of the pseudocritical temperature in the case of a liquid-like fluid mentioned above. However at very high heat transfer rates the property change may be quite large, and the flow field photographs still show some "pockets" or clusters of different density fluid near the heated surface, (see Figure 49). These "pockets" are not as distinct as those appearing in a liquid-like fluid, and do not appear

to alter the basic turbulent flow pattern in any way.

The largest heat transfer coefficients measured in the present study occured with freestream fluid temperatures 1-2°F. below the pseudocritical and heated surface temperatures 1-2°F. above the pseudocritical. The photographs of the heated flow field (see Figure 47) indicate a certain amount of secondary free convective flow superimposed on the basic forced flow pattern. This free convection produces about a 30% increase in the heat transfer coefficient when compared with the heated surface facing downwards (see Figure 39). However except for this secondary flow, the basic heat transfer mechanism is apparently that of forced convection, and the turbulent "pockets" of hot fluid described above were not observed. Again the large peaks recorded in the heat transfer coefficient must be due simply to the large values of thermal transport properties of the fluid occuring near the pseudocritical temperature.

The experiments of Fritsch and Grosh (11), and Larson and Schoenhals (14) were conducted with very small temperature differences in a fluid slightly below as well as slightly above the pseudocritical temperature. They concluded that the heat transfer coefficient variation could be accounted for by considering the property variations within the fluid, and that no unusual heat transfer

mechanismoccurred inthe vicinity of the critical point. The flow field observations in the present study essentially confirm these conclusions for the case of a fluid very near the pseudocritical temperature with small temperature differences. It should also be pointed out that even though heat transfer coefficients are large, the corresponding small temperature differences still result in fairly low heat transfer rates.

## C. The Analogy with Boiling Heat Transfer

Some of the heat transfer results for liquid-like supercritical fluids bear a resemblance to certain regions in subcritical or boiling heat transfer. Since actual bubbles can not form in a supercritical fluid, the heat transfer mechanisms are not perfectly analagous. Nonetheless, useful ideas about the heat transfer process in a supercritical fluid can be gained by exploiting the similarity to subcritical heat transfer.

Before considering the analogy between subcritical and supercritical heat transfer let us first examine the various regimes of normal boiling, and how they change as the pressure is increased above the critical pressure. When both freestream and surface temperature are below the saturation temperature in a subcritical fluid, heat is transferred by a normal convection process. If the surface is increased above the saturation temperature, vapor bubbles form at various locations on the heated surface. The formation of bubbles marks the beginning of the nucleate boiling regime, and is accompanied by very large increases in heat removed from the heater surface with only very small further increases in surface temperature. The initial portion of nucleate boiling, called

the isolated bubble regime, is characterized by the fact that the bubbles which grow and rise off the surface produce a strong convective motion in the heated liquid. This strong convective motion is very similar to turbulent natural convection (60). It is this natural convection, not the actual latent heat absorbed by the bubble while on the surface, that is responsible for the major portion of heat transported in this region. Further increases in heat transfer rate cause the isolated bubbles to coalesce into vapor columns, so that in the latter stages of nucleate boiling the latent heat transported by the vapor columns becomes the principal heat transfer mechanism. The rising vapor columns interfere with the colder fluid returning to the heated surface, eventually become unstable and collapse into vapor patches on the heated surface. This collapse limits the heat removal from the surface by nucleate boiling and is sometimes called "peak nucleate flux".

The formation of vapor patches on the heater surface causes the heat transfer rate to decrease because of the poorer thermal conductivity of the vapor phase. As the heated surface temperature is increased, the vapor patches grow and eventually form a vapor film over the surface. The liquid-vapor film interface is always hydrodynamically unstable and small disturbances cause it to distort

and rupture into large clusters of vapor which enter the liquid. However the heat transfer rate is large enough to continuously generate and maintain this vapor film, so that liquid which moves toward the heated surface to replace the broken-off vapor clusters is always evaporated before actually reaching the surface. This heat transfer region is often called "stable" film boiling because of the continuous vapor blanket, even though the vapor flow in itself may be laminar or turbulent, and the liquid-like vapor film interface is constantly breaking up. The actual heat transfer coefficient in this region is governed by the vapor film on the heated surface.

If the pressure is increased towards the critical, the heat flux at onset of nucleate boiling, the peak nucleate heat flux, and heat flux at the onset of stable film boiling all converge. Recent experiments indicate that at the critical pressure they become equal (61). Thus at supercritical pressures, the entire nucleate and partial film boiling regions are not expected and indeed are not observed to occur. The heat flux versus temperature difference curves for a supercritical fluid have a smooth transition between the lower portions representing the convection region and the upper portions representing stable film boiling. In a manner of speaking, the heat transfer mechanism in a supercritical fluid proceeds directly from normal convection to

stable film boiling (62).

Re-examining the heat transfer mechanisms observed with liquid-like supercritical fluids (Section B of this Chapter), it was seen that for both freestream and surface temperature below the pseudocritical temperature, heat is transferred by normal turbulent forced convection which is directly analagous to subcritical turbulent forced convection. When the surface was raised above the pseudo-critical temperature, "pockets" of warmer fluid having much lower density than the liquid-like freestream fluid were observed in the heated boundary layer. These "pockets" appeared near the heated surface, and diffused rapidly into the colder freestream fluid. The actual heat transfer coefficient is reduced in this region due to the poor thermal transport properties of the fluid on the heated surface, which is apparently undisturbed by these pockets. The fluid next to the heated surface can thus be considered as a "pseudo-vapor film". The "pockets" of hot fluid which rise from this pseudo-vapor film act in a manner similar to the vapor bubbles leaving the liquid-vapor interface in stable film boiling. Both the supercritical "pockets" and subcritical bubbles induce free convection and turbulent energy exchange in the region of the "interface", but the heat transfer coef-ficients in both cases are still governed by the insulating vapor or

pseudo-vapor film on the heated surface. Hence the heat transfer mechanism occurring in a liquid-like supercritical fluid when the surface is far above the pseudocritical temperature may be properly described as "pseudo-film boiling".

Finally it should be noted that the heat transfer mechanism occurring when the surface is very near the pseudocritical temperature is not strictly analagous to either the forced convection preceding or "pseudo-film boiling" following it, but may well be a complicated interaction of the two.

## D. Stability of the Heated Flow Field

In Chapter II it was stated Goldmann (26) has proposed that sudden large increases in heat transfer rates recorded when the freestream and surface straddle the pseudocritical temperature may be explained by hydrodynamic stability arguments. He visualized the "interface" between the liquid-like freestream and vapor-like surface fluid as becoming "wavy" under certain conditions of heat transfer and fluid property variations, leading to a "break-up" of the vapor film. The stability and break-up criterion for the film can be determined with arguments similar to those used in such "parallel flows" as boundary layers or stratified flows.

The stability of parallel flows to infinitesmal disturbances is known to be greatly affected by curvature of the velocity profile, viscous amplification of the disturbance, variations in fluid properties, and body forces such as gravity (63, 64). A very rough classification of various types of stability problems in terms of these factors is shown in Table 2. The entries in the Table indicate authors of successful approaches to particular problems.

The broad class of stability problems is quiescent fluids that may or may not include property variations, viscous effects,

and interfacial accelerations between layered media are known as Rayleigh-Taylor problems because of the early works of Rayleigh (65) and Taylor (66). An instability different from the Rayleigh-Taylor type can occur when either a continuously stratified or a layered media has a constant shearing motion imposed on it (either a linear or discontinuous velocity profile). These instabilities are called Kelvin-Helmholtz instabilities. The actual works of Rayleigh, Taylor, Kelvin and Helmholtz neglected viscous effects, and failed to predict the observed instability in flows having smoothly curved velocity profiles such as boundary-layer flows. Tollmien (83) and later Schlichting (84) showed that viscosity could actually amplify disturbances of certain wave length and thereby cause instability in boundary layer flows. The class of problem which encounters viscosity amplified waves is called Tollmien-Schlichting instability.

The classical stability problems outlined in Table 2 are concerned with initially laminar flows, and strictly speaking do not apply to flows which are already fully turbulent. However very recently, Betchov and Criminale (89) have shown that these classical methods can be directly applied to turbulent boundary layers as well. Visual and hot wire studies in both wakes and

boundary layers indicate the edges of the turbulence are well defined from the lower turbulence freestream flow (see Figure 15). The "interface" or "superlayer" between the fully turbulent boundary layer and low turbulence freestream exhibits a definite wavelength or "intermittency" factor (90). Betchov and Criminale equate the turbulent boundary layer to a laminar flow having variable viscosity (which corresponds to the turbulent eddy viscosity) and apply classical stability techniques to compute the stability of this "superlayer". Their results for disturbance wavelength and phase velocities provide acceptable agreement with those actually observed at the edge of the turbulent layer. More important for purposes of the present discussion, their results indicate that very little mutual interaction exists between the unstable superlayer and the normal laminar sublayer next to the surface, so that laminar sublayer "break-up" should not occur.

In the heated turbulent boundary layer of a supercritical fluid, an "interface" exists between the liquid-like and vapor-like fluid whenever the pseudocritical temperature occurs within the flow. This interface has actually been experimentally observed in vertical pipe flows by Wood and Smith (40). Following the reasoning of Betchov and Criminale, it may be possible to predict the stability

characteristics of this interface by the classical Kelvin-Helmholtz approach. As a starting point one would assume a steady-state velocity and temperature field, and consider the properties of the fluid as functions of height from the wall only (stratified flow). In this case the energy disturbance equation is uncoupled from the problem and only a modified Orr-Sommerfeld equation need be considered. The classical results indicate that regardless of viscosity variation or velocity profile, the interface is unstable for heavier fluids above lighter fluids. Thus once the surface temperature surpasses the pseudocritical, there will always be some unstable wavelengths present in the flow. However since disturbances for any problem are constrained to die out on the surface, it seems reasonable to conclude that the instability of the proposed interface in a supercritical fluid does not affect the laminar sublayer, much as the laminar sublayer was not affected in the Betchov-Criminale study. These arguments seem to indicate that "break-up" of the vapor film, resulting in sharp improvements in heat transfer, does not occur in parallel flow for any surface temperature above the pseudocritical, although the "interface" is always unstable for these surface temperatures. The experimental results of the present study confirm this supposition.

It is interesting to note that the analogy to film boiling may also extend to the hydrodynamic stability problem discussed above. Berenson (91) considered the stability of the vapor-liquid interface occurring in film boiling using the classical Rayleigh-Taylor and Kelvin-Helmholtz approach. His results indicate that the spacing between bubbles departing from the interface at the onset of stable film boiling is exactly the same as the most unstable wavelength predicted by analysis. Even though the liquid-vapor interface is always unstable after the onset of film boiling, the actual film itself is stable in the sense that it does not "break-up". This is precisely the nature of the "pseudo-film" instability described for supercritical fluids. One might also expect that with sufficient information on the variation of fluid properties, eddy viscosity and "film" thickness in a supercritical fluid, some estimate of the size of "pockets" appearing in a supercritical fluid could be made before hand by computing the corresponding disturbance wavelengths.

It should be emphasized that although no sharp changes in heat transfer occur because of hydrodynamic stability effects for flat plate or pipe flows, such phenomena can actually occur in other geometries. The results of Knapp (20) show that sharp changes in heat transfer can occur under certain conditions of fluid properties

and heat transfer rate during natural convection from a horizontal cylinder. The improvements in heat transfer are seemingly caused by an instability in the heated flow field. This instability is apparently unrelated to any of the types discussed above for flat plate geometries, and more closely resembles three-dimensional vorticies which sometimes occur in curved flows. Further studies are required on stability effects for such geometries.

## E. Comments on Previous Investigations

### 1. Experimental Studies

Many of the previous studies listed in Chapter II cite unusual phenomena such as pressure fluctuations, "singing noises", and sudden large departure in heat transfer coefficient. No such anomalies were observed in the present investigation, nevertheless it is desirable to discuss these unusual effects in light of the results of this study.

Some of the pressure fluctuations in forced and natural flow loops have been definitely identified as travelling simple acoustic waves (5, 8) or fluctuations driven by certain portions of the experimental apparatus acting as acoustic resonators (28), and need not be considered further. The results of Chalfant (22), and Cornelius and Parker (29), both obtained during forced convection heating in loop geometries, show that the frequencies of fluctuation in heat transfer coefficient and pressure did not correspond to any simple acoustic modes.

To account for the unusual results of Chalfant, Goldmann proposed the "boiling hypothesis" described in Chapter II. Cornelius and Parker have also cited Goldmann's proposal as the cause of

their unusual observations. The visual observations of the heated flow field presented in this study indicate that occurrence of "boiling", leading to improved heat transfer, does not seem to exist in flat plate or pipe flows. Moreover, it is entirely possible that modes of acoustic oscillation different from ordinary travelling waves may occur. Referring to the variation in speed of sound for $CO_2$ near the critical point (53), it may be seen that the acoustic velocity can decrease by a factor of 2 between a freestream at 80°F. and a heated surface of 85°F. in $CO_2$ at 1,100 psia. Such changes in acoustic velocity could produce complicated refractions and reflections of the sound waves within the heated layer, and may well result in the experimental apparatus exhibiting fluctuations far removed from a simple acoustic mode.

A second mechanism for driving pressure fluctuations was proposed by Hines and Wolf (27). They pointed out that because of the large variations in viscosity with temperature, small temperature fluctuations could well produce pressure fluctuations near the surface through a reversal in the direction of the pressure gradient. The discussion in Part D of this Chapter does not preclude this type of instability, rather, the results of Betchov and Criminale give some indication that such fluctuations actually exist. The present

investigation can in no way refute this proposal, so that viscosity variations may indeed result in the pressure oscillations.

The low frequency pressure fluctuations of Cornelius and Parker may actually have been triggered by still a third mechanism. The fluid used in their experiments (Freon-114) could apparently undergo chemical reactions in the vicinity of 600-700°F. and form "deposits" on the heater walls. Since some of their results reported for the low frequency fluctuations show wall temperatures as high as 530°F., it is quite possible that the reaction played some part in triggering the observed oscillations in wall temperature and fluid pressure.

2. Theoretical Studies

Perhaps the most applicable theoretical study of predicting heat transfer to turbulent flow of fluids near the critical point is that of Deissler (47). However, his method yields estimates of heat transfer as much as 40% too low when extreme straddling of the pseudocritical temperature occurs (see comparison in 43).

Based on the visual observations of the flow field in this study, two factors in Deissler's analysis may be cited as being poor approximations to the actual heat transfer mechanism. First, Deissler makes use of the eddy viscosity concept in order to integrate the equations for shear stress and heat transfer. The particular analytical expression used is taken from one successfully employed in turbulent flow of constant property fluids with no heat transfer. Although no gross instability or break-up of the basic forced flow pattern was observed in this study, the photographs of the actual flow lead one to believe that significant changes in the structure of the turbulence may occur when the freestream and heated surface straddle the pseudocritical temperature. A better understanding of the eddy viscosity variations, accounting for the observed turbulent interaction, may well improve the accuracy of the method.

Secondly, Deissler's method is not designed to take into

account the effects of body forces on the flow fields. Some steps to rectify this were proposed by Hsu and Smith (48) for vertical flows, however studies for horizontal and inclined surfaces would also be desirable. The experimental results of the present investigation indicate that reversal of the direction of gravity during heat transfer from a horizontal surface may change the heat transfer coefficient by 40% when the surface is sufficiently above the pseudocritical temperature. Thus gravity forces should not be ignored in any theoretical predictions of heat transfer coefficients even with fairly high Reynolds number flows.

# VIII. SUMMARY AND CONCLUSIONS

A series of experiments have been performed measuring heat transfer rates during forced convection from a flat plate to $CO_2$ in the region of its thermodynamic critical point. The majority of the tests were performed with freestream pressures slightly above the critical, and freestream temperatures both above and below the pseudocritical. The investigations conducted at supercritical pressures with temperatures below the pseudocritical included heat transfer rates sufficiently large so that the flat plate surface temperature exceeded the pseudocritical. The heated plate was in a horizontal position, and measurements were made with the heated surface facing both up and down. The effect of freestream temperature and velocity on the heat transfer rate was also measured.

In order to gain some information on the basic heat transfer mechanisms in supercritical fluids, photographs of the heated boundary layer were taken using a modified semi-focusing color schlieren apparatus. The photographs enable comparisons to be made between the flow fields occuring in a supercritical fluid and the flow fields when the fluid property variations are not as severe. Additional information about the flow field was obtained by measuring the turbulence levels present in the immediate vicinity of the

heated flat plate at various heat transfer rates and flow conditions. The measurements were performed using a hot wire anemometer located at a fixed position over the flat plate.

The experimental results indicate that at supercritical pressures the heat transfer coefficient is a sensitive function of freestream and surface temperature. With the freestream temperature at a fixed value below the pseudocritical temperature, and freestream pressure and velocity also constant, the heat transfer coefficient reached a peak value when the surface was at the pseudocritical temperature. When the surface temperature was either increased or decreased from the pseudocritical, the heat transfer coefficient decreased sharply. Nevertheless the actual heat transfer rate increased monotonically with increasing surface temperature for all values of surface temperature investigated.

When the freestream pressure, velocity and surface heat transfer rate were held constant, increasing the freestream from below to above the pseudocritical temperature produced a sharp peak in heat transfer coefficient when the freestream temperature was 1-2°F. below the pseudocritical temperature. This peak occurred when the heat transfer rate was such that the surface temperature exceeded the pseudocritical by 1-2°F.

Both the peaks associated with either freestream or surface temperature near the pseudocritical occured regardless of free-stream velocity, or whether the horizontal surface was facing up or down. Comparison of the photographs of the flow fields occurring at the peak heat transfer coefficients with those when the fluid had essentially constant properties show that no unusual flow is present at the locations of the peaks. Secondary free convective effects were observed to be superimposed on the basic forced flow patterns very near the heated surface, but the flow pattern resembled normal turbulent flow in all other respects. No increases in the turbulence level were recorded by the hot wire probe at the peak heat transfer coefficients, and a time trace of the fluctuations appeared similar to normal turbulence.

On the basis of the flow field observations and turbulence measurements, it is concluded that the peaks in heat transfer coefficient are caused by the rather large thermodynamic and transport properties of the fluid which occur near the critical point, and not by the occurrence of any new or unusual flow field or heat transfer mechanism.

When the freestream fluid was 10-15 °F. below the pseudo-critical temperature and at supercritical pressures, increasing the

surface above the pseudocritical temperature caused the heat transfer coefficient to drop sharply, and resulted in an unusual type of turbulent flow superimposed on the basic forced convection flow field. "Pockets" of hot, low density fluid were observed to form due to temperature fluctuations near the heated surface, rise from the surface, and rapidly diffuse into the cooler freestream fluid. The "pockets" of different density fluid do not have sharply defined edges, but could still be positively identified in the flow photographs and oscilloscope traces of the hot wire current fluctuation. The "pockets" of different density fluid and the resulting flow field are slightly different from the flow occurring in normal heated turbulent boundary layers. Heat transfer in this region is apparently analagous to the film boiling region occurring below the critical pressure. The "pseudo-film" of vapor-like fluid on the heated surface governs the heat transfer mechanism, and appears to blanket the surface for all temperatures above the pseudocritical. Hydrodynamic stability arguments lead one to believe that this film should not "break-up" or become unstable. The sharp changes in heat transfer coefficient previously reported for pipe flows in this region are apparently caused by mechanisms other than such a vapor-like film break-up.

The conclusion that the sharp peaks in heat transfer coef-

ficient for flat plate and pipe flows are due to fluid property variations, and not any unusual flow fields or new heat transfer mechanisms, does not preclude the occurance of unusual flows in other geometries. The observation of "bubbles", which result in improved heat transfer during natural convection from a horizontal cylinder, suggests that further studies on the nature of such bubbles and their possible occurrence in various other geometries and fluid flow situations are desireable.

The present study also indicates that further investigations of the velocity and temperature fluctuations near the heated surface in supercritical fluids are needed. In addition, direct observation of the laminar sub-layer in turbulent flow may suggest models for use in future theoretical predictions of shear stress and heat transfer rates in supercritical fluids.

# REFERENCES


1. Schmidt, E., E. Eckert, and U. Grigull, "Wärmetransport durch Flussigkeiten in der Nahe ihres kritischen Zustandes," Jb. Dtsch. Luft., Vol. 2, 53 (1939).

2. Schmidt, E., "Wärmetransport durch naturliche Konvektion in Stoffen bei kritischem Zustand," Int. J. Heat Mass Transf., Vol. 1, 92-101 (1960).

3. Hahne, E. W. P., "Wärmetransport durch naturliche Konvektion in Medien nahe ihrem kritischen Zustand," Int. J. Heat Mass Transf., Vol. 8, 481-497 (1965).

4. Friedrich, R., "Eine Gasturbine mit gekuhlten Schaufeln fur Gastemperaturen uber 1000°C," Brennst-Warmekr., Vol. 14, 368 (1962).

5. Boggs, J. P. and J. H. Holman, "Heat Transfer to Freon-12 Near the Critical State in a Natural Circulation Loop," J. of Heat Transf., Vol. 82, 221-226 (1960).

6. Van Putte, D. A. and R. J. Grosh, "Heat Transfer to Water in the Near-Critical Region," Tech. Rep. No. 4, Purdue University, ANL, Subcontract 31-109-38-704 (1960).

7. Harden, D. G. and J. H. Boggs, "Transient Flow Characteristics of a Natural Circulation Loop Operated in the Critical Region," Proc. Heat Trans. and Fl. Mech. Inst., Stanford University Press, 38-45 (1964).

8. Harden, D. G., "Transient Behavior of a Natural Circulation Loop Operating Near the Thermodynamic Critical Point," Argonne National Lab. Report, ANL-6710 (May 1963).

9. Walker, W. J. and D. G. Harden, "Heat-Driven Pressure and Flow Transients in the Supercritical Thermodynamic Region," ASME Paper No. 64-WA/HT-37 (1964).

10. Eckert, E. R. G. and H. A. Simon, "Laminar Free Convection in Carbon Dioxide Near its Critical Point," Int. J. Heat Mass Transf., Vol. 6, 681-690 (1963).

11. Fritsch, C. A. and R. J. Grosh, "Free Convective Heat Transfer to Supercritical Water Experimental Measurements," Trans. ASME, Vol. 85, Series C, 289-294 (1963).

12. Fritsch, C. A. and R. J. Grosh, "Free Convective Heat Transfer to a Supercritical Fluid," Proceedings of 1961 International Heat Transfer Conference, Part V, Paper 121, 1010-1016 (August 1961).

13. Brodowicz, K. and I. Bialokoz, "Free Convection Heat Transfer from a Vertical Plate to Freon-12 Near the Critical State," Archiwum Budowy Maszyn, Vol. 10, No. 4, 289 (1963).

14. Larson, J. R. and R. J. Schoenhals, "Turbulent Free Convection in Near Critical Water," ASME Paper 65-HT-57 (1965).

15. Doughty, D. L. and R. M. Drake, "Free Convection Heat Transfer from a Horizontal Right Circular Cylinder to Freon-12 Near the Critical State," Trans. ASME, Vol. 78, 1843-1850 (1956).

16. Bonilla, C. F. and L. A. Sigel, "High-Intensity Natural Convection Heat Transfer Near the Critical Point," Chem. Eng. Progr. Symp. Ser., Vol. 57, No. 32, 87-95 (1961).

17. Griffith, J. D. and R. H. Sabersky, "Convection in a Fluid at Supercritical Pressures," ARS Jour., Vol. 30, No. 3, 289-291 (1960).

18. Holt, V. E., "An Experimental Investigation of High-Flux Free Convection Heat Transfer to Water up to Near Critical Conditions," Argonne Nat. Lab., Rep. ANL 6400 (August 1961).

19. Graham, R. W., R. C. Hendricks, and R. C. Ehlers, "Analytical and Experimental Study of Pool Heating of Liquid Hydrogen over a Range of Accelerations," NASA TND-1883 (February 1965).

20. Knapp, K. K., Ph. D. Thesis, California Inst. of Technology, Pasadena, Calif. (September 1964).

21. Yamagata, K. et al, "Free Convective Heat Transfer to a Supercritical Fluid," (2nd. report) Technology Rept., Kyushu University, Vol. 37, No. 1, 47 (1964).

22. Chalfant, A. I., "Heat Transfer and Fluid Friction Experiments for the Supercritical Water Reactor," P. W. A. C. - 109, (June 1954).

23. Randall, D. G., "Some Heat Transfer and Fluid Friction Experiments with Supercritical Water," Reactor Heat Transfer Conference, (November 1956).

24. Goldmann, K., "Heat Transfer to Supercritical Water at 5000 psi Flowing at High Mass Flow Rates through Round Tubes," Proceedings of 1961 International Heat Transfer Conference, Part III, Paper 66, 561-568 (August 1961).

25. Goldmann, K., "Heat Transfer to Supercritical Water and Other Fluids with Temperature-Dependent Properties," AIChE Chem. Eng. Progress Symposium Series, Nuclear Engineering, Part 1, Vol. 50, No. 11, 105-113 (1954).

26. Goldmann, K., "Special Heat Transfer Phenomena for Supercritical Fluids," NDA 2-31, (November 1956).

27. Hines, W. S. and H. Wolf, "Heat Transfer Vibrations with Hydrocarbon Fluids at Supercritical Pressures and Temperatures," presented at A. R. S. Propellants, Combustion and Liquid Rockets Conference, (April 1961).

28. Thurston, R. S., "Pressure Oscillations Induced by Forced Convective Heat Transfer to Two-Phase and Supercritical Hydrogen," Los Alamos Report, LAMS-3070 (February 1964).

29. Cornelius, A. J. and J. D. Parker, "Heat Transfer Instabilities Near the Thermodynamic Critical Point," Proc. Heat Trans. and Fl. Mech. Inst., 317-329 (1965).

30. Dean, L. E. and L. M. Thompson, "Study of Heat Transfer to Liquid Nitrogen," ASME Paper No. 56-SA-4 (1956).

31. Powell, W. B., "Heat Transfer to Fluids in the Region of the Critical Temperature," Jet Propulsion, Vol. 27, 776-783 (1957).

32. Bringer, R. P. and J. M. Smith, "Heat Transfer in the Critical Region," AIChE Jour., Vol. 3, No. 1, 49-55 (1957).

33. Dickinson, N. L. and C. P. Welch, "Heat Transfer to Supercritical Water," Trans. ASME, Vol. 80, 746-752 (1958).

34. Del Bene, J. V. and J. P. Barger, "Heat Transfer to Supercritical Freon-12," Mass. Inst. of Techn., Contract NONR 1891-(14), Technical rept. to Office of Naval Research (1959).

35. Koppel, L. B., Ph. D. Thesis, Northwestern University, Evanston, Ill. (1960).

36. Petukhov, B. S., E. A. Krasnoschekov, and V. S. Protopopov, "An Investigation of Heat Transfer to Fluids Flowing in Pipes Under Supercritical Conditions," Proc. 1961 Int. Heat Trans. Conf., Part III, Paper No. 67, 569-578 (1961).

37. Armand, A. A., N. V. Tarasova, and A. S. Conkov, "An Investigation of Heat Transfer from Wall to Steam Near Critical Region," (in Russian), Heat Transfer at High Heat Flux and Other Special Conditions, papers edited by A. A. Armand (Gosenergoizdat, Moscow-Leningrad), 41-50 (1959).

38. Miropolsky, Z. L. and M. E. Shitzman, "Heat Transfer to Water and Steam with Varying Specific Heat (In the Near Critical Region)," (in Russian), Journal of Technical Physics, Vol. 27, No. 10, 2359-2372 (1951).

39. Szetela, E. J., "Heat Transfer to Hydrogen Including Effects of Varying Fluid Properties," ARS Journal, Vol. 32, No. 8, 1289-1292 (1962).

40. Wood, R. D. and J. M. Smith, "Heat Transfer in the Critical Region -- Temperature and Velocity Profiles in Turbulent Flow," AIChE Jour., Vol. 10, No. 2, 180-186 (1964).

41. Domin, G., "Wärmebergang in Kritischen und uberkritischen Bereichen von Wasser in Rohren," B. W. K., Vol. 15, No. 11, 527-532 (1963).

42. Shitzman, M. E., "Heat Transfer to Water, Oxygen, and Carbon Dioxide in the Critical Region," (in Russian) Teploenergetika, Vol. 6, No. 1, 68-72 (1959).

43. Swenson, H. S., C. R. Kakarala, and J. R. Carver, "Heat Transfer to Supercritical Water in Smooth-Bore Tubes," ASME Paper No. 64-WA/HT-25 (1964).

44. Hendricks, R. C., et al, "Correlation of Hydrogen Heat Transfer in Boiling and Supercritical Pressure States," Am. Rocket Soc. Propellants, Combustion and Liquid Rockets Conf., (April 1961).

45. Hess, H. L. and H. R. Kunz, "A Study of Forced Convection Heat Transfer to Supercritical Hydrogen," ASME Paper No. 63-WA-205 (1963).

46. Koppel, L. B. and J. M. Smith, "Laminar Flow Heat Transfer for Variable Physical Properties," ASME Paper No. 61-SA-32 (1961).

47. Deissler, R. G., "Heat Transfer and Fluid Friction for Fully Developed Turbulent Flow of Air and Supercritical Water with Variable Fluid Properties," Trans. ASME, Vol. 76, 73-85 (1954).

48. Hsu, Y. Y. and J. M. Smith, "The Effect of Density Variation on Heat Transfer in the Critical Region," Trans. ASME, Vol. 82, Series C, 176-182 (1961).

49. Kennedy, J. T. and G. Thodos, "Reduced Density Correlation for Carbon Dioxide," J. Chem. Eng. Data, Vol. 5, 293-297 (1960).

50. Michels, A., J. V. Sengers, and P. S. van der Gulik, "The Thermal Conductivity of $CO_2$ in the Critical Region," Physica, Vol. 28, 1201-1237 (1962).

51. Sengers, J. V., "Thermal Conductivity and Viscosity of Simple Fluids," Int. J. Heat Mass Transf., Vol. 8, 1103-1116 (1965).

52. Schlichting, H., Boundary Layer Theory, McGraw-Hill, New York (1960).

53. Hirschfelder, J. O., C. F. Curtiss, and R. B. Bird, Molecular Theory of Gases and Liquids, John Wiley, New York (1954).

54. "Flow Measurement", ASME publ. PTC 19.5, 4 (1959).

55. Schubauer, G. B. and H. K. Skramstad, "Laminar Boundary Layer Oscillations and Stability of Laminar Flow," NACA War-time Rep. W-8.

56. Dryden, H. L. and G. B. Schubauer, "The Use of Damping Screens for the Reduction of Wind Tunnel Turbulence," J. Aero. Sci., Vol. 14, 221-228 (1947).

57. Kantrowitz, A. and R. L. Trimpi, "A Sharp-Focusing Schlieren System," J. Aero. Sci., Vol. 17, 311-314 (1950).

58. North, R. J., "A Colour Schlieren System Using Multicolour Filters of Simple Construction," NPL/Aero/266 (1954).

59. Kovasznay, L. G., Physical Measurements in Gas Dynamic and Combustion, Vol. IX, High Speed Aerodynamics and Jet Propulsion Series, Princeton University Press, Art. F, 2, 219-285 (1954).

60. Zuber, N., "Nucleate Boiling. The Region of Isolated Bubbles and the Similarity with Natural Convection," Int. J. Heat Mass Trans., Vol. 6, 53-78 (1963).

61. Skripov, V. P. and G. P. Nikolaev, "Heat Transfer from Boiling Carbon Dioxide at Pressures Near the Critical," Izv. Vyssh. Ucheb. Zav. Energetika, No. 4, 66 (1964).

62. Sabersky, R. H., Turbulent Flows and Heat Transfer, Vol. V, High Speed Aerodynamics and Jet Propulsion Series, Princeton University Press, Art. E, 2, 313-335 (1959).

63. Lin, C. C., Theory of Hydrodynamic Stability, Cambridge University Press, Cambridge (1955).

64. Chandrasekhar, S., Hydrodynamic and Hydromagnetic Stability, Oxford University Press, London (1961).

65. Rayleigh, Lord, "Investigation of the Character of the Equilibrium of an Incompressible Heavy Fluid of Variable Density," Scientific Papers, Cambridge, Part II, 200-207 (1900).

66. Taylor, G. I., "The Instability of Liquid Surfaces when Accelerated in a Direction Perpendicular to their Planes," Proc. Roy. Soc. (London), Part A, Vol. 201, 192-196 (1950).

67. Harrison, W. J., "The Influence of Viscosity on the Oscillations of Superposed Fluids," Proc. London Math. Soc., Vol. 6, 396-405 (1908).

68. Bellman, R. and R. H. Pennington, "Effects of Surface Tension and Viscosity on Taylor Instability," Quart. Appl. Math., Vol. 12, 151-162 (1954).

69. Teng Fan, T. Y., "The Character of the Instability of an Incompressible Fluid of Constant Kinematic Viscosity and Exponentially Varying Density," J. Astrophys., Vol. 21, 408-417 (1955).

70. Morton, B.R., "On the Equilibrium of a Stratified Layer of Fluid," Quart. J. Mech. Appl. Math., Vol. 9, 22-34 (1956).

71. Kelvin, Lord, Mathematical and Physical Papers, Part IV, Hydrodynamics and General Dynamics, Cambridge, 69-85 (1950).

72. Helmholtz, H., "Über discontinuirliche Flussigkeits-bewegungen," transl. in Phil. Mag., Ser. 4, Vol. 36, 337-346 (1868).

73. Rayleigh, Lord, Scientific Papers, Part I, 474 (1880).

74. von Mises, R., Jahresbericht Dt. Math. Vereinigung, (1912).

75. Hopf, L., Ann. d. Phys., Vol. 44, 1 (1914).

76. Taylor, G.I., "Effect of Variation in Density on the Stability of Superposed Streams of Fluid," Proc. Roy. Soc. (London), Part A, Vol. 132, 499-523 (1931).

77. Goldstein, S., "On the Stability of Superposed Streams of Fluid of Different Densities," Proc. Roy. Soc. (London), Part A, Vol. 132, 524-548 (1931).

78. Feldman, S., "On the Hydrodynamic Stability of Two Viscous Incompressible Fluids in Parallel Uniform Shearing Motion," J. Fluid Mech., Vol. 2, Pt. 4, 343-370 (1957).

79. Miles, J.W., "The Hydrodynamic Stability of a Thin Film in Uniform Shearing Motion," J. Fluid Mech., Vol. 8, Pt. 4, 593-611 (1960).

80. Case, K.M., "Stability of an Idealized Atmosphere. Discussion of Results," Phys. of Fluids, Vol. 3, 149-154 (1960).

81. Plesset, M.S. and D.Y. Hsieh, "A General Analysis of the Stability of Superposed Fluids," Calif. Inst. of Tech., Div. of Eng. and Appl. Sci. Rep. No. 85-26, Pasadena, Calif. (1963).

82. Curle, N., Aero. Res. Council, London, Unpublished Rep. No. 18426 (1956).

83. Tollmien, W., "Uber die Enstehung der Turbulenz," NACA TM - 609 (1931).

84. Schlichting, H., "Zur Enstehung der Turbulenz bei der Plattenstromung," Nach. Ges. Wiss. Gottingen, Math. Phys. Klasse, 182-208 (1933).

85. Lin, C. C., "On the Stability of Two-Dimensional Parallel Flows," Quart. Appl. Math., Vol. 3, 117-142, 218-234, 277-301 (1945-46).

86. Drazin, P. G., "The Stability of a Shear Layer in an Unbounded Heterogeneous Inviscid Fluid," J. Fluid Mech., Vol. 4, 214-224 (1958).

87. Schlichting, H., "Turbulence and Heat Stratification," NACA TM - 1262 (1935).

88. Lees, L. and C. C. Lin, "Investigation of the Stability of the Laminar Boundary Layer in a Compressible Fluid," NACA TN-1115 (1946).

89. Betchov, R. and W. O. Criminale, "Oscillations of a Turbulent Flow," Physics of Fluids, Vol. 7, No. 12, 1920-1926 (1964).

90. Townsend, A. A., The Structure of Turbulent Shear Flow, Cambridge University Press, Cambridge (1956).

91. Berenson, P. J., "Film-Boiling Heat Transfer from a Horizontal Surface," J. Heat Transf., Vol. 83, 351-358 (1961).

92. National Bureau of Standards, Circular #564, Chapter 4, "The Thermodynamic Properties of Carbon Dioxide," 138-195 (1955).

93. Liepmann, H. and A. Roshko, Elements of Gasdynamics, John Wiley, New York, 153-161 (1960).

94. Holder, D. W. and R. J. North, Schlieren Methods, Notes on Applied Science No. 31, Her Majesty's Stationery Office, London, 5-7 (1963).

95. Greenleaf, A. R., Photographic Optics, Mac millan, New York, 26 (1950).

96. Fish, R. W. and K. Parnham, "Focusing Schlieren Systems," Aero. Res. Counc. C. P. -54 (1950).

97. Eckert, E. R. G. and R. M. Drake Jr., Heat and Mass Transfer, McGraw-Hill, New York, 241-243 (1959).

# LIST OF SYMBOLS

| | |
|---|---|
| $A$ | heated surface area |
| $A_o$ | flow channel area |
| $a$ | unintercepted height of light source |
| $B$ | luminance of light source |
| $b$ | width of light source |
| $C$ | contrast of schlieren system |
| $C_d$ | discharge coefficient |
| $c$ | circle of confusion, sonic velocity |
| $c_1$, $c_2$, $c_3$ | constants |
| $c_p$ | specific heat at constant pressure |
| $d$ | diameter of thermocouple plug |
| $d_i$ | venturi inlet diameter |
| $d_t$ | venturi throat diameter |
| $f$ | focal length of lens |
| $H$ | maximum spacing between light sources |
| $h$ | heat transfer coefficient, height of light source, enthalpy |
| $h_t$ | heat transfer coefficient for thermocouple plug |
| $I$ | illumination on film plane |
| $i$ | instantaneous hot wire current |

| | |
|---|---|
| $i_o$ | mean hot wire current |
| $K_i$ | head loss coefficient |
| k | thermal conductivity |
| l | thermocouple plug length |
| Nu | Nusselt number |
| m | magnification of image on film plane |
| $\dot{m}$ | mass flow rate |
| n | constant |
| Pr | Prandtl number |
| $p_o$ | freestream pressure |
| Q | heat transfer rate |
| Re | Reynolds number |
| S | sensitivity of schlieren system, entropy |
| T | fluid temperature |
| $T_o$ | freestream fluid temperature |
| $T_w$ | heated surface temperature |
| $T_t$ | thermocouple plug temperature |
| u | instantaneous local fluid velocity |
| $u_o$ | mean local fluid velocity |
| $u^+$ | shear velocity $u^+ = \sqrt{\tau_w / \rho}$ |
| $V_o$ | freestream velocity |

| | |
|---|---|
| W | power input to plate |
| X | distance from lens to image plane |

Greek Letters

| | |
|---|---|
| $\alpha$ | inclination of light rays = h/f |
| $\beta$ | inclination of light rays = H/f |
| | dimensionless temperature = $\frac{Q}{c_p\sqrt{\rho \tau_w}}$ |
| $\delta^*$ | displacement thickness of boundary layer |
| $\epsilon$ | deflection of light rays |
| $\mu$ | dynamic viscosity |
| $\rho$ | fluid density |
| $\tau$ | turbulence level |
| $\tau_w$ | wall shear stress |

# Appendix A

# PROPERTIES OF CARBON DIOXIDE

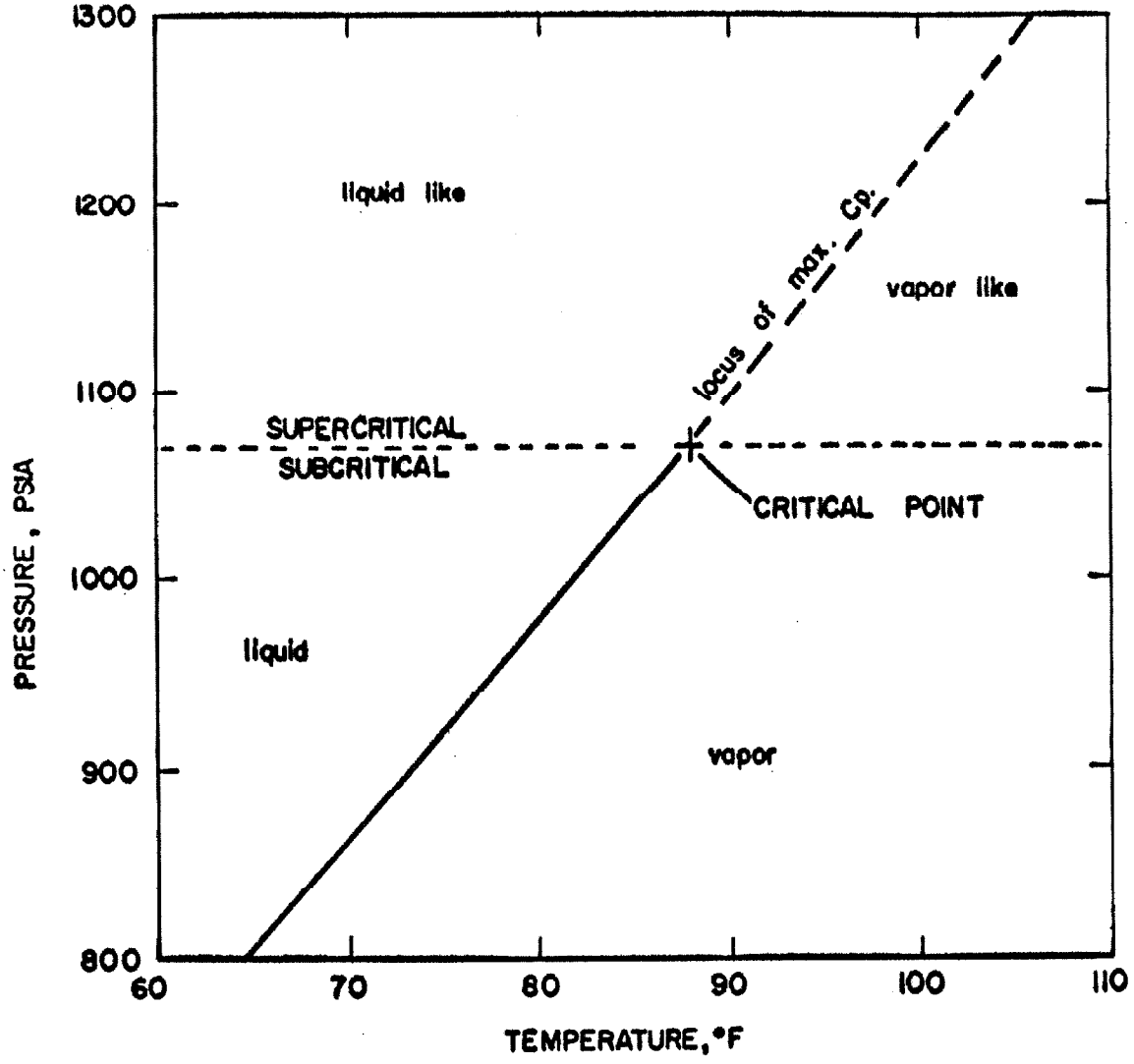


FIG. 1. VAPOR PRESSURE CURVE FOR CARBON DIOXIDE
(Data taken from (20, 92) ).

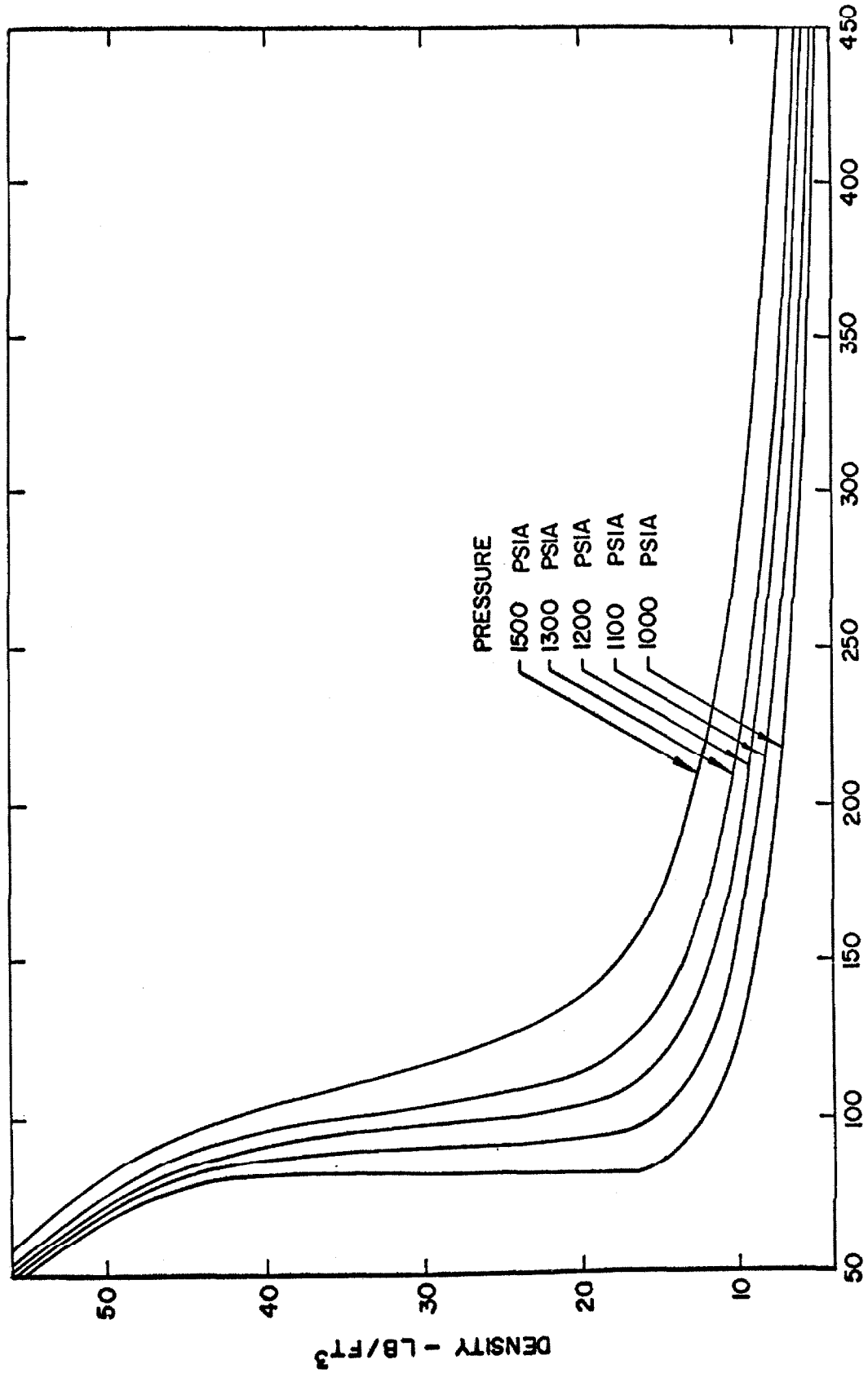


FIG. 2. DENSITY OF CARBON DIOXIDE
(Data taken from (20) ).

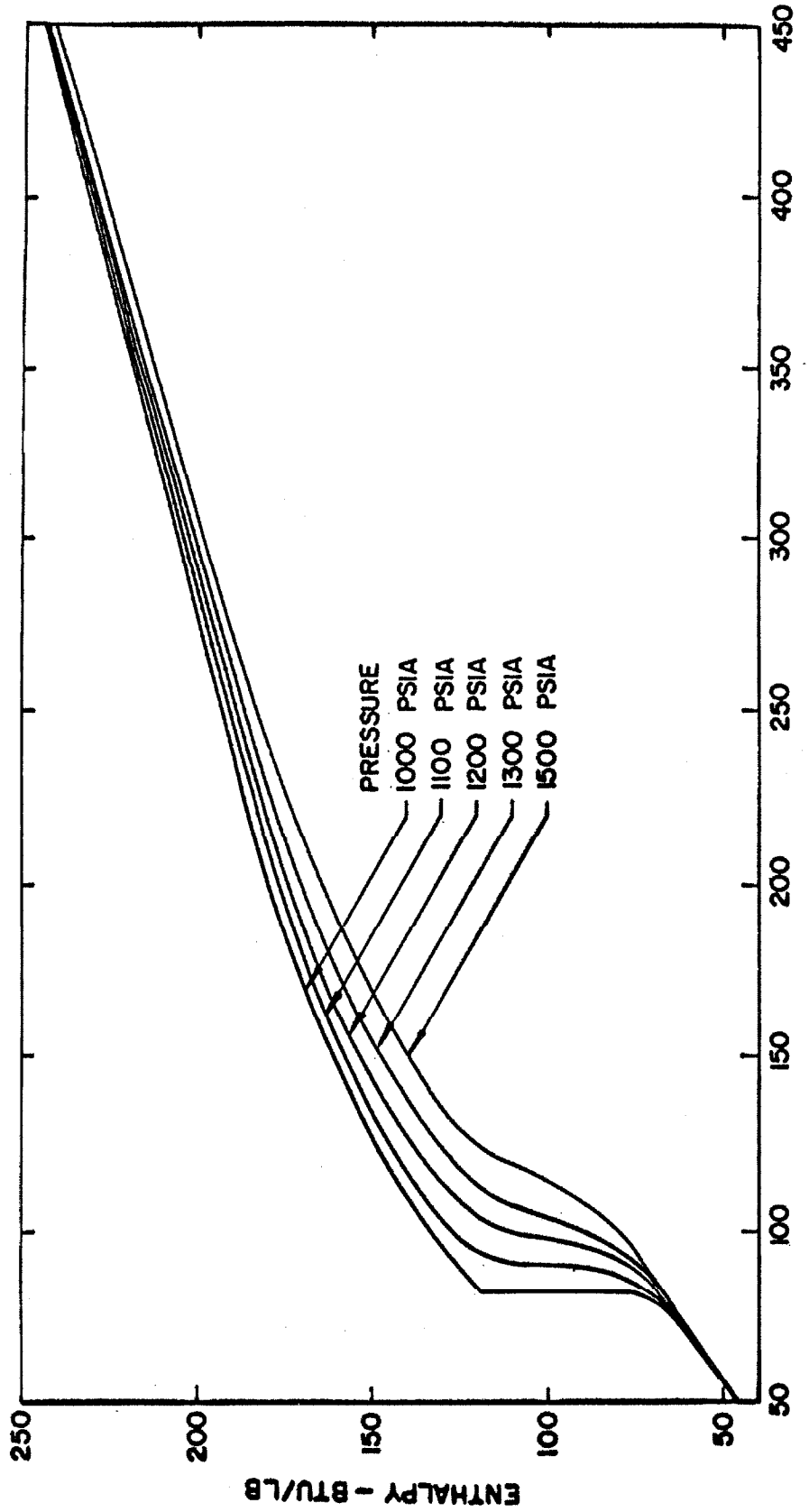


FIG. 3. ENTHALPY OF CARBON DIOXIDE
(Data taken from (20) ).

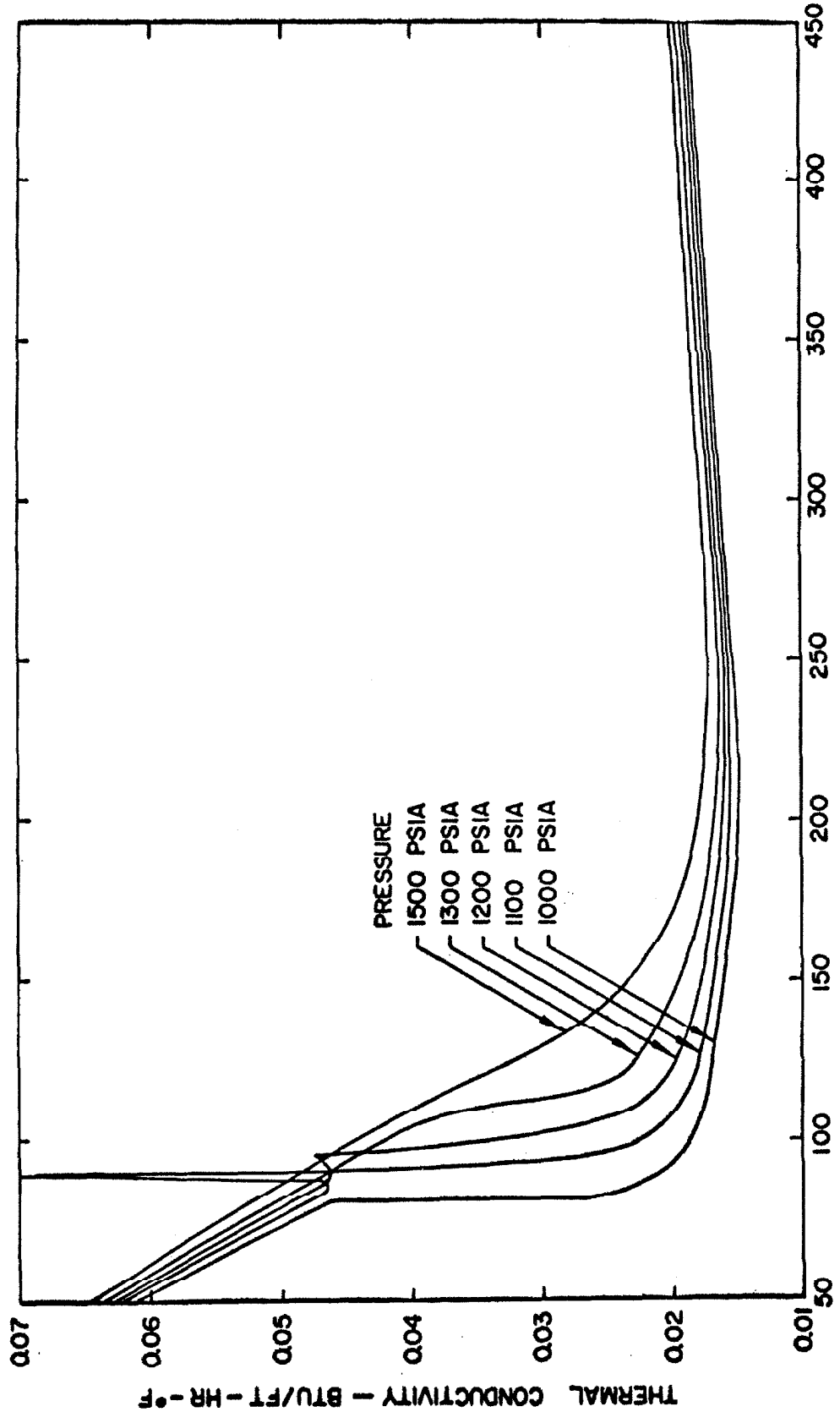


FIG. 4. THERMAL CONDUCTIVITY OF CARBON DIOXIDE
(Data taken from (20) ).

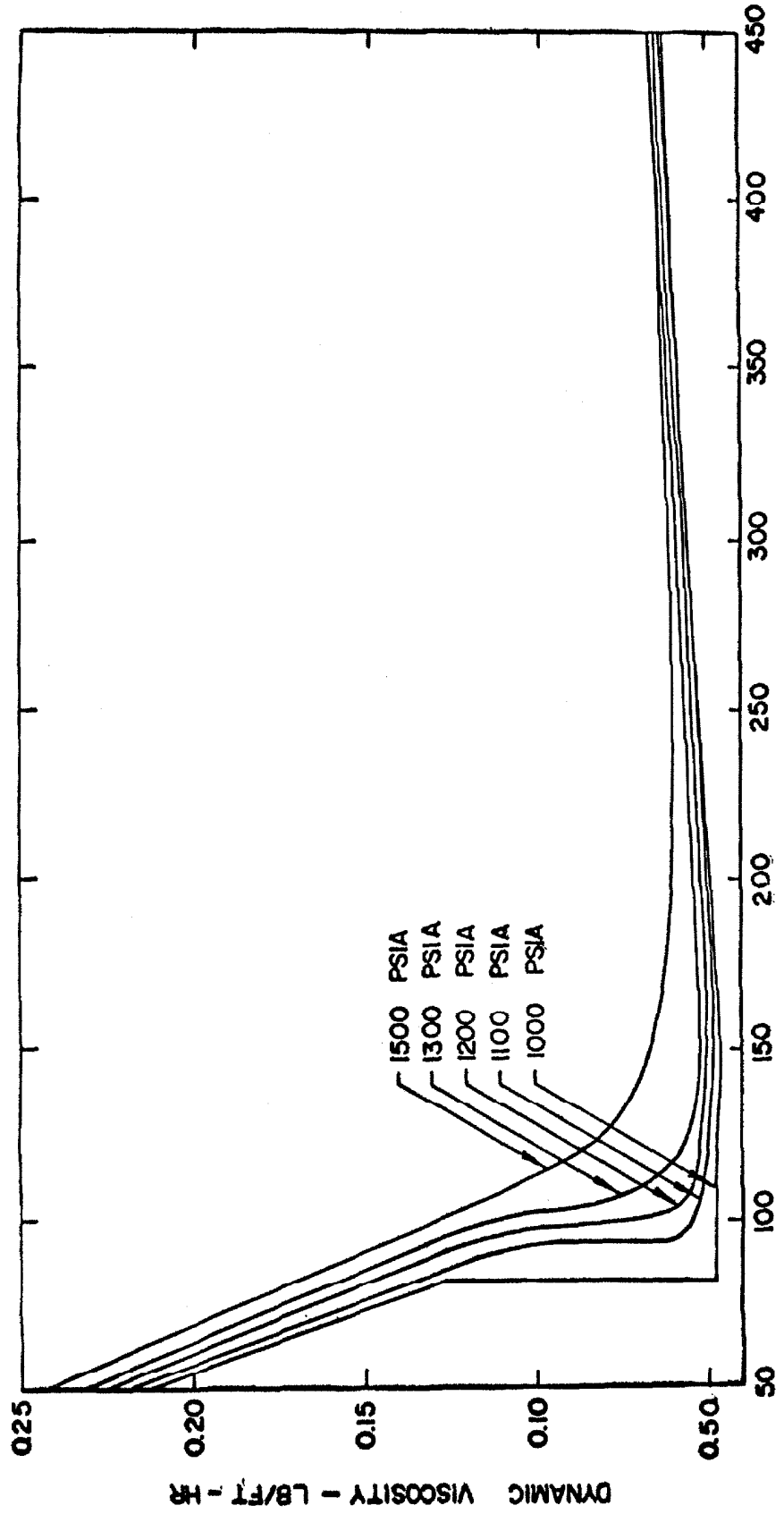


FIG. 5. DYNAMIC VISCOSITY OF CARBON DIOXIDE
(Data taken from (20) ).

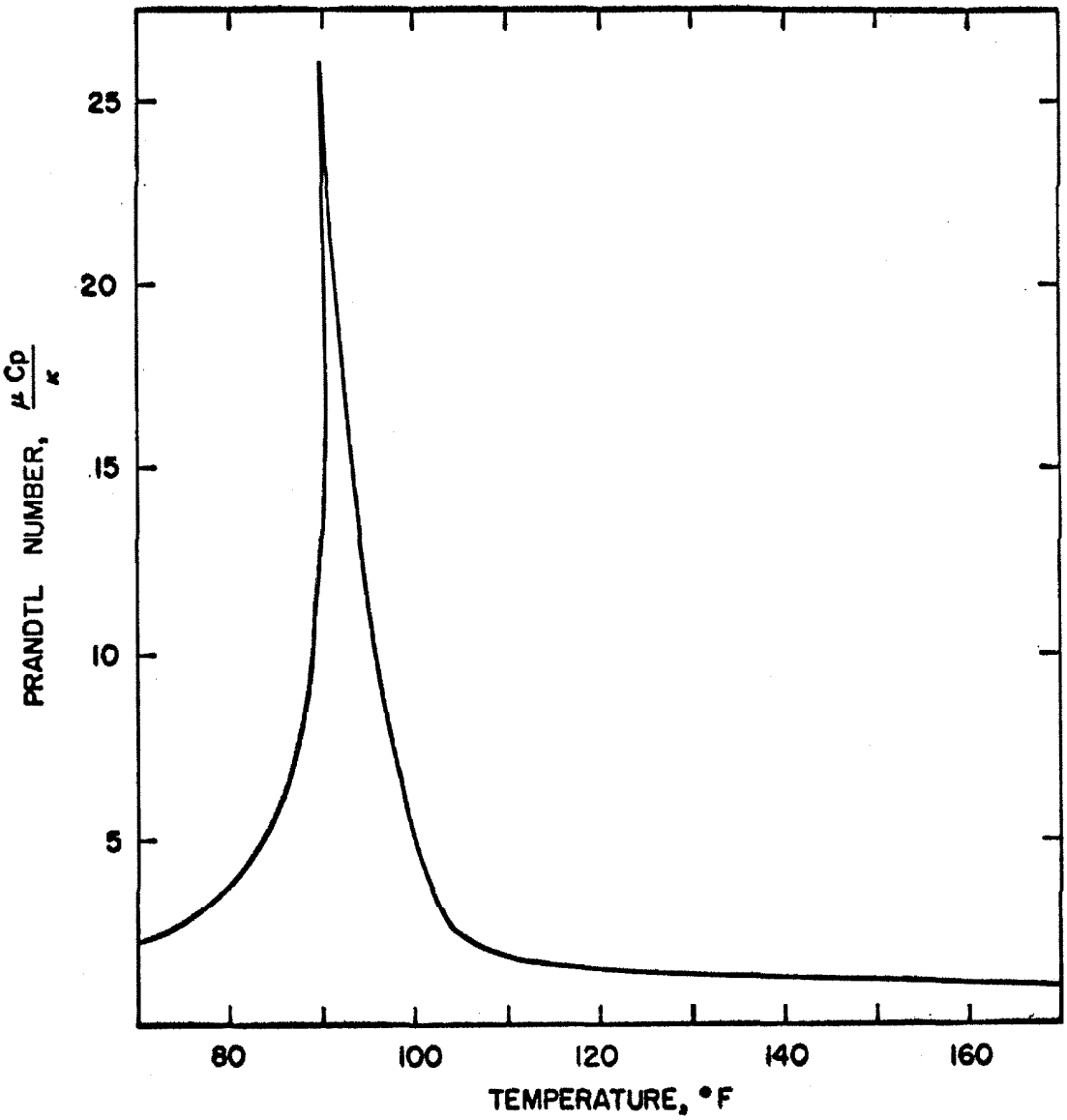


FIG. 6. PRANDTL NUMBER OF CARBON DIOXIDE AT 1,100 psia (*Data taken from* (50) ).

# Appendix B

# EXPERIMENTAL APPARATUS

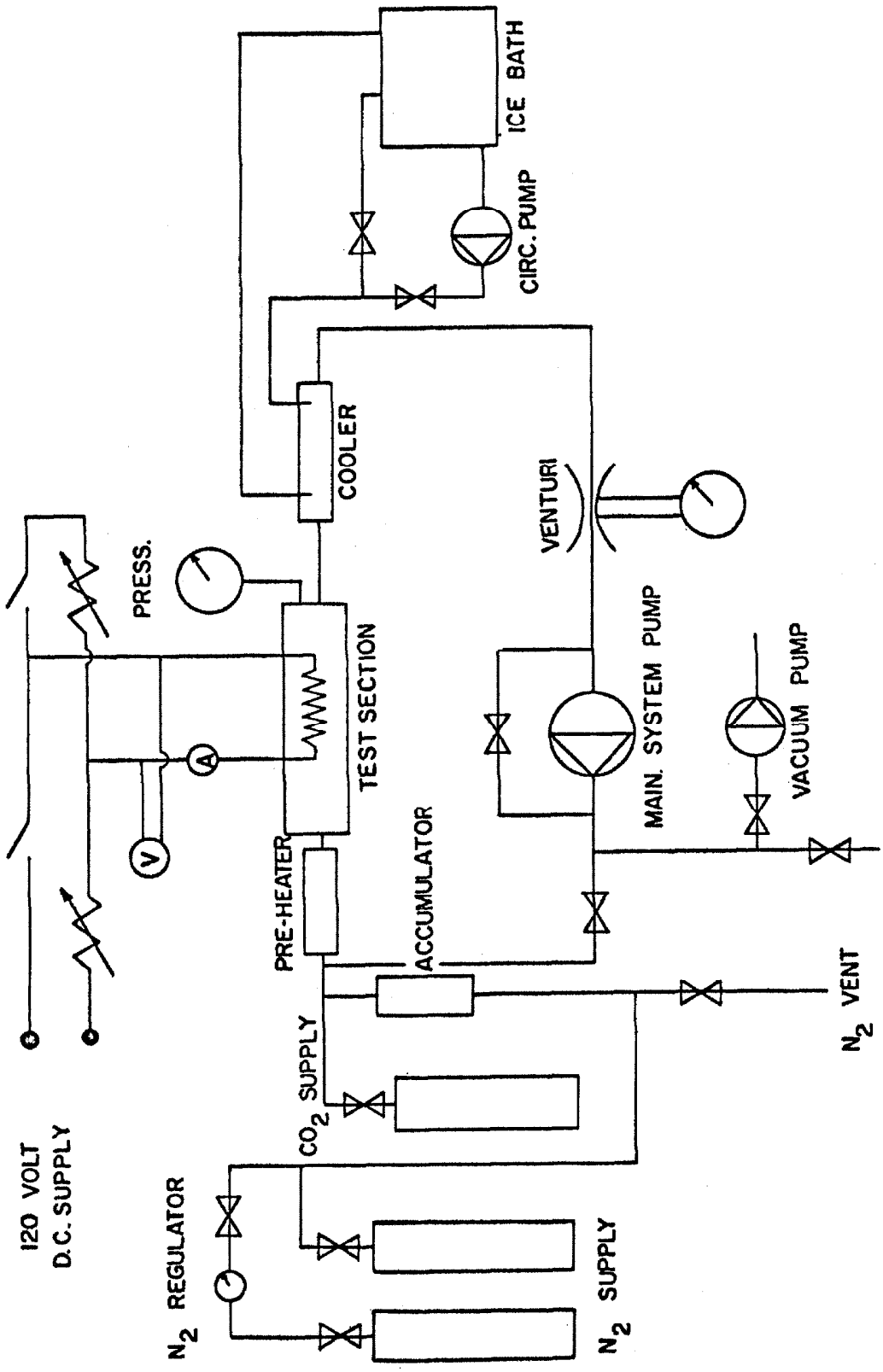


FIG. 7. SCHEMATIC DIAGRAM OF FORCED CONVECTION APPARATUS

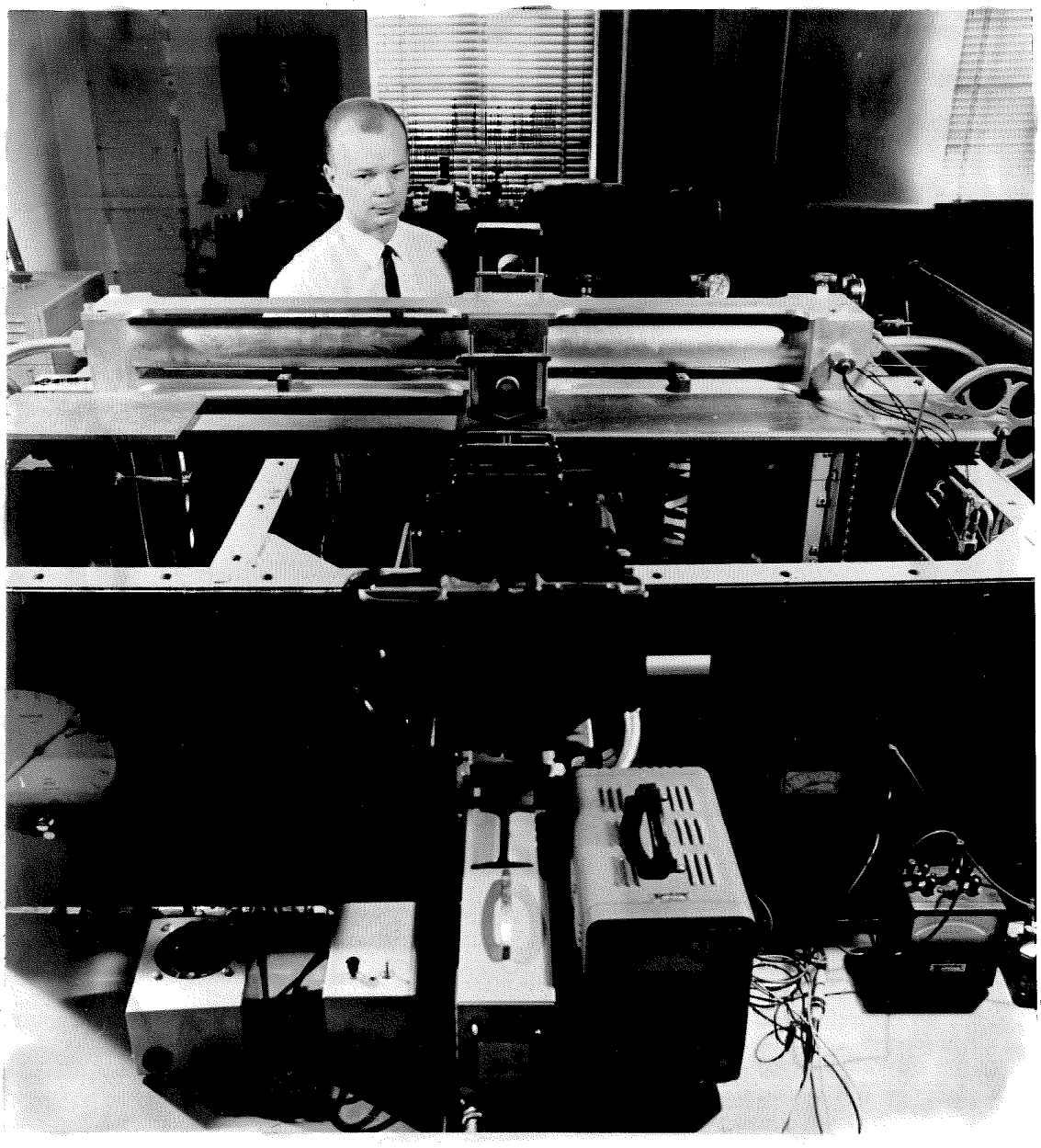

FIG. 8. OVERALL VIEW OF FORCED CONVECTION APPARATUS.

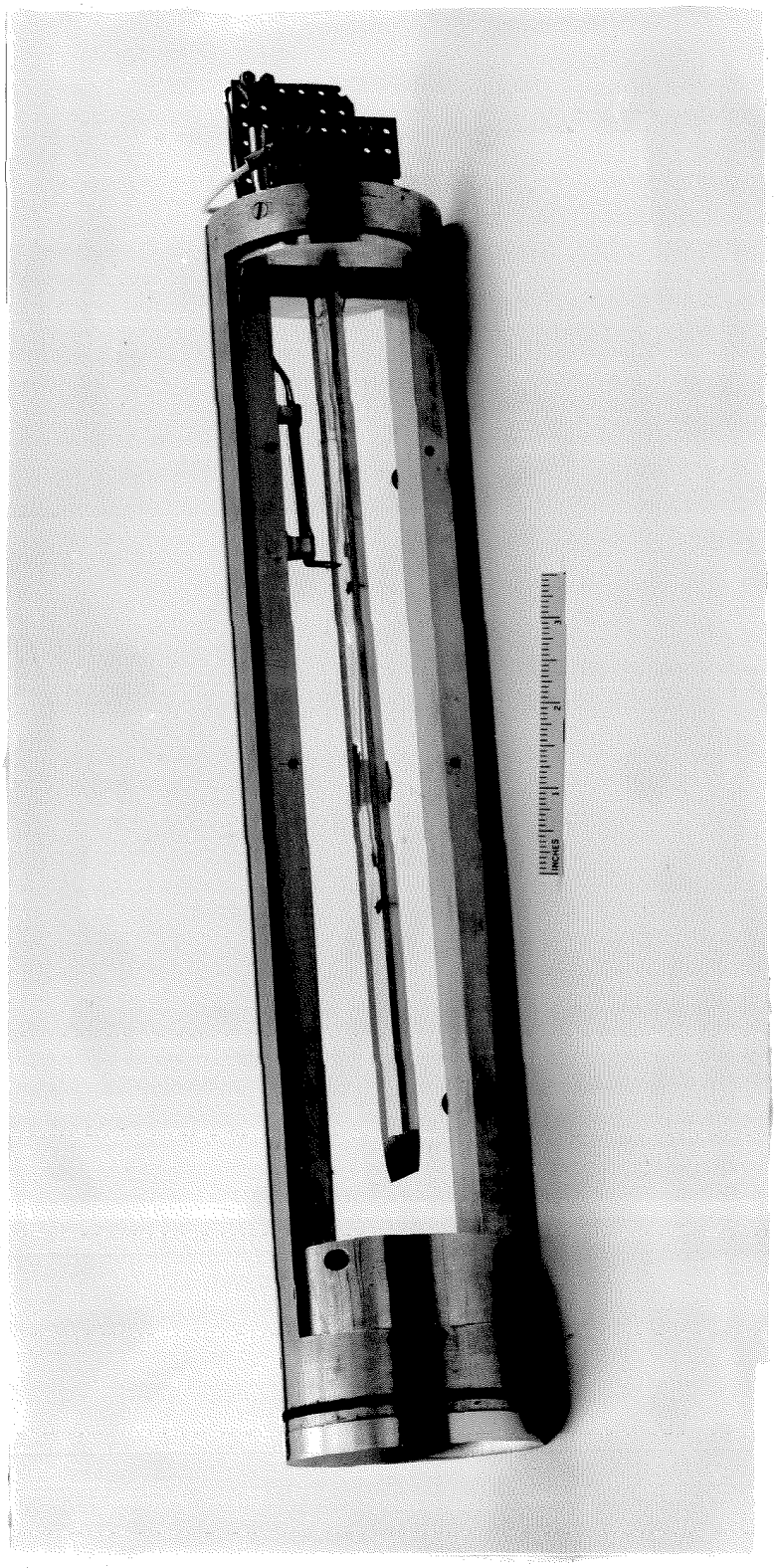

FIG. 9. RECTANGULAR FLOW CHANNEL.

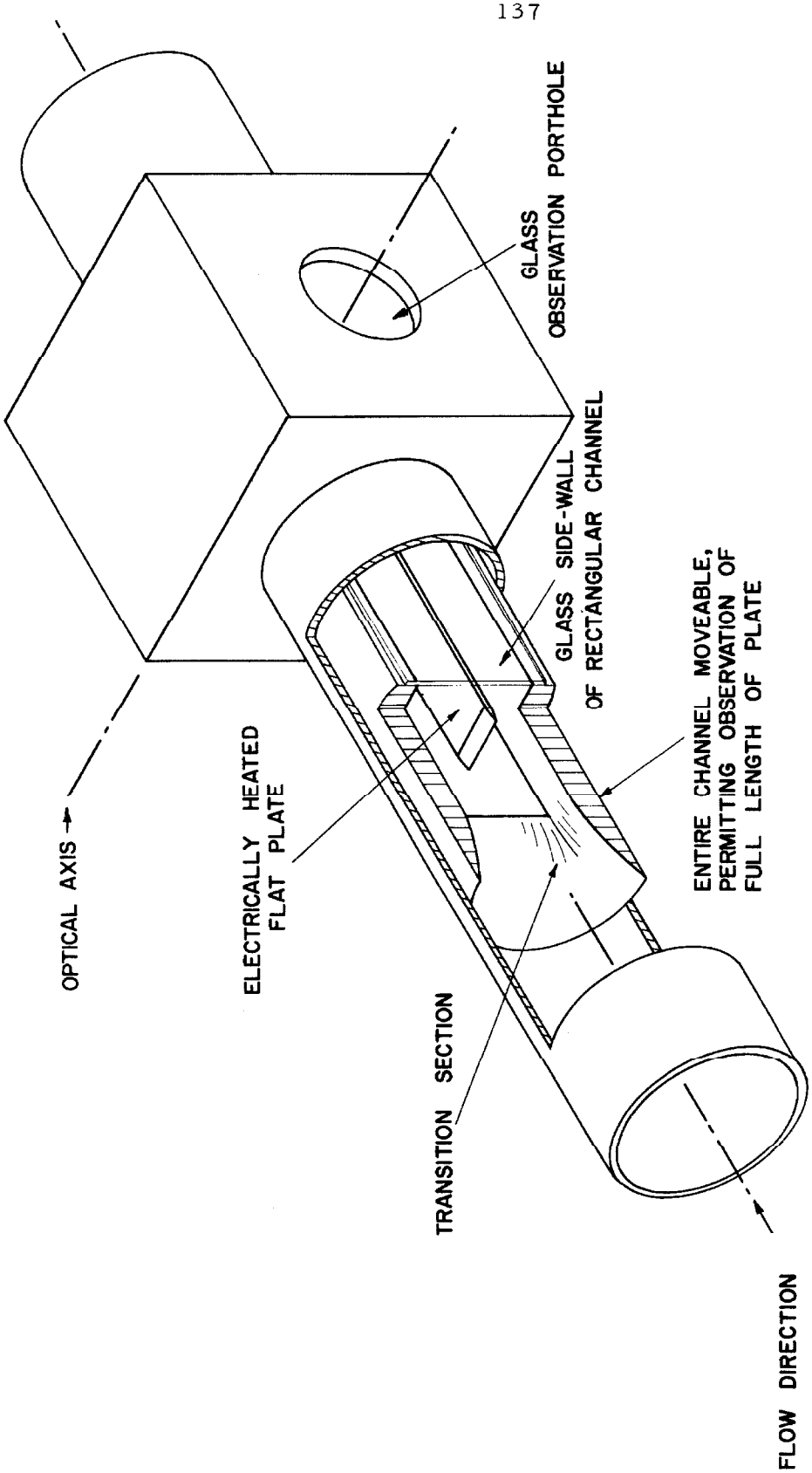


FIG. 10. SECTIONED VIEW OF FORCED CONVECTION APPARATUS TEST SECTION.

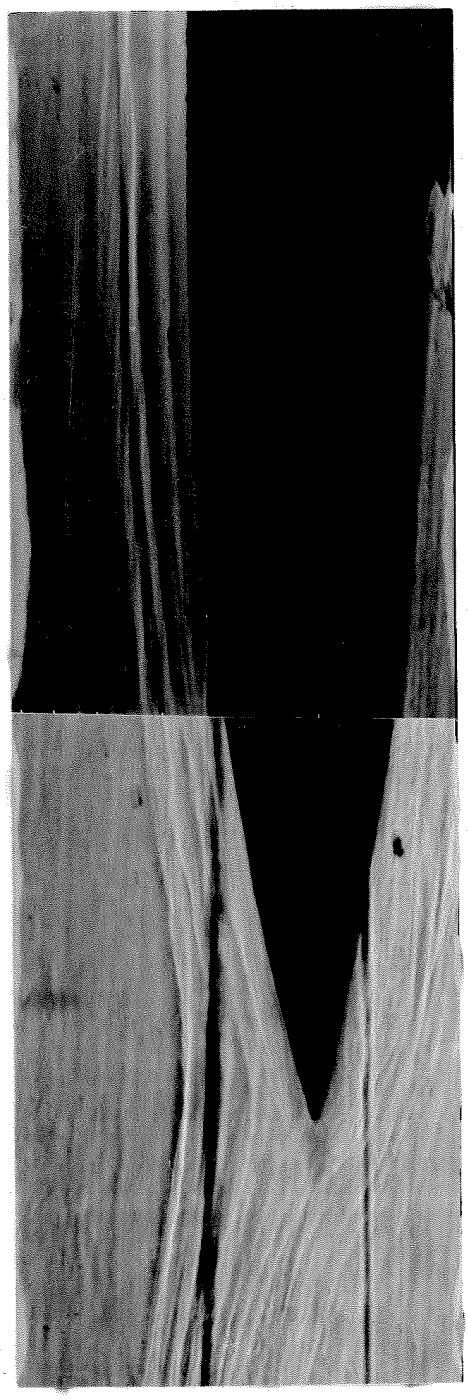

FIG. 11. FLOW FIELD OVER LEADING EDGE OF HEATED FLAT PLATE (10 x enlarged).

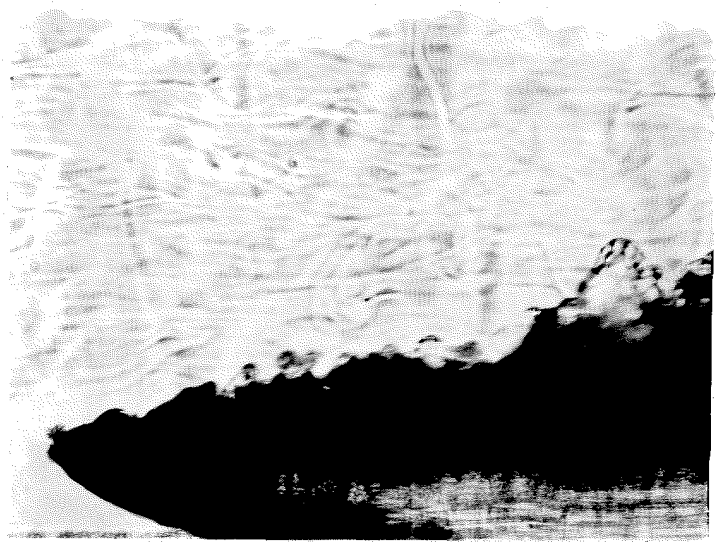

A. CONVENTIONAL SCHLIEREN

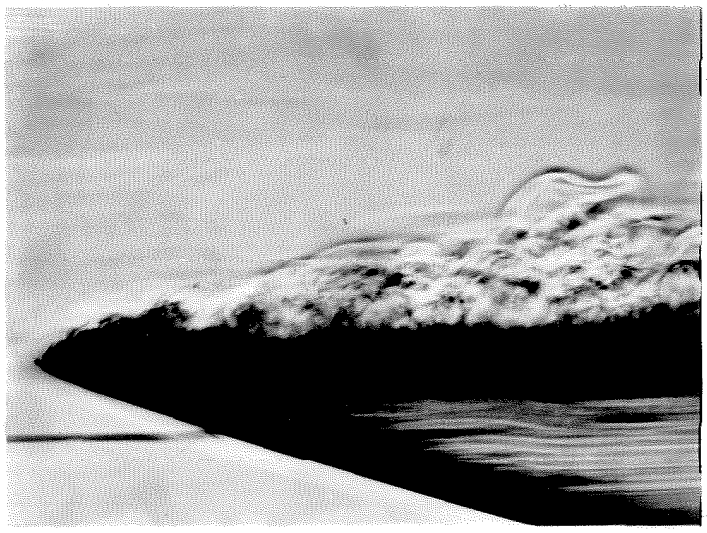

B. SEMI-FOCUSING SCHLIEREN

FIG. 12. IDENTICAL FLOWS OVER HEATED PLATE IN SUPERCRITICAL $CO_2$.

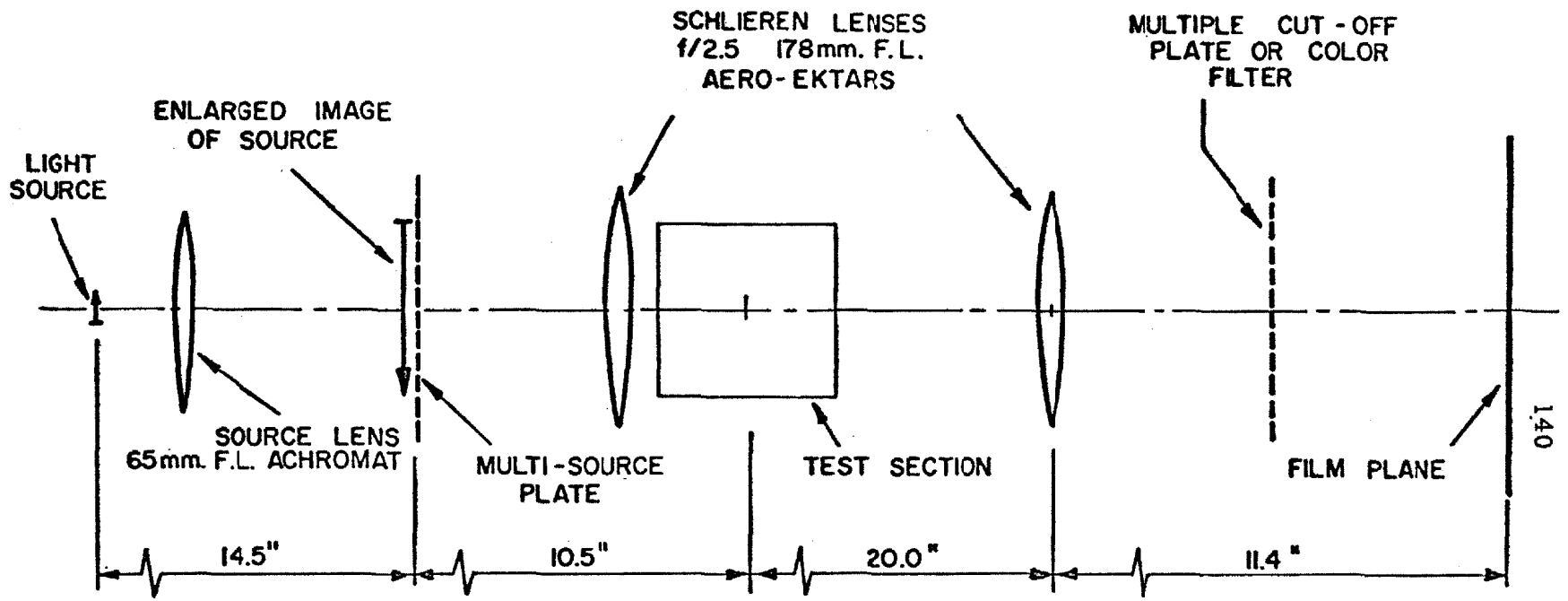


FIG. 13. ELEMENTS OF OPTICAL BENCH

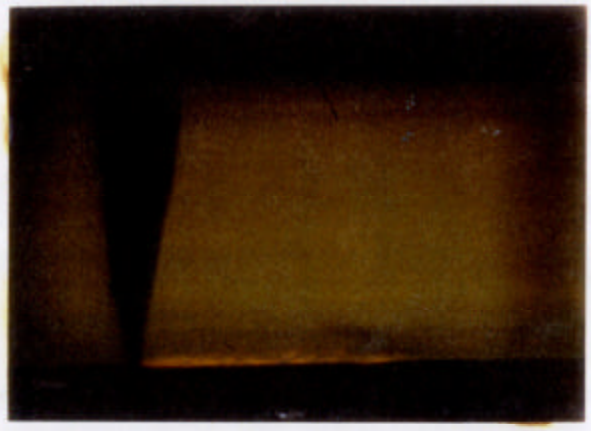

FIG. 14. THERMAL WAKE OF HOT WIRE ANEMOMETER IN SUPERCRITICAL $CO_2$ (5 x enlarged).

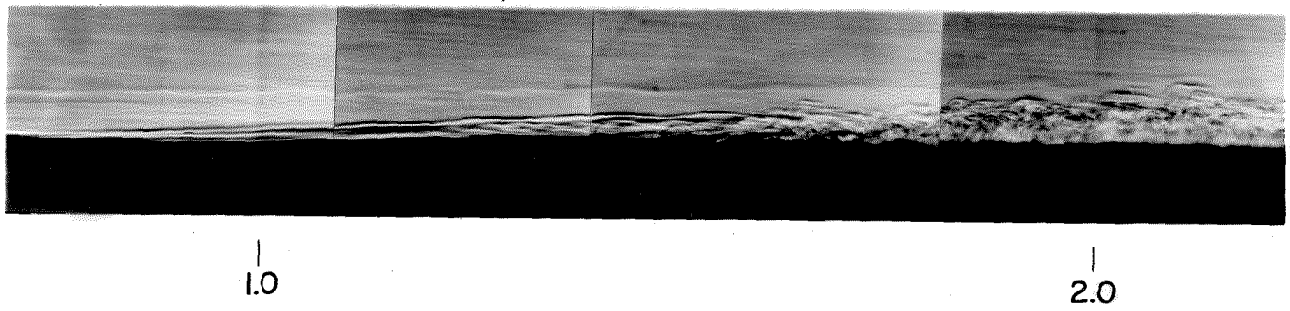


FIG. 15. BOUNDARY LAYER TRANSITION ON HEATED PLATE IN SUPERCRITICAL $CO_2$.
(Numbers indicate distance from leading edge in inches).

# Appendix C

# EXPERIMENTAL RESULTS

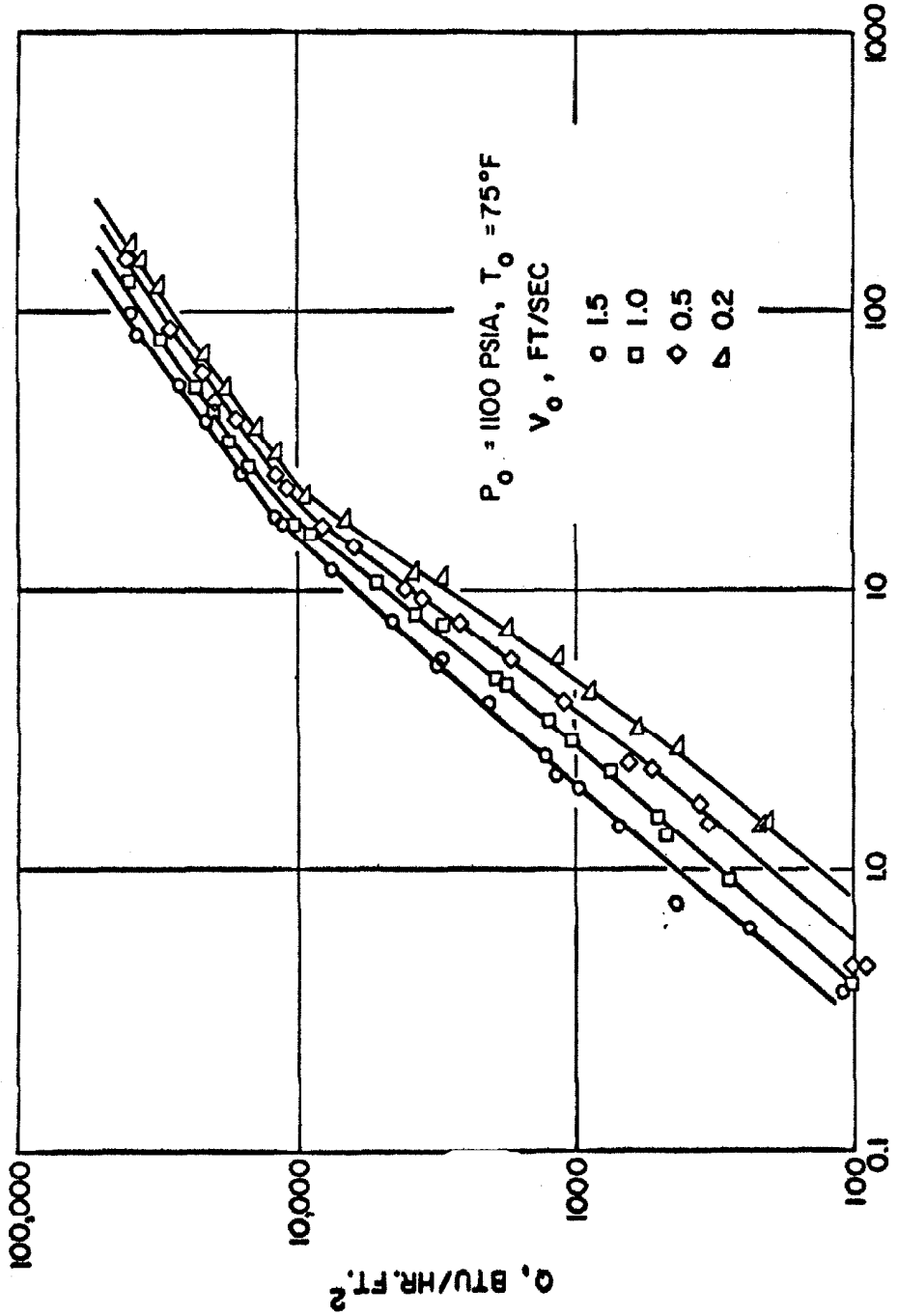


FIG. 16. FORCED CONVECTIVE HEAT TRANSFER FROM A FLAT PLATE TO SUPERCRITICAL $CO_2$ AT 1,100 psia AND 75°F.

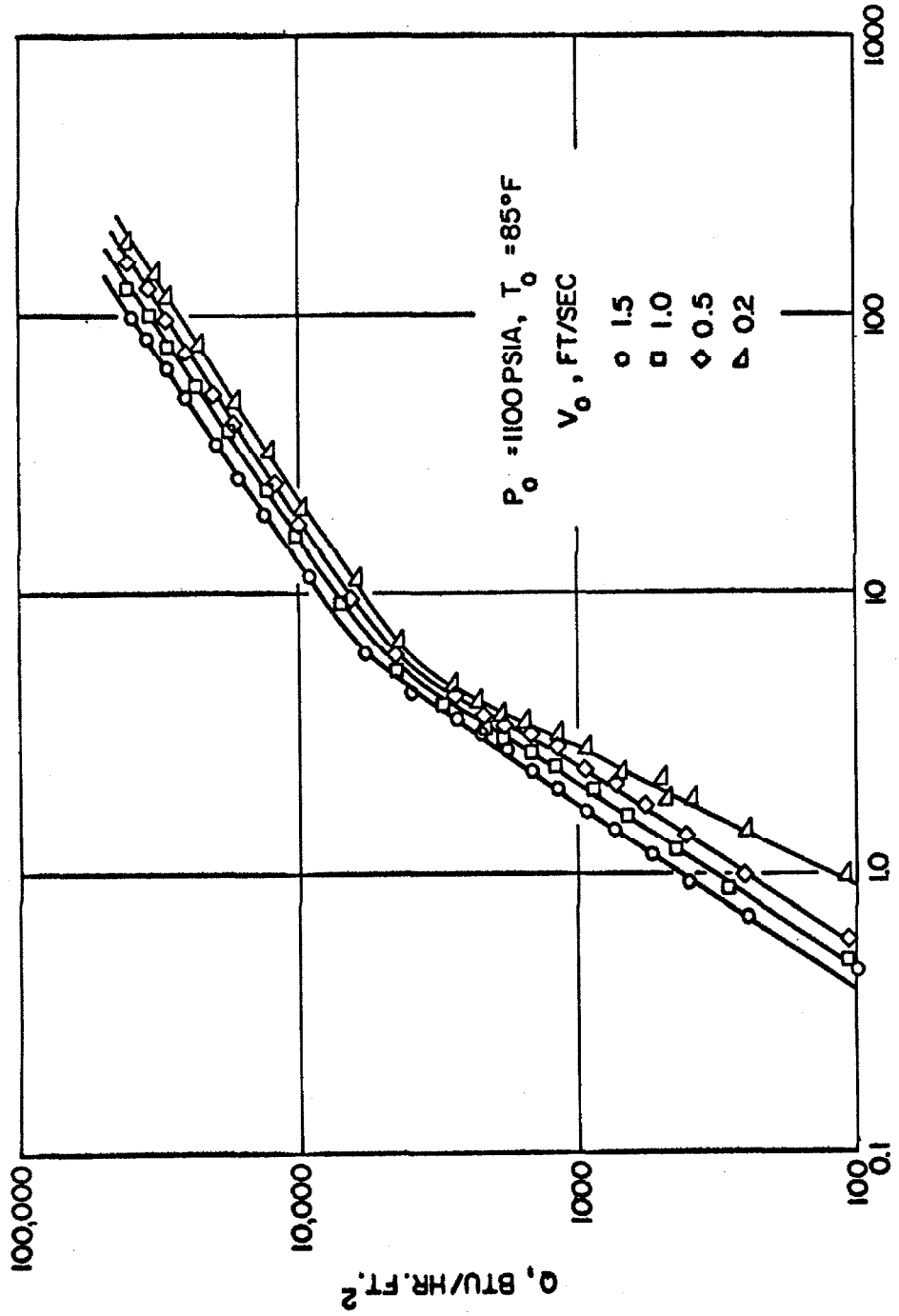


FIG. 17. FORCED CONVECTIVE HEAT TRANSFER FROM A FLAT PLATE TO SUPERCRITICAL $CO_2$ AT 1,100 psia AND 85°F.

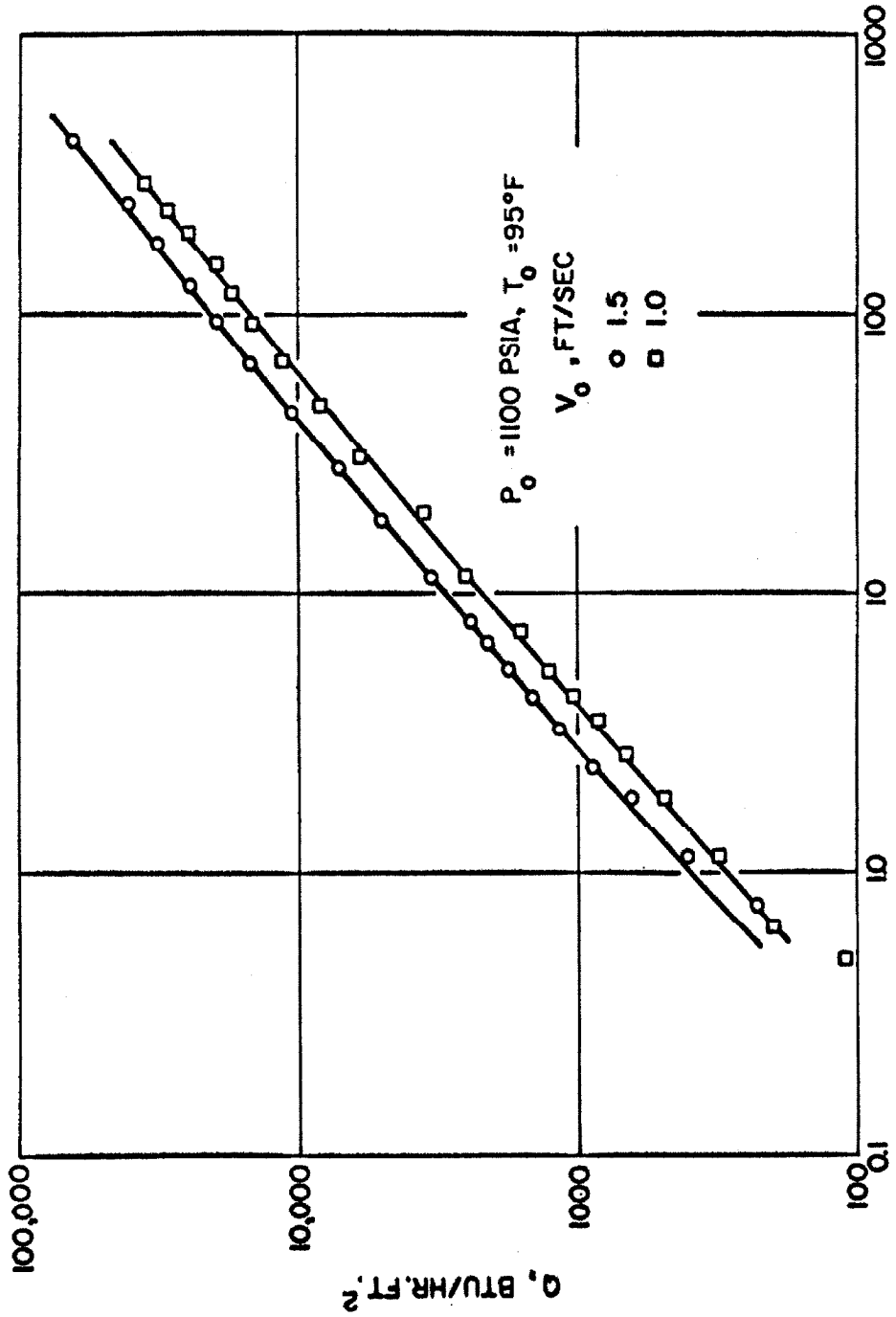


FIG. 18. FORCED CONVECTIVE HEAT TRANSFER FROM A FLAT PLATE TO SUPERCRITICAL $CO_2$ AT 1,100 psia AND 95°F.

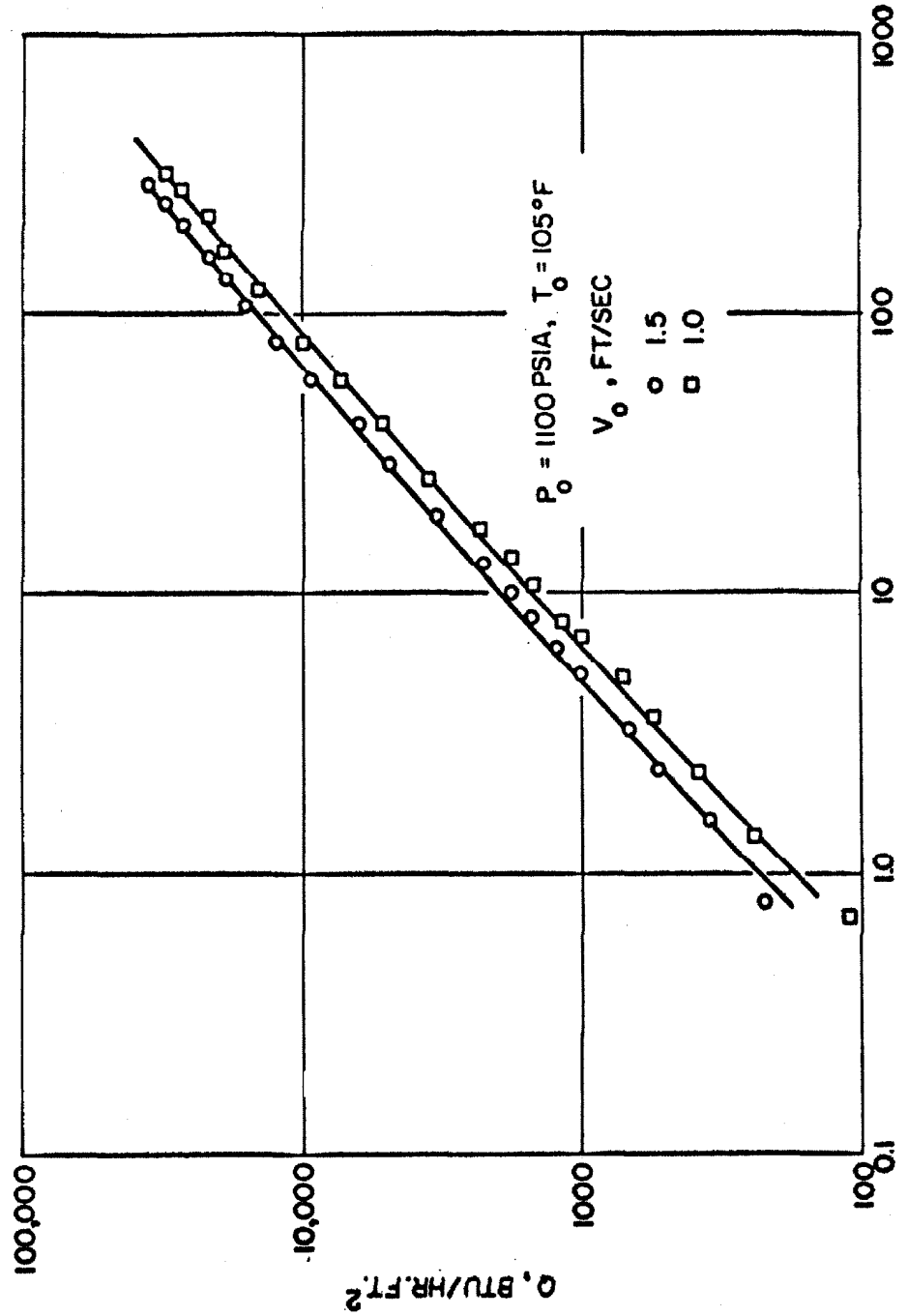


FIG. 19. FORCED CONVECTIVE HEAT TRANSFER FROM A FLAT PLATE TO SUPERCRITICAL $CO_2$ AT 1,100 psia AND 105°F.

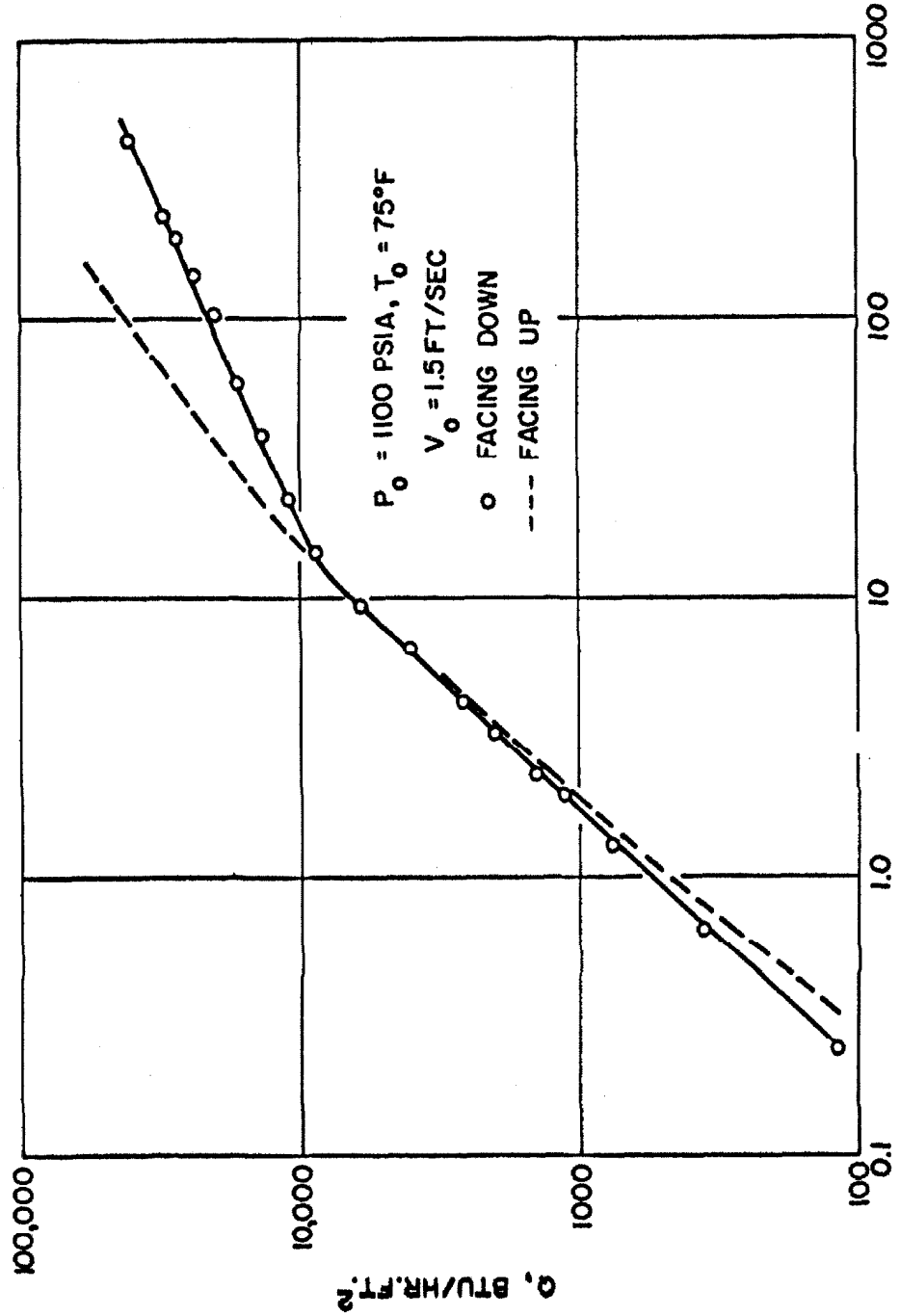


FIG. 20. EFFECT OF GRAVITY ON FORCED CONVECTIVE HEAT TRANSFER FROM A FLAT PLATE TO SUPERCRITICAL $CO_2$ AT 1,100 psia AND 75°F.

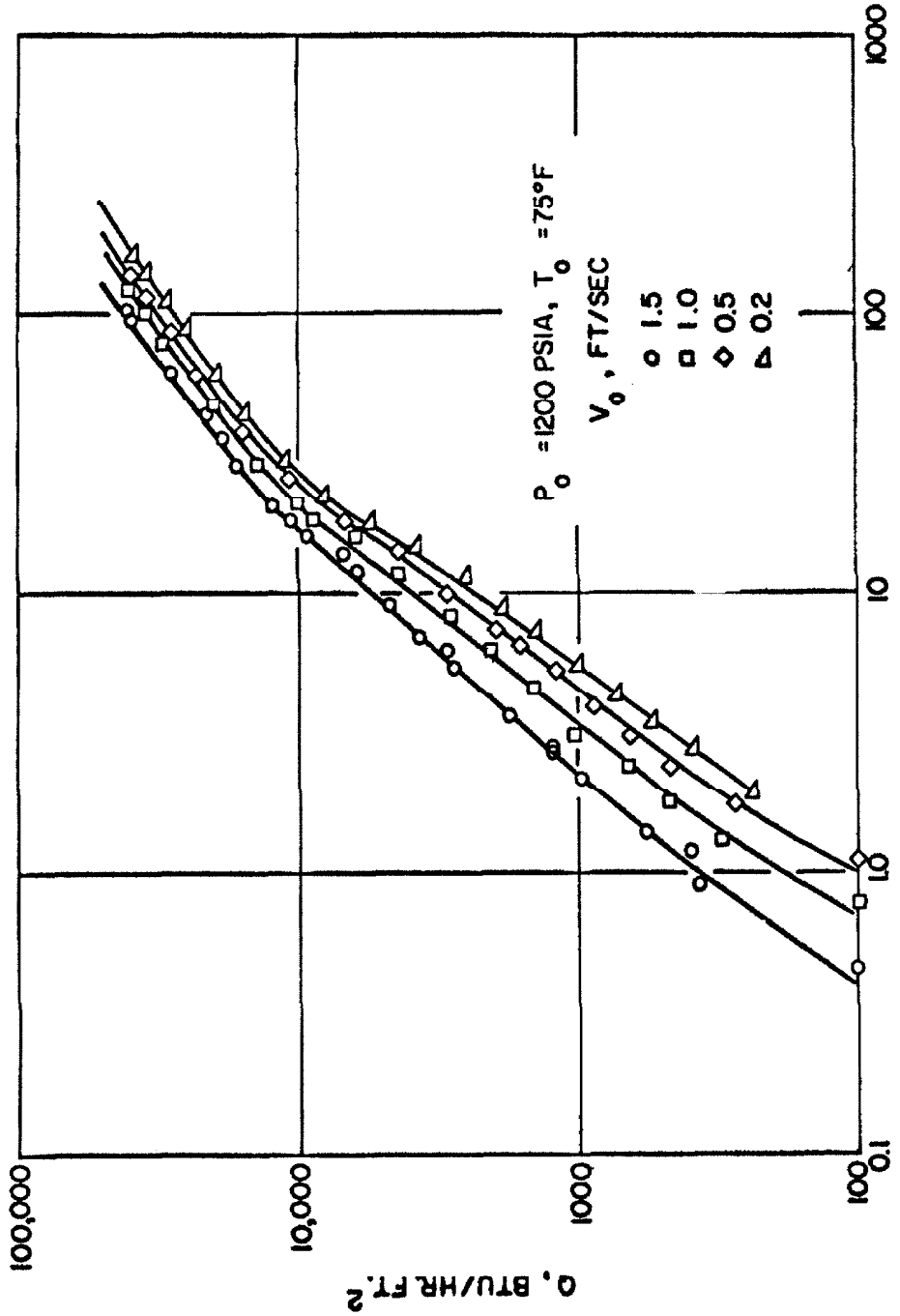


FIG. 21. FORCED CONVECTIVE HEAT TRANSFER FROM A FLAT PLATE TO SUPERCRITICAL $CO_2$ AT 1,200 psia AND 75°F.

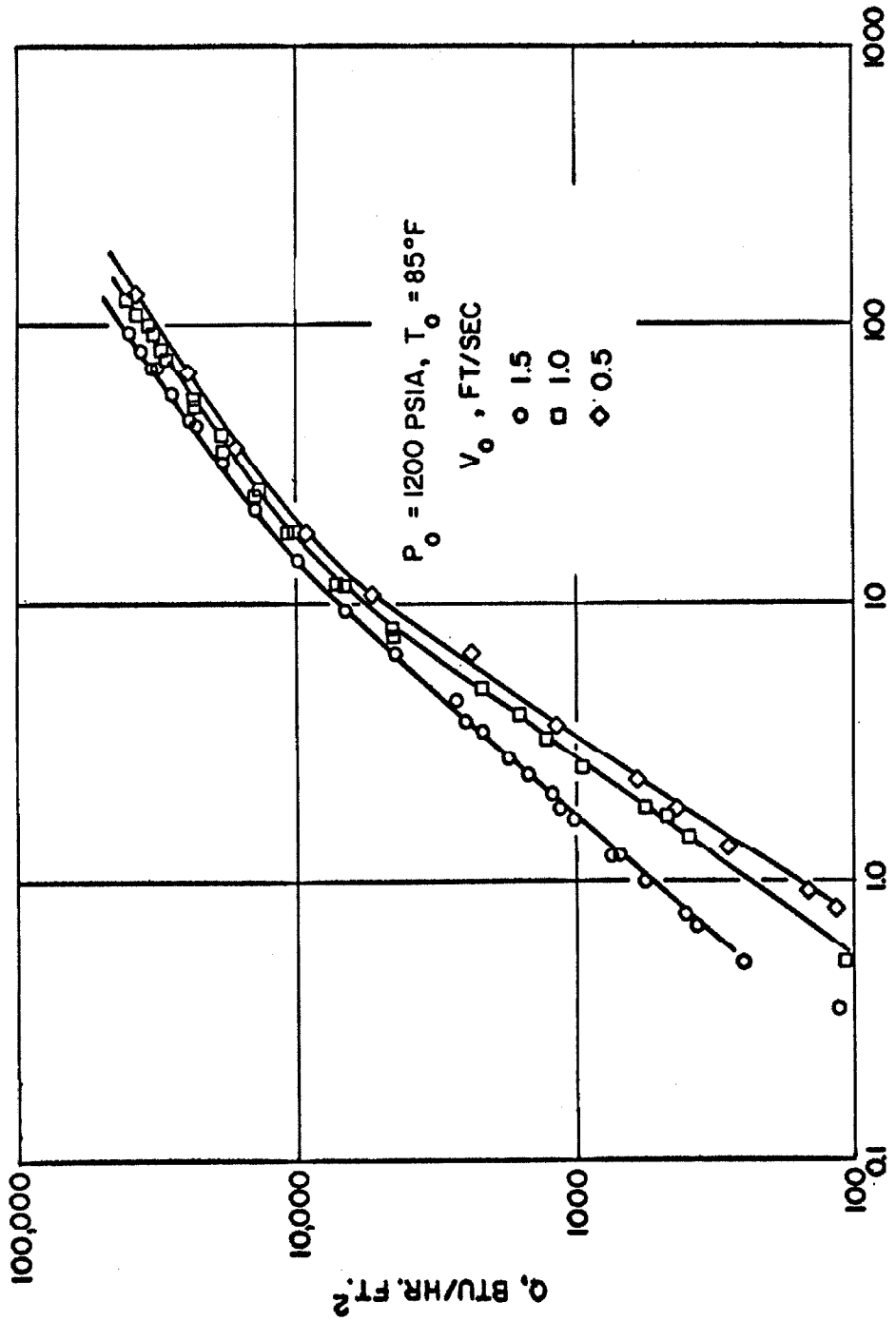


FIG. 22. FORCED CONVECTIVE HEAT TRANSFER FROM A FLAT PLATE TO SUPERCRITICAL $CO_2$ AT 1,200 psia AND 85°F.

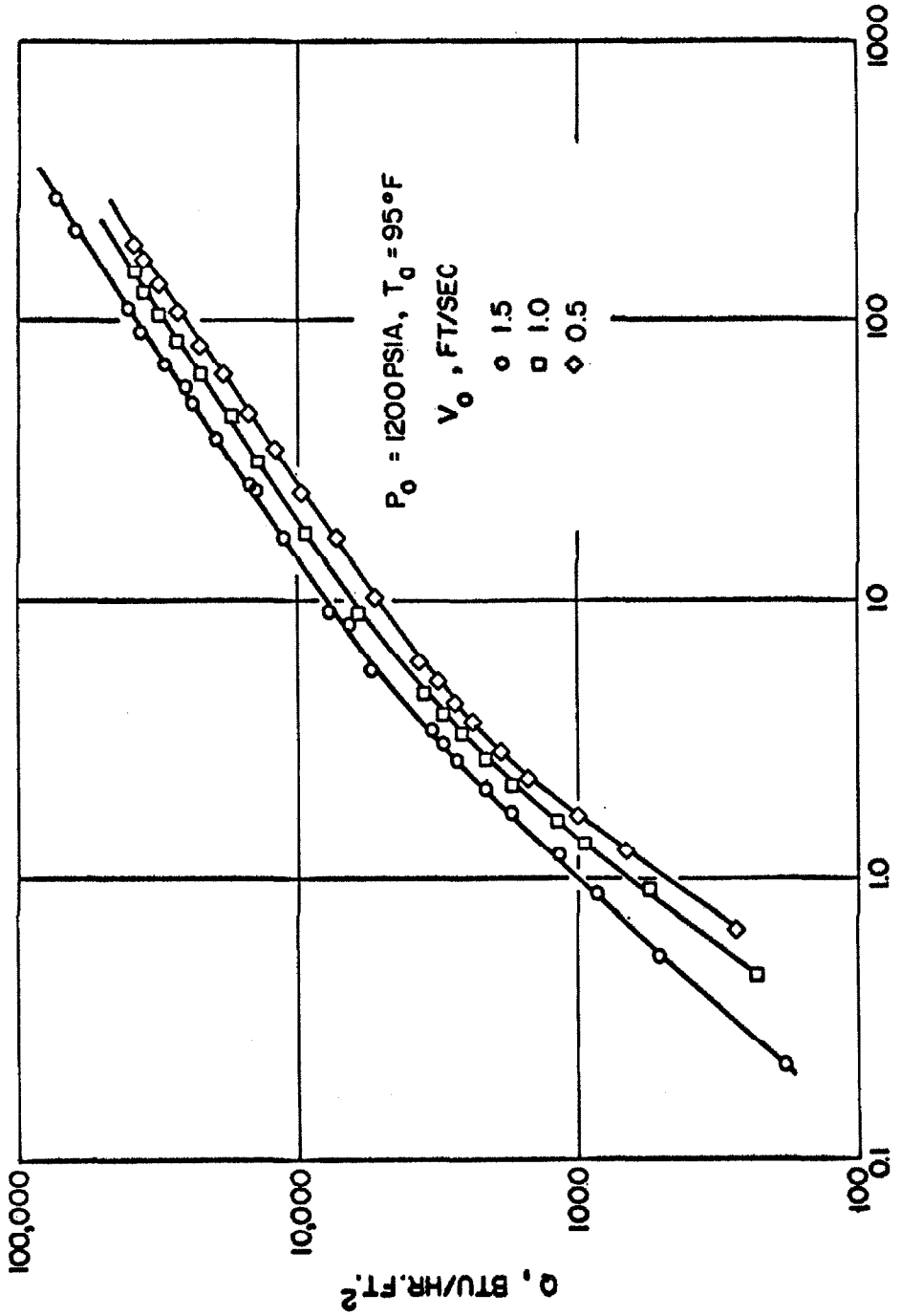


FIG. 23. FORCED CONVECTIVE HEAT TRANSFER FROM A FLAT PLATE TO SUPERCRITICAL $CO_2$ AT 1,200 psia AND 95°F.

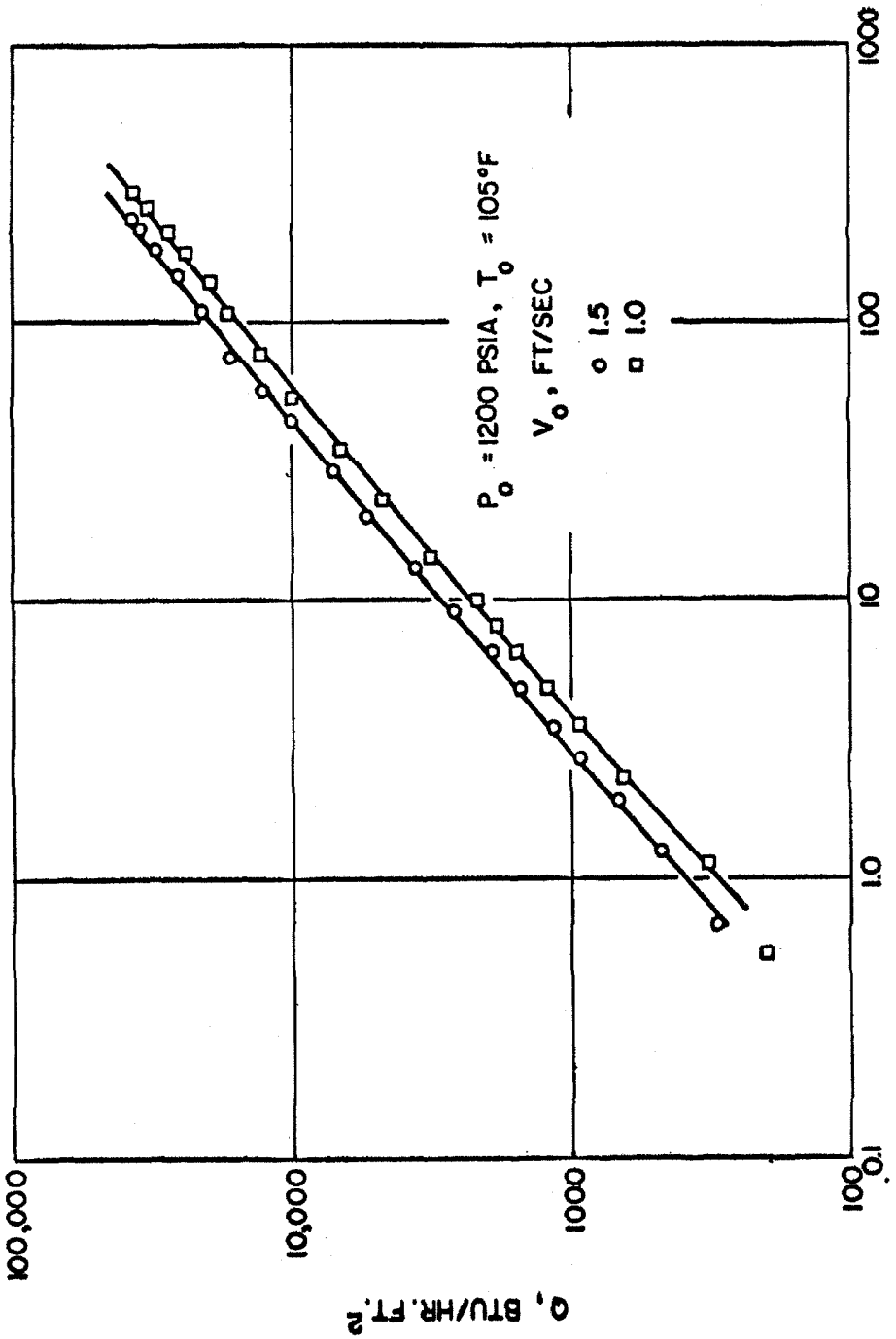


FIG. 24. FORCED CONVECTIVE HEAT TRANSFER FROM A FLAT PLATE TO SUPERCRITICAL $CO_2$ AT 1,200 psia AND 105°F.

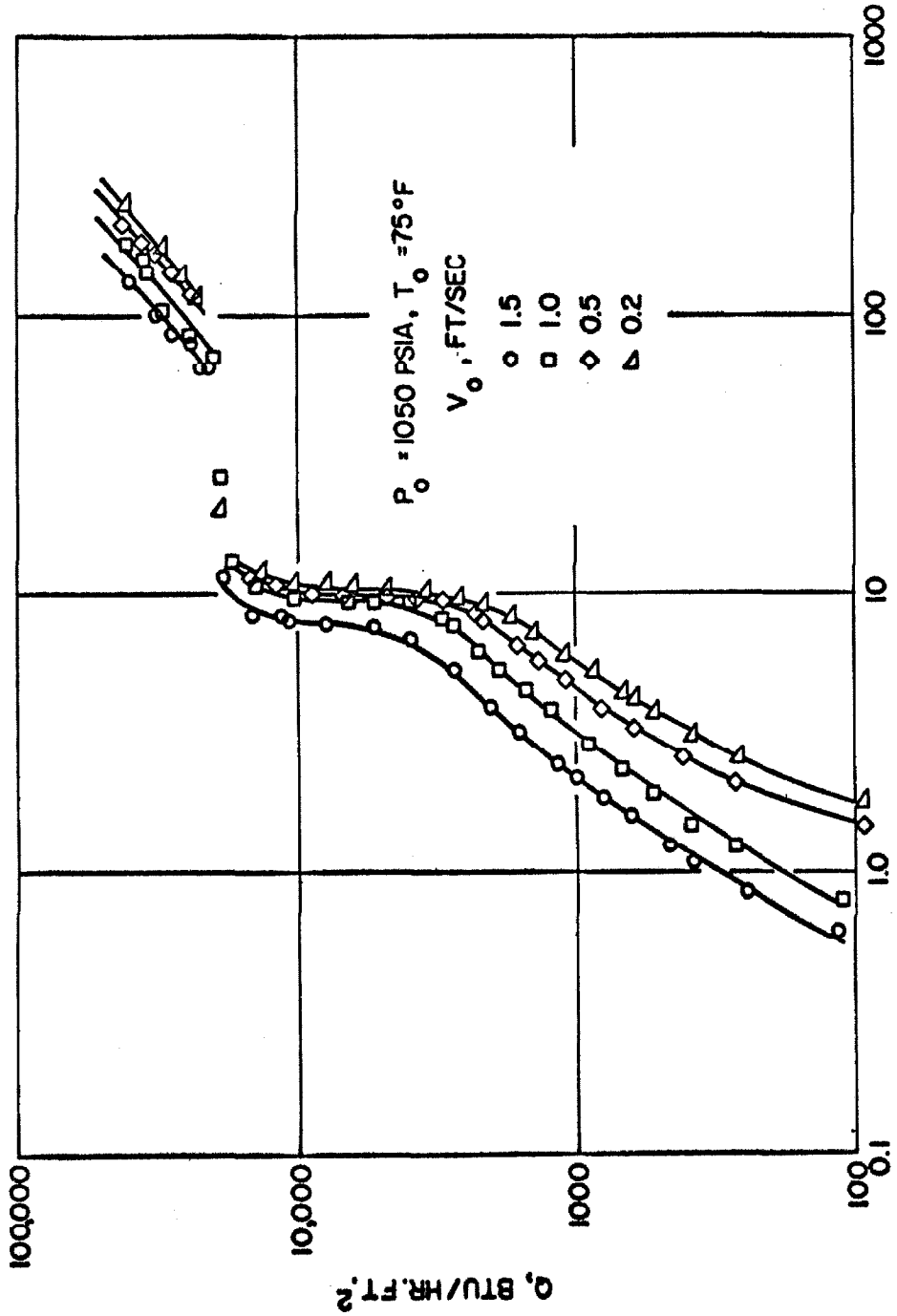


FIG. 25. FORCED CONVECTIVE HEAT TRANSFER FROM A FLAT PLATE TO SUBCRITICAL $CO_2$ AT 1,050 psia AND 75°F.

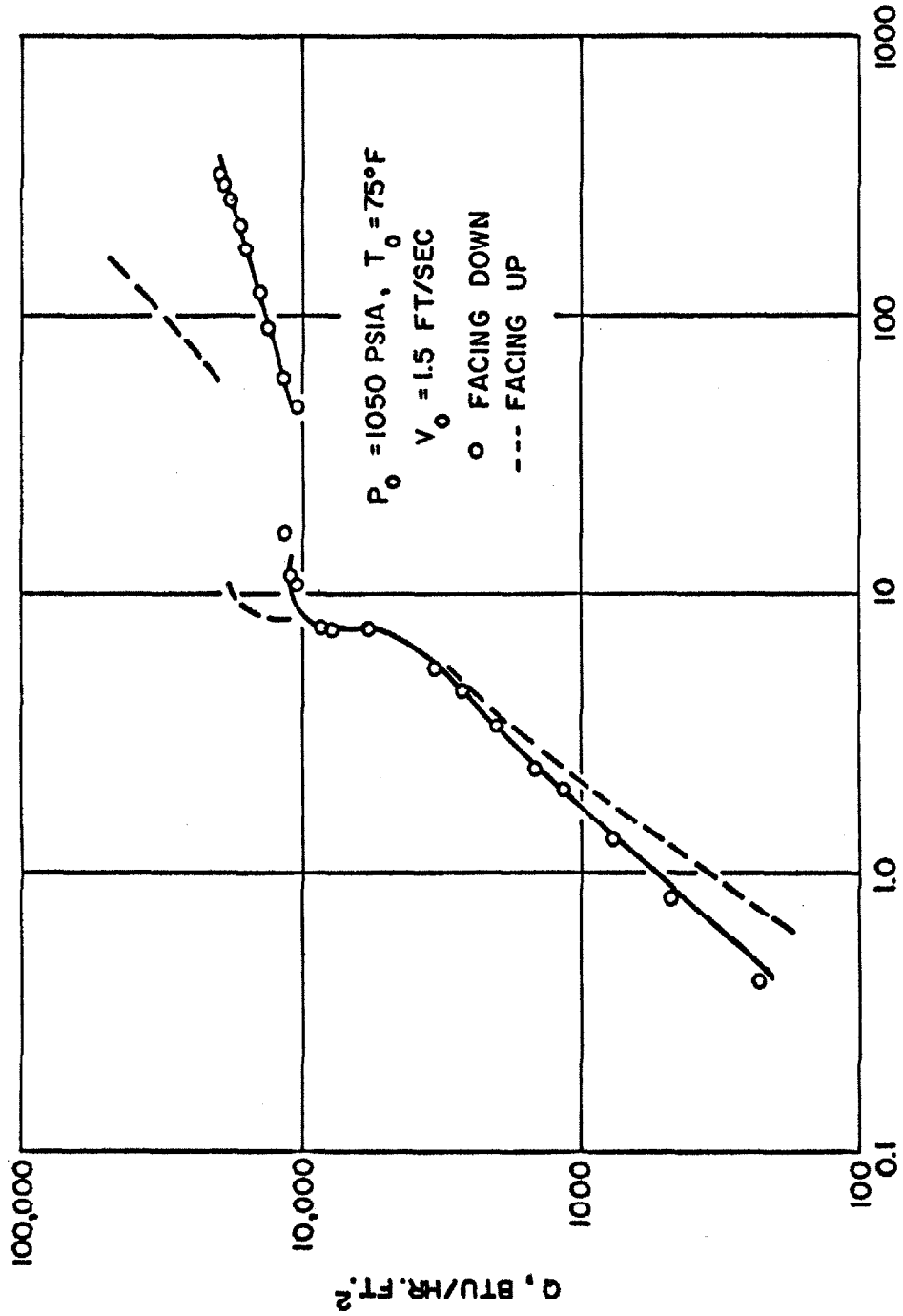


FIG. 26. EFFECT OF GRAVITY ON FORCED CONVECTIVE HEAT TRANSFER FROM A FLAT PLATE TO SUBCRITICAL $CO_2$ AT 1,050 psia AND 75°F.

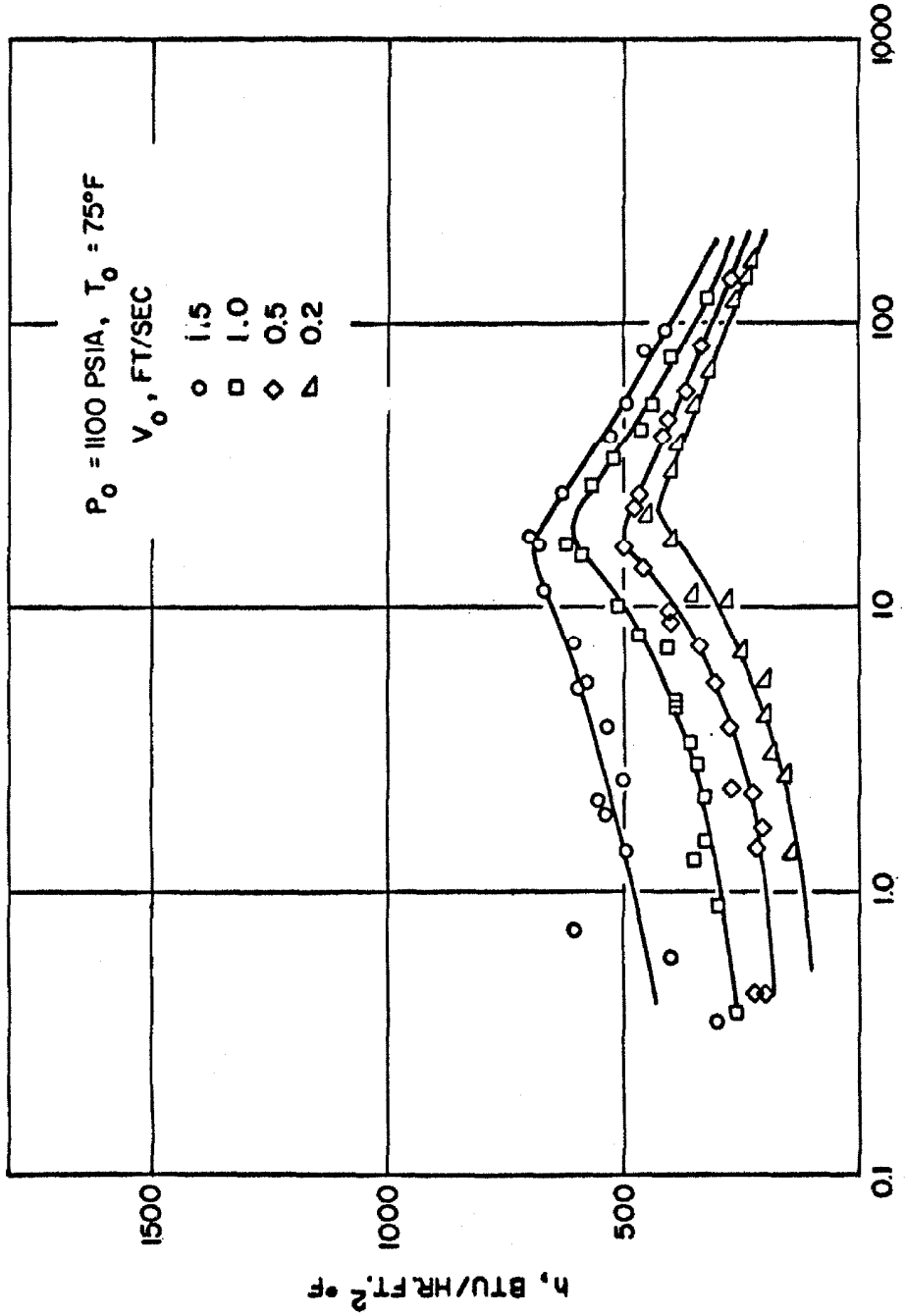


FIG. 27. HEAT TRANSFER COEFFICIENT FOR A FLAT PLATE IN SUPERCRITICAL $CO_2$ AT 1,100 psia AND 75°F.

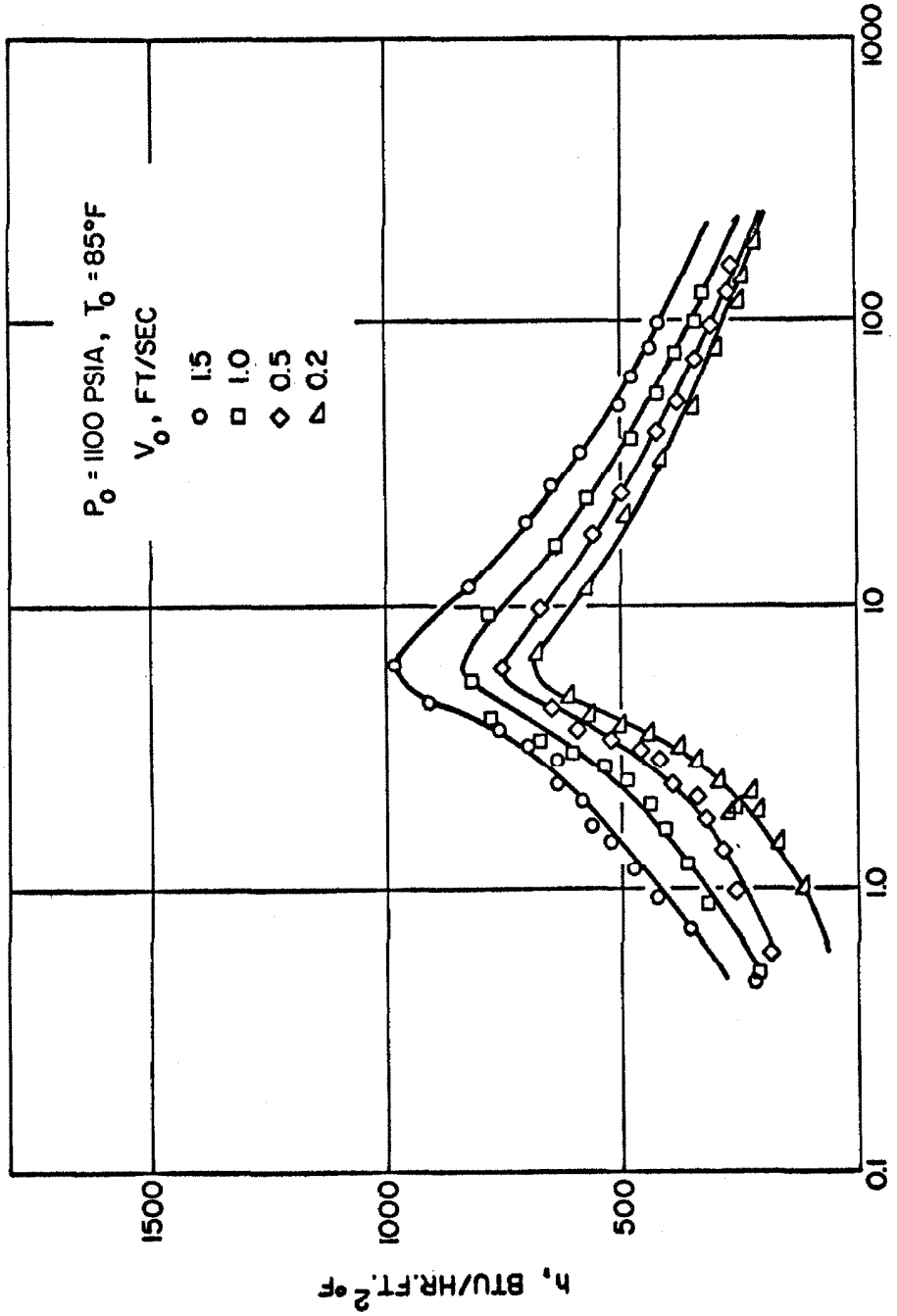


FIG. 28. HEAT TRANSFER COEFFICIENT FOR A FLAT PLATE IN SUPERCRITICAL $CO_2$ AT 1,100 psia AND 85°F.

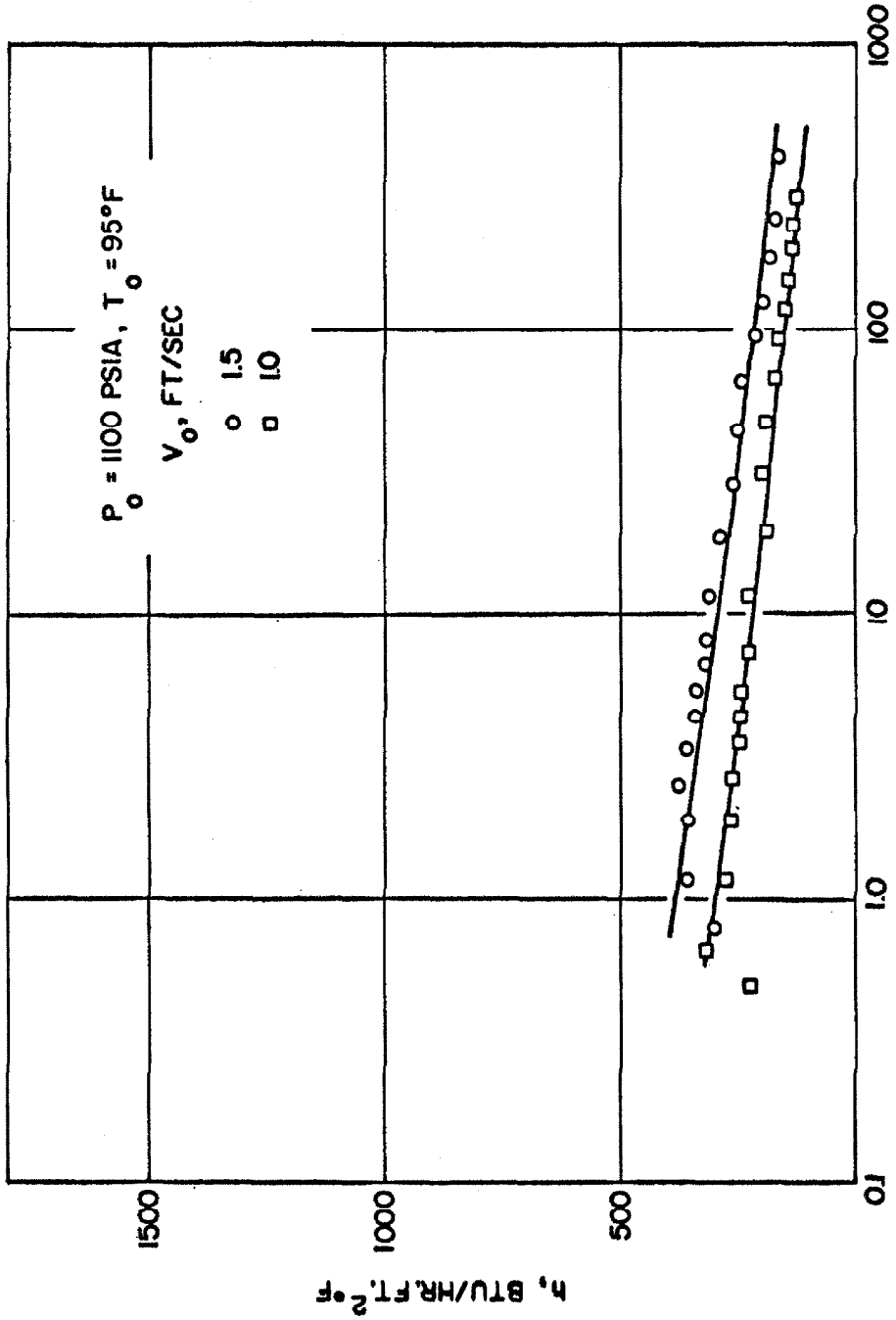


FIG. 29. HEAT TRANSFER COEFFICIENT FOR A FLAT PLATE IN SUPERCRITICAL $CO_2$ AT 1,100 psia AND 95°F.

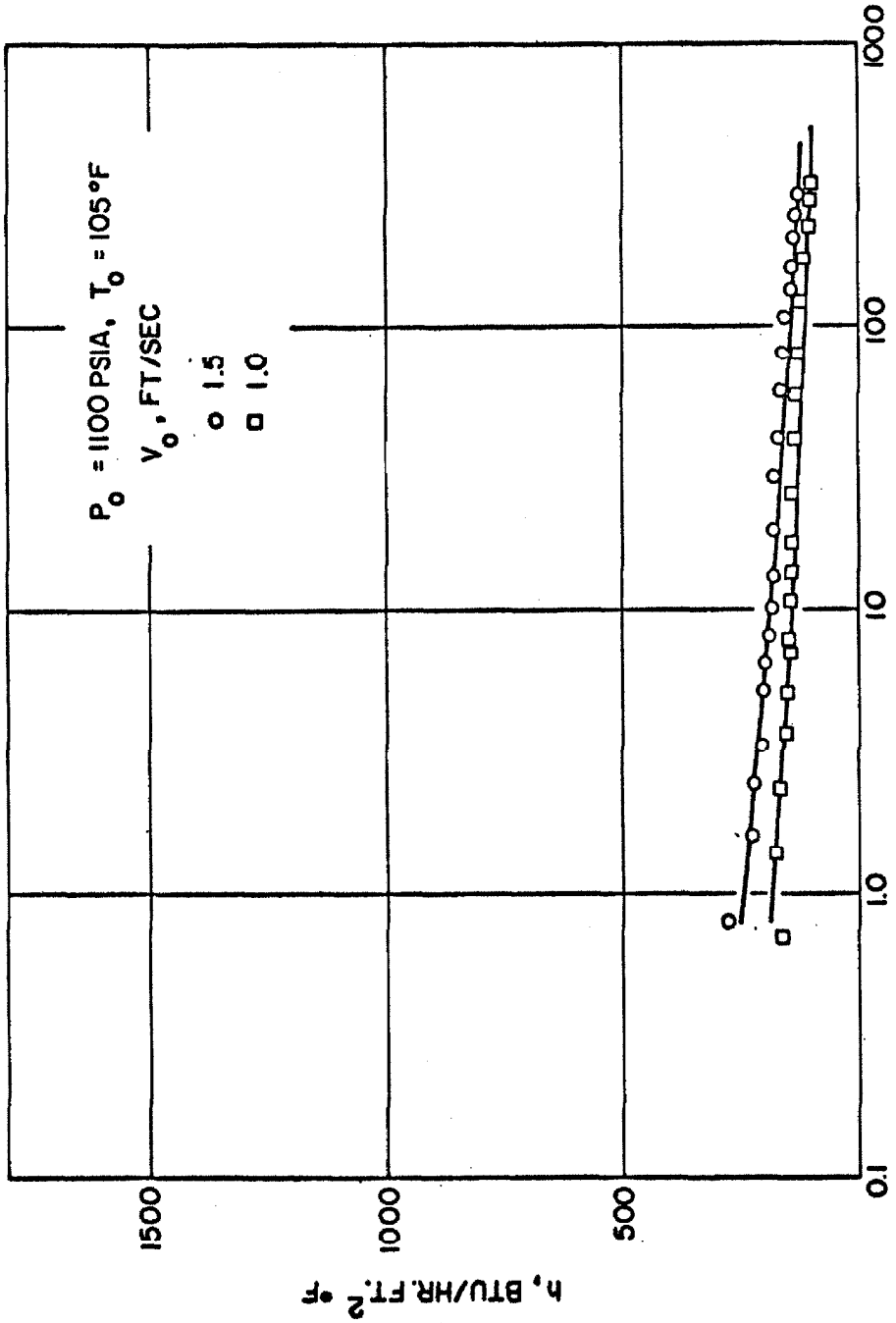


FIG. 30. HEAT TRANSFER COEFFICIENT FOR A FLAT PLATE IN SUPERCRITICAL $CO_2$ AT 1,100 psia AND 105°F.

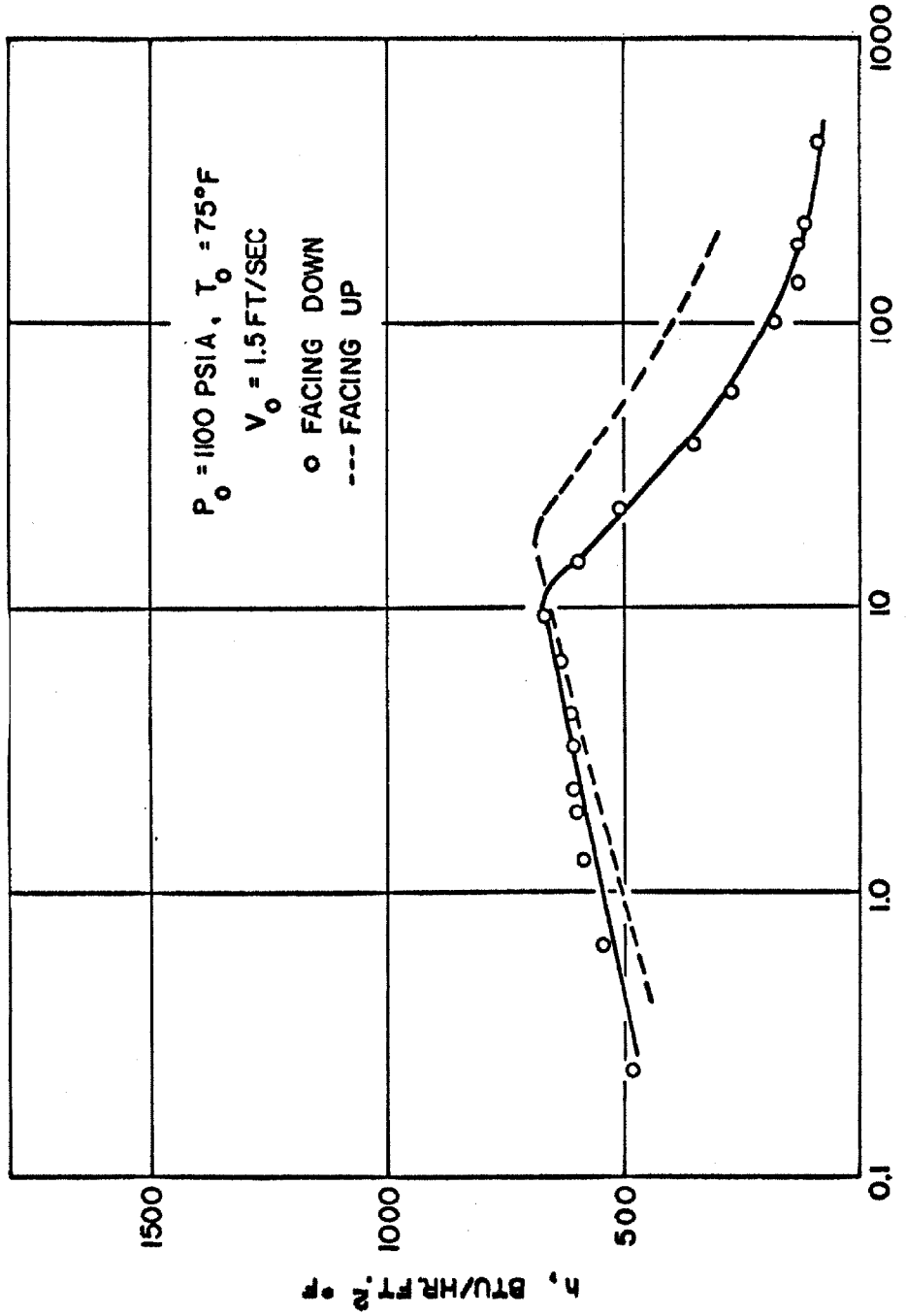


FIG. 31. EFFECT OF GRAVITY ON HEAT TRANSFER COEFFICIENT FOR A FLAT PLATE IN SUPERCRITICAL $CO_2$ AT 1,100 psia AND 75°F.

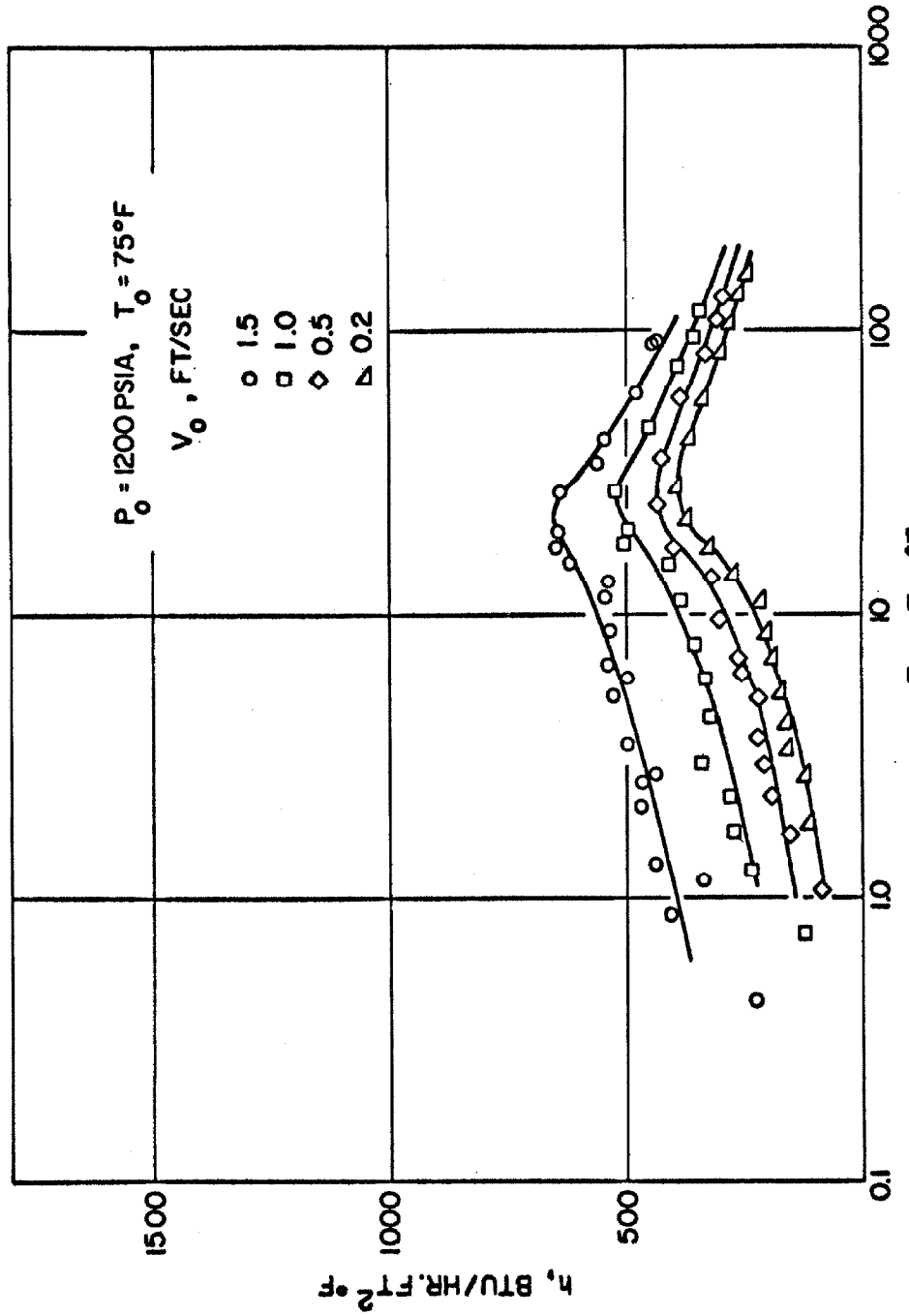


FIG. 32. HEAT TRANSFER COEFFICIENT FOR A FLAT PLATE IN SUPERCRITICAL $CO_2$ AT 1,200 psia AND 75°F.

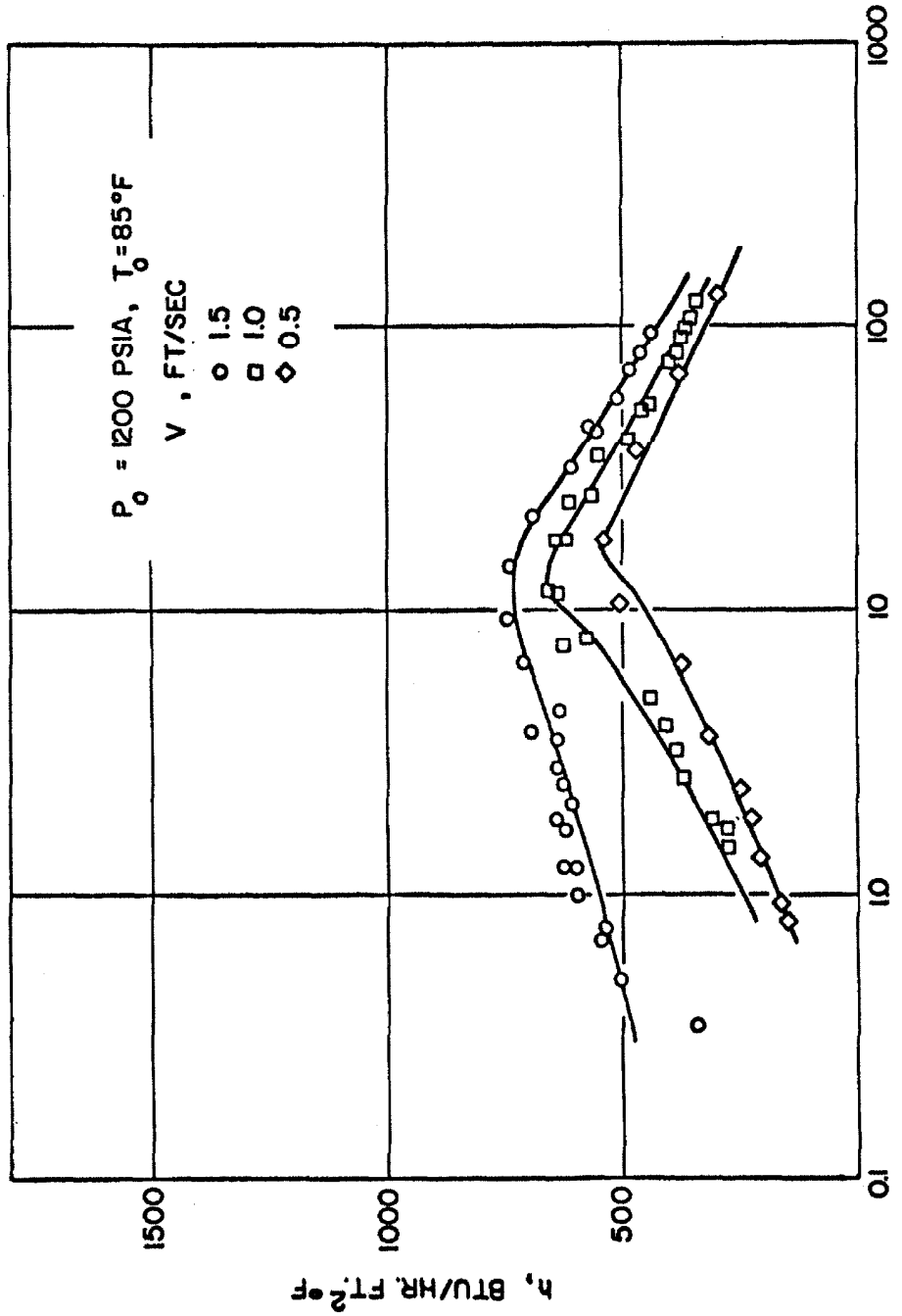


FIG. 33. HEAT TRANSFER COEFFICIENT FOR A FLAT PLATE IN SUPERCRITICAL $CO_2$ AT 1,200 psia AND 85°F.

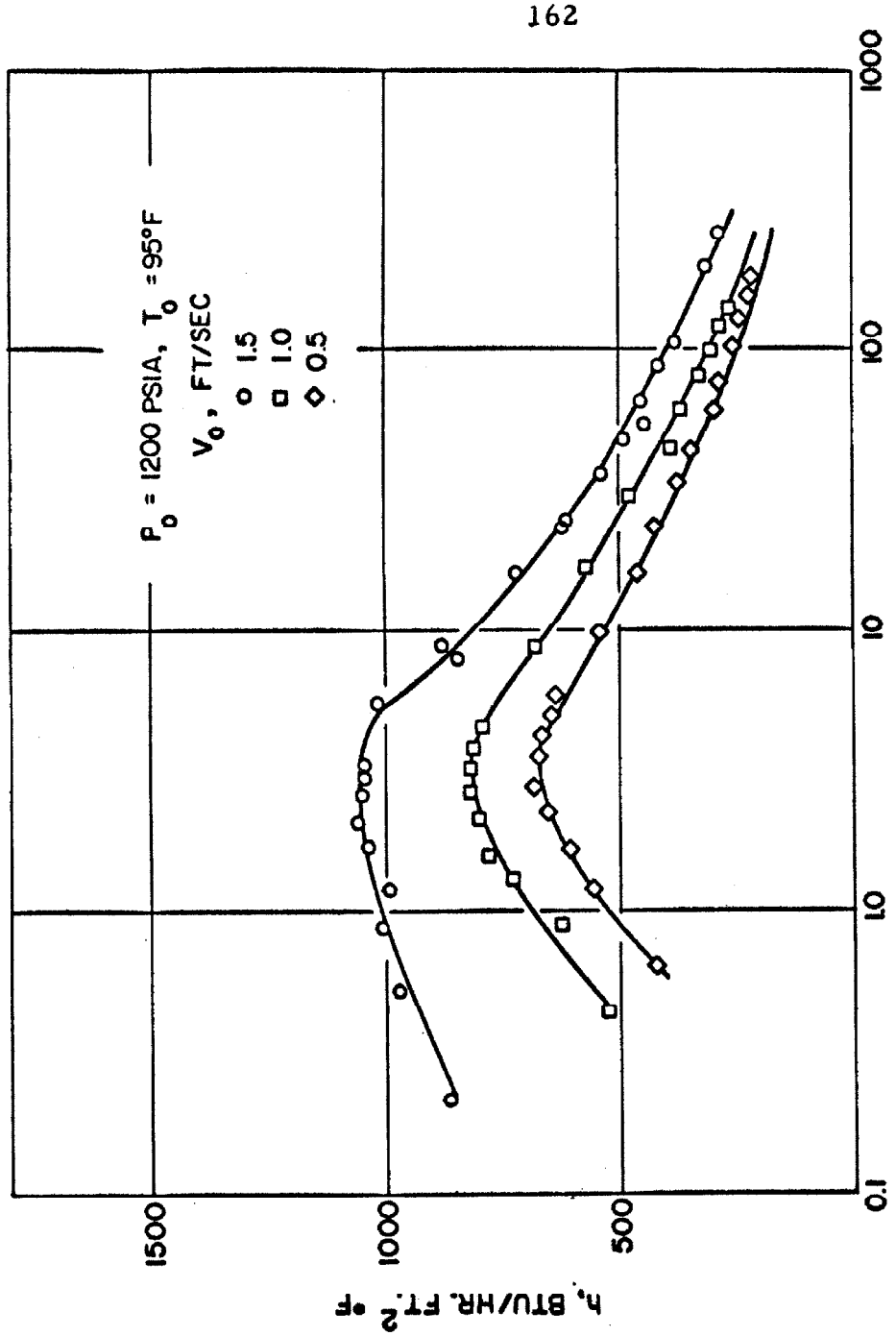


FIG. 34. HEAT TRANSFER COEFFICIENT FOR A FLAT PLATE IN SUPERCRITICAL $CO_2$ AT 1,200 psia AND 95°F.

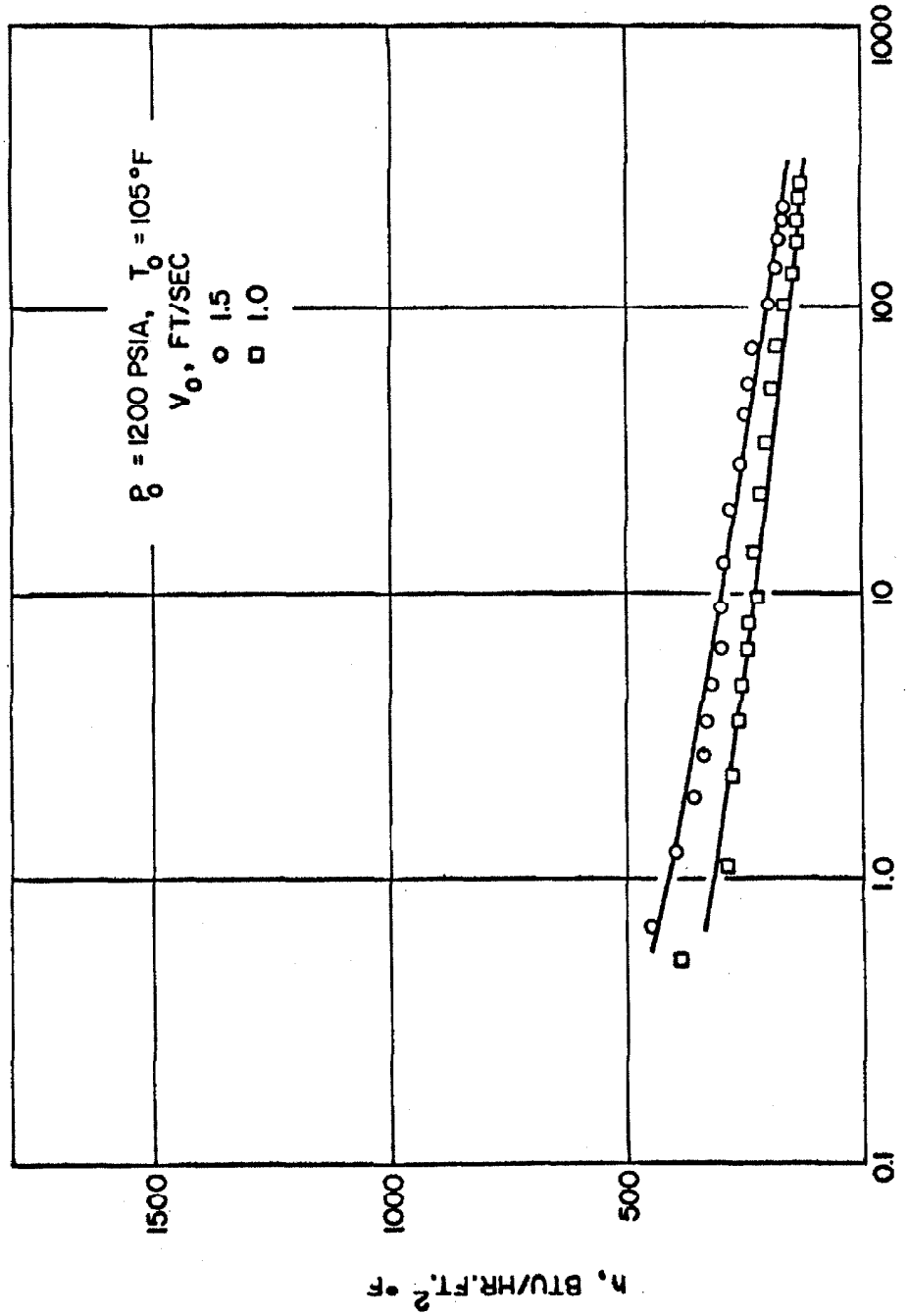


FIG. 35. HEAT TRANSFER COEFFICIENT FOR A FLAT PLATE IN SUPERCRITICAL $CO_2$ AT 1,200 psia AND 105°F.

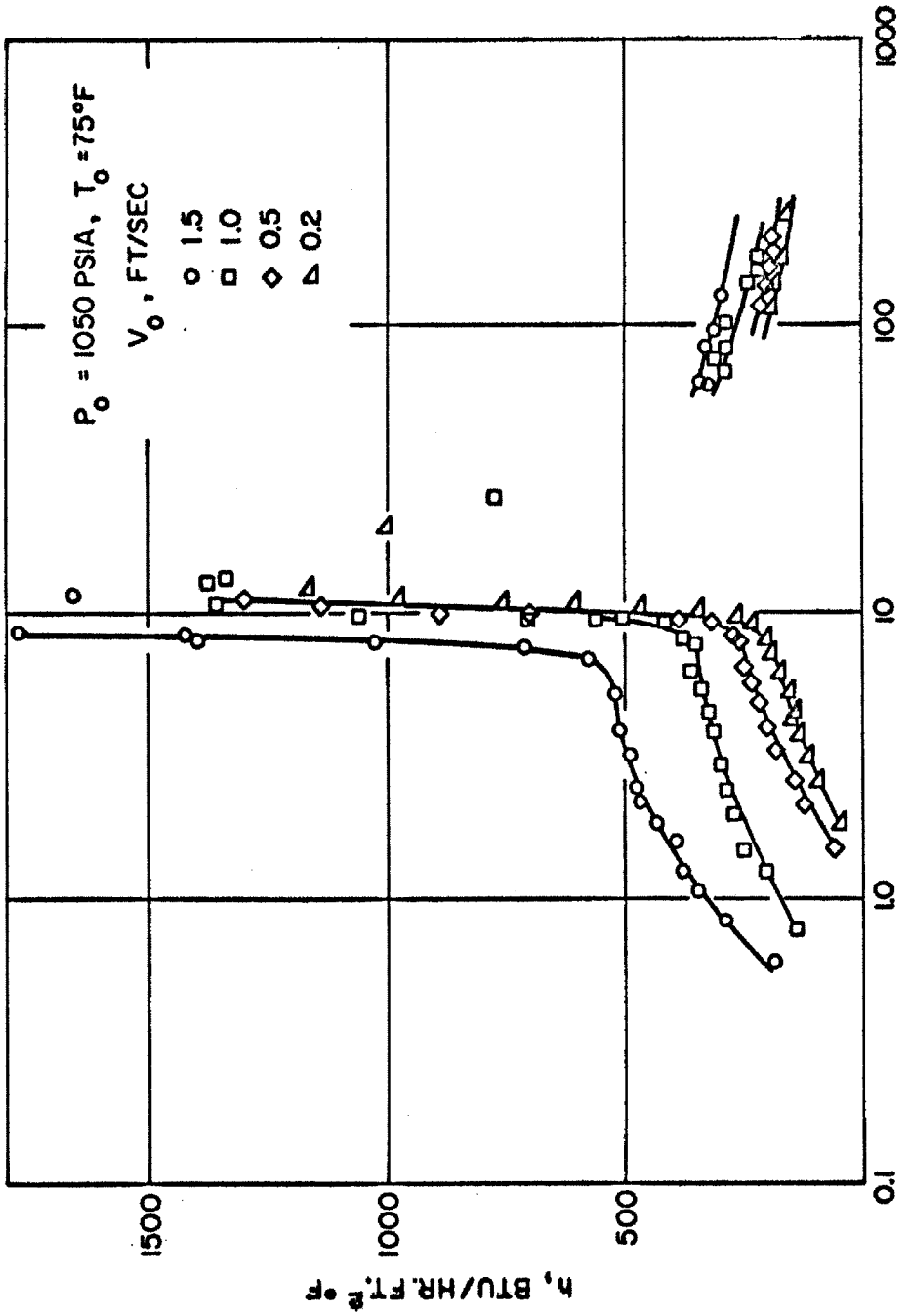


FIG. 36. HEAT TRANSFER COEFFICIENT FOR A FLAT PLATE IN SUBCRITICAL $CO_2$ AT 1,050 psia AND 75°F.

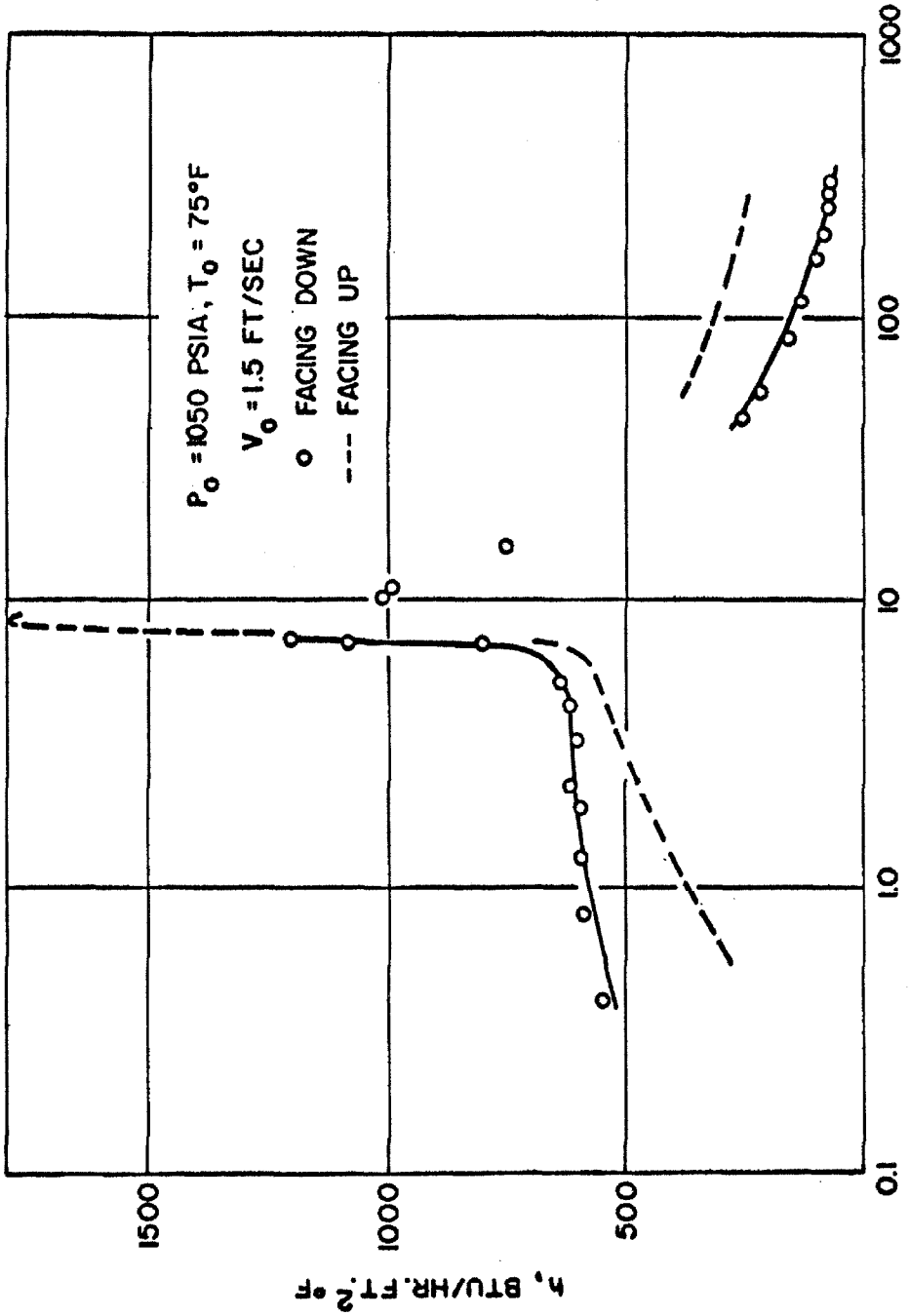


FIG. 37. EFFECT OF GRAVITY ON HEAT TRANSFER COEFFICIENT FOR A FLAT PLATE IN SUBCRITICAL $CO_2$ AT 1,050 psia AND 75°F.

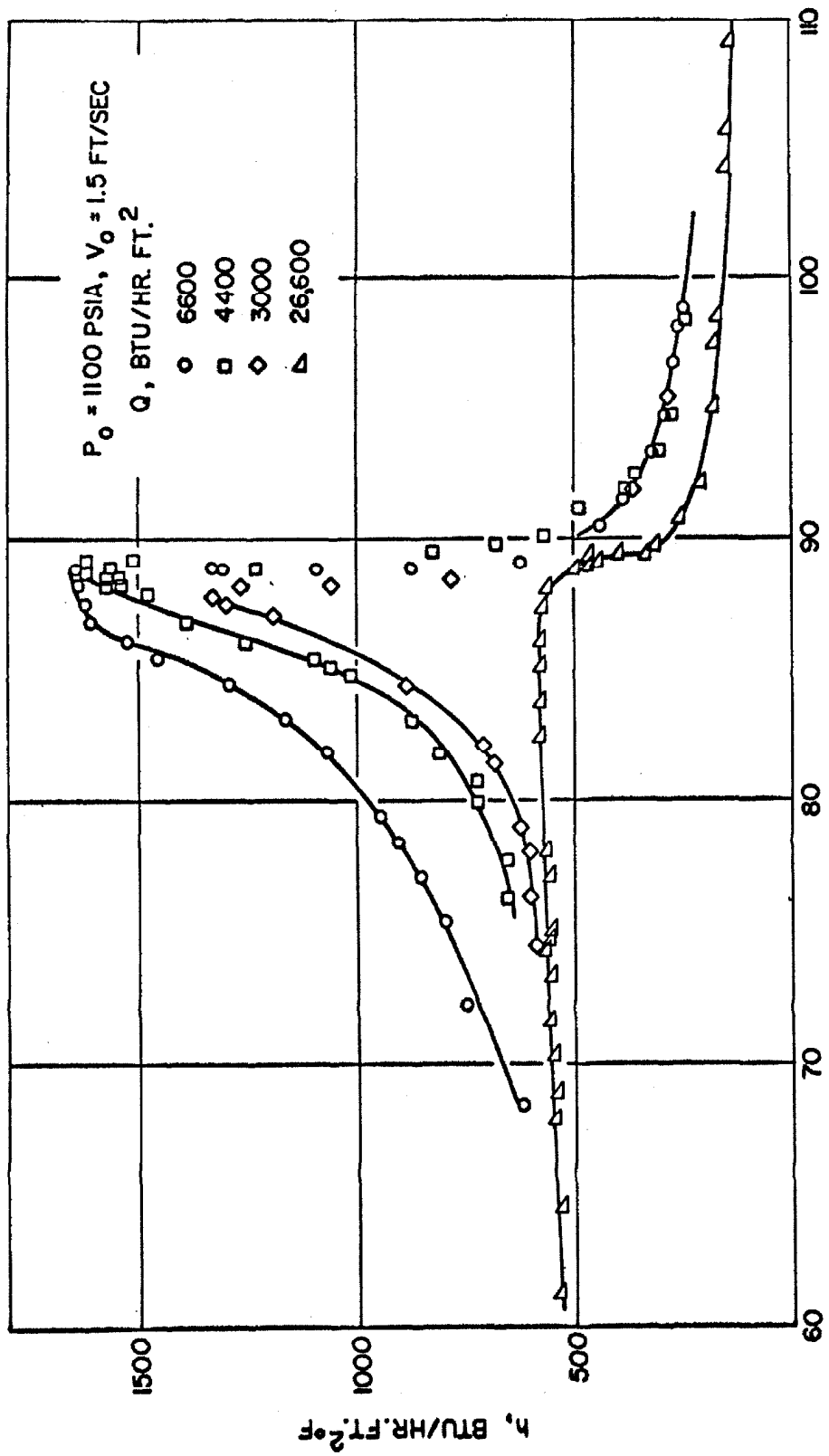


FIG. 38. HEAT TRANSFER COEFFICIENT DEPENDENCE ON FREESTREAM TEMPERATURE FOR A FLAT PLATE IN SUPERCRITICAL $CO_2$ AT 1,100 psia.

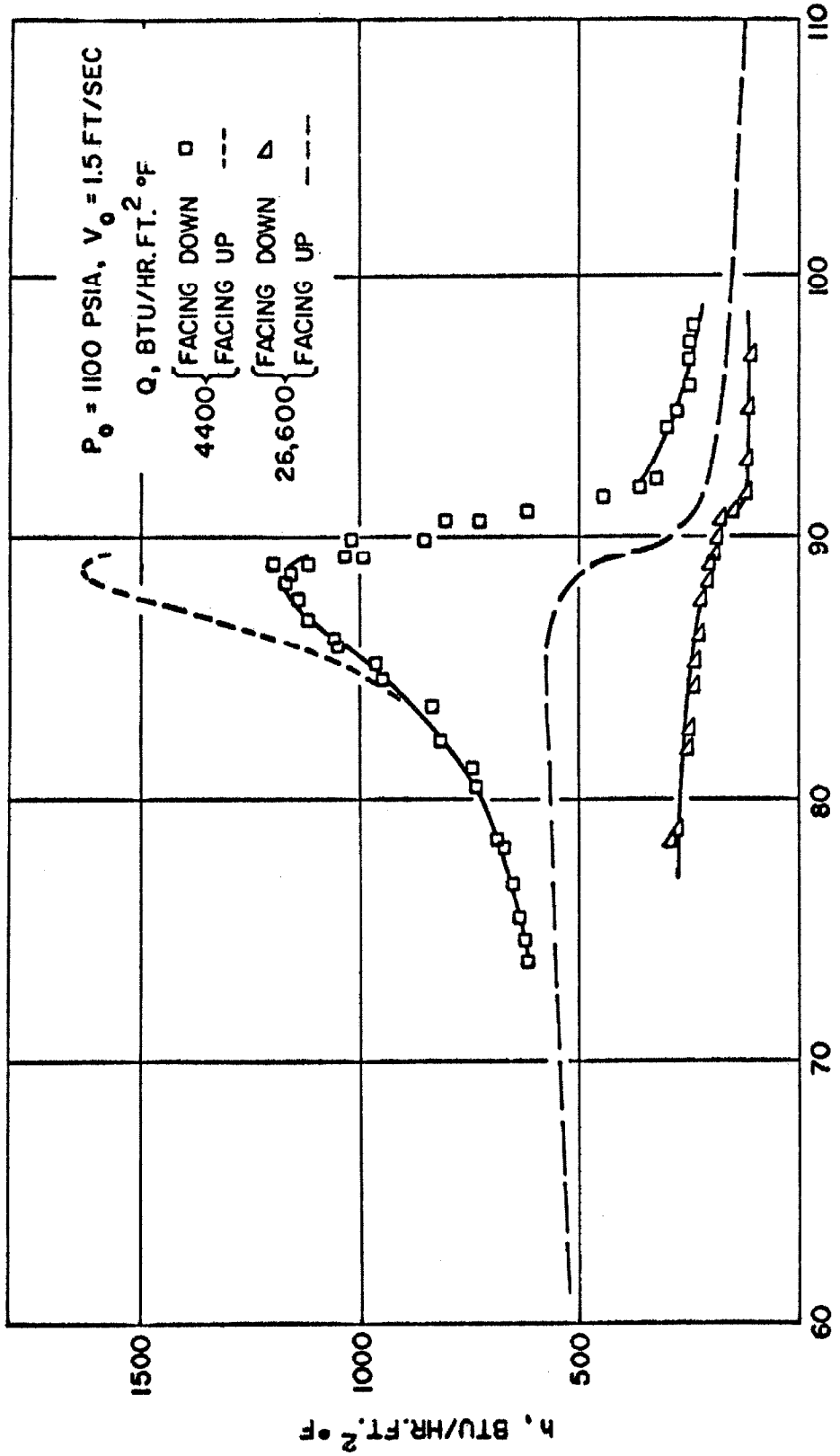


FIG. 39. HEAT TRANSFER COEFFICIENT DEPENDENCE ON FREESTREAM TEMPERATURE FOR A FLAT PLATE FACING DOWNWARDS IN SUPERCRITICAL $CO_2$ AT 1,100 psia.

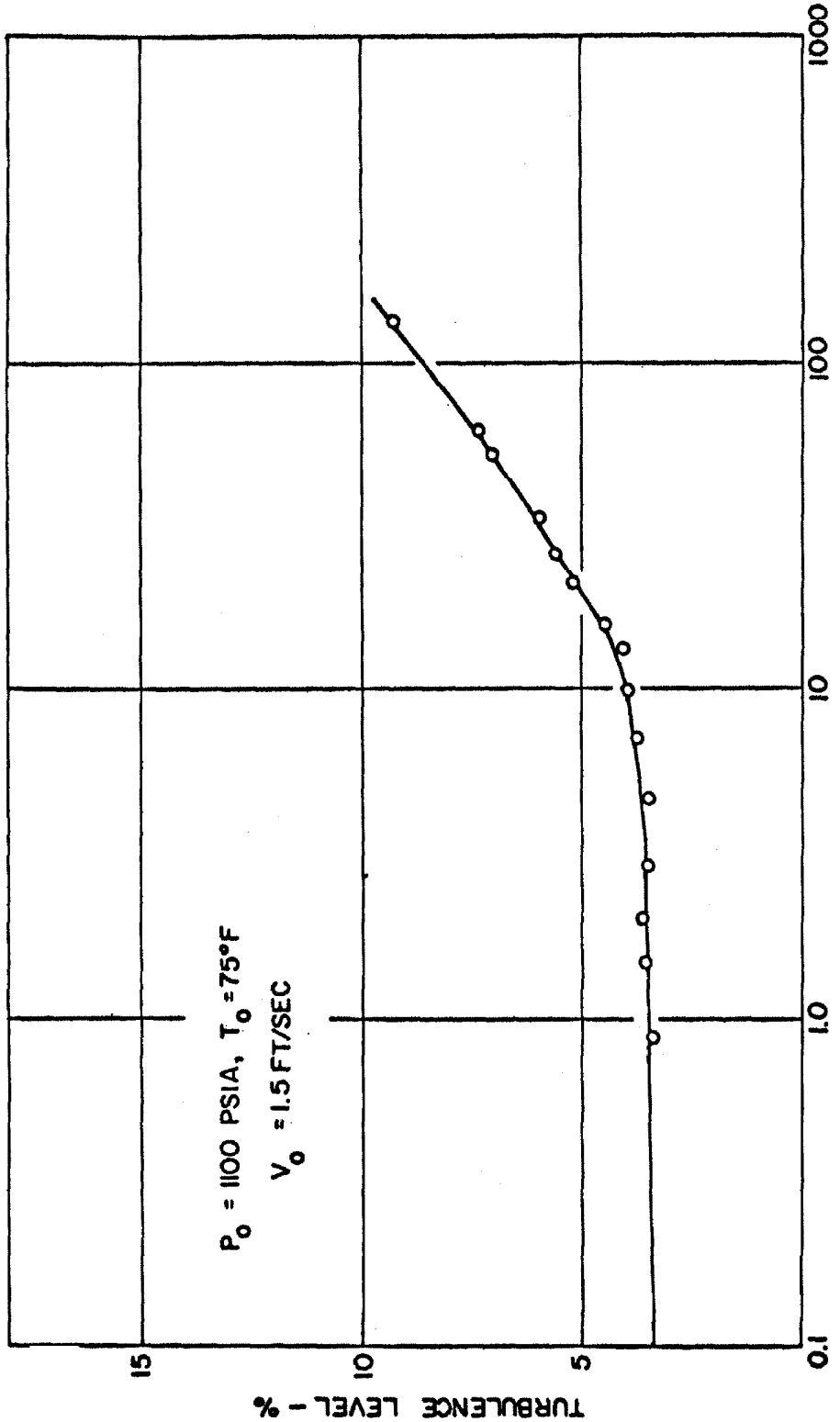


FIG. 40. TURBULENCE LEVELS NEAR A HEATED FLAT PLATE DURING FORCED CONVECTION HEAT TRANSFER TO SUPERCRITICAL $CO_2$ AT 1,100 psia AND 75°F.

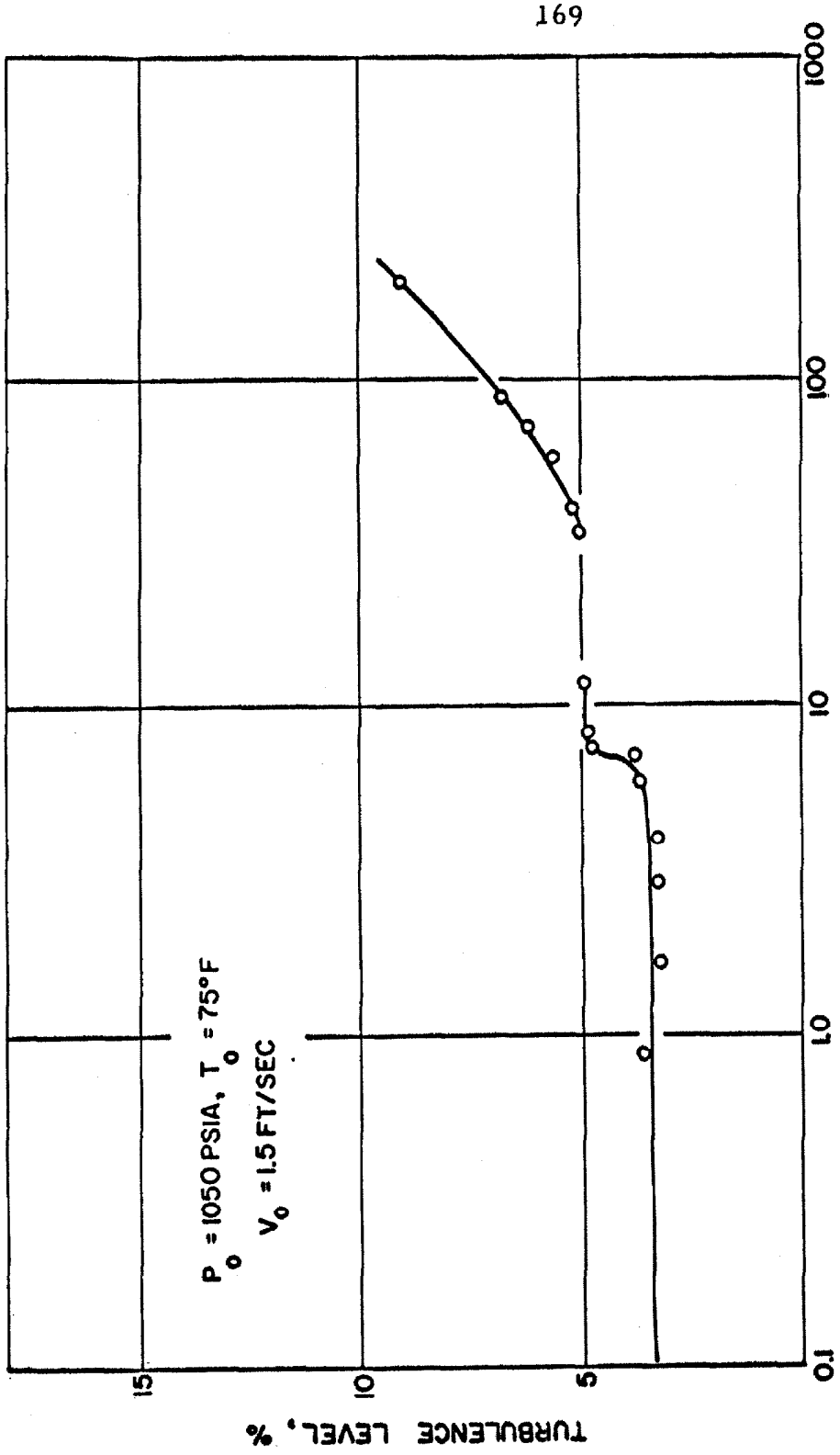


FIG. 41. TURBULENCE LEVELS NEAR A HEATED FLAT PLATE DURING FORCED CONVECTION HEAT TRANSFER TO SUBCRITICAL $CO_2$ AT 1,050 psia AND 75°F.

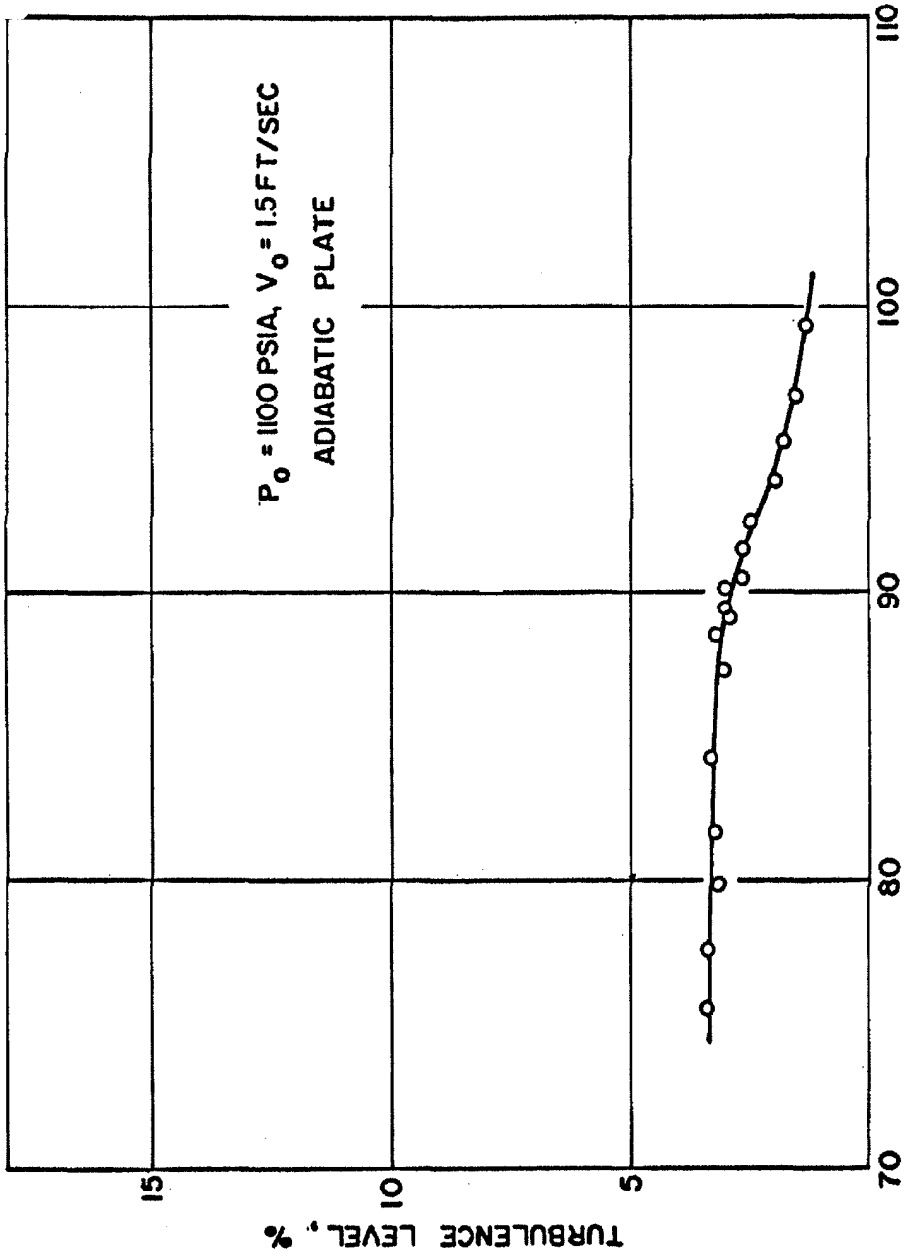


FIG. 42. TURBULENCE LEVELS NEAR AN ADIABATIC FLAT PLATE IN SUPERCRITICAL $CO_2$ AT 1,100 psia.

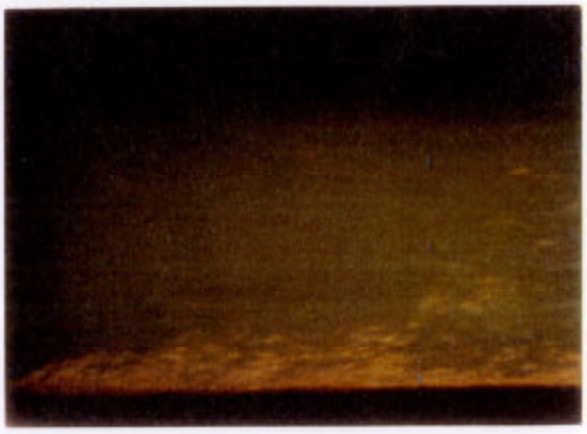

FIG. 43. HEATED FLOW FIELD OVER A FLAT PLATE IN SUPERCRITICAL $CO_2$ AT 1,100 psia AND 75°F. *

($V_o$ = 1.5 ft./sec., $T_w - T_o$ = 3.4°F.)

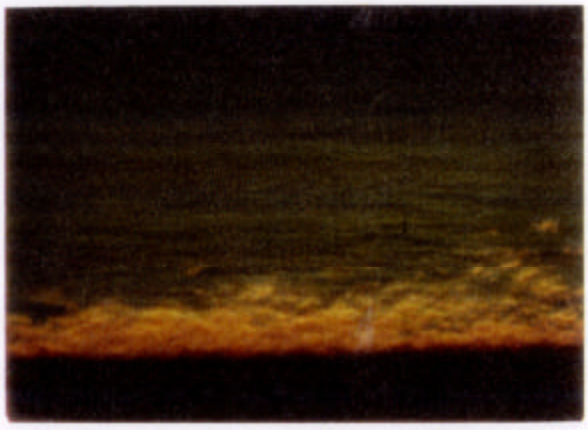

FIG. 44. HEATED FLOW FIELD OVER A FLAT PLATE IN SUPERCRITICAL $CO_2$ AT 1,100 psia AND 75°F. *

($V_o$ = 1.5 ft./sec., $T_w - T_o$ = 8.9°F.)

---

* see p. 175

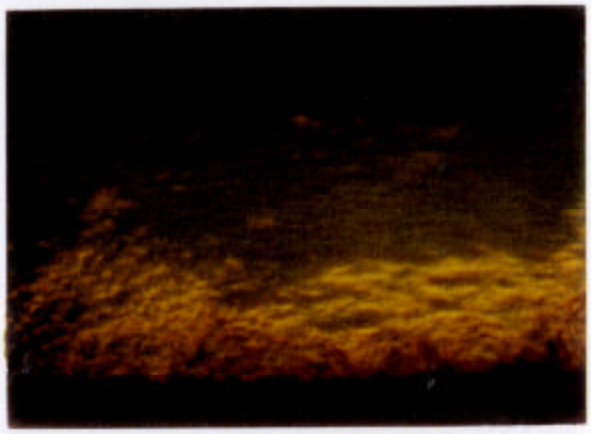

FIG. 45. HEATED FLOW FIELD OVER A FLAT PLATE IN SUPERCRITICAL $CO_2$ AT 1,100 psia AND 75°F. *

($V_o$ = 1.5 ft./sec., $T_w - T_o$ = 17.8°F.)

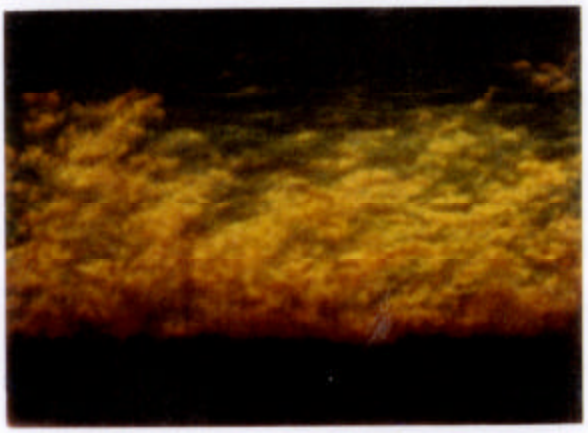

FIG. 46. HEATED FLOW FIELD OVER A FLAT PLATE IN SUPERCRITICAL $CO_2$ AT 1,100 psia AND 75°F. *

($V_o$ = 1.5 ft./sec., $T_w - T_o$ = 60.6°F.)

---

* see p. 175

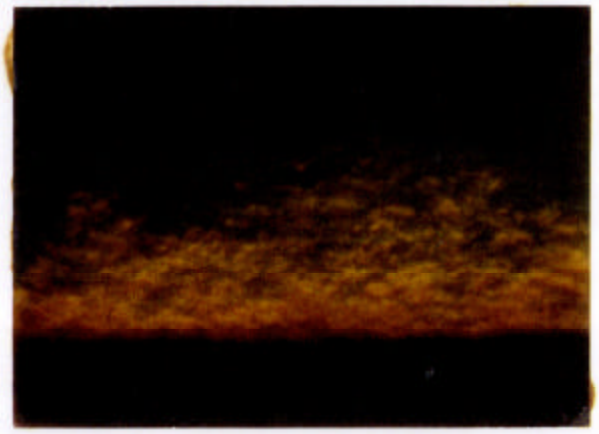

FIG. 47. HEATED FLOW FIELD OVER A FLAT PLATE IN SUPERCRITICAL $CO_2$ AT 1,100 psia AND 87.8°F. *

($V_o$ = 1.5 ft./sec., $T_w - T_o$ = 4.3°F.)

FIG. 48. HEATED FLOW FIELD OVER A FLAT PLATE IN SUPERCRITICAL $CO_2$ AT 1,100 psia AND 105.9°F. *

($V_o$ = 1.5 ft./sec., $T_w - T_o$ = 32.6°F.)

---

* see p. 175

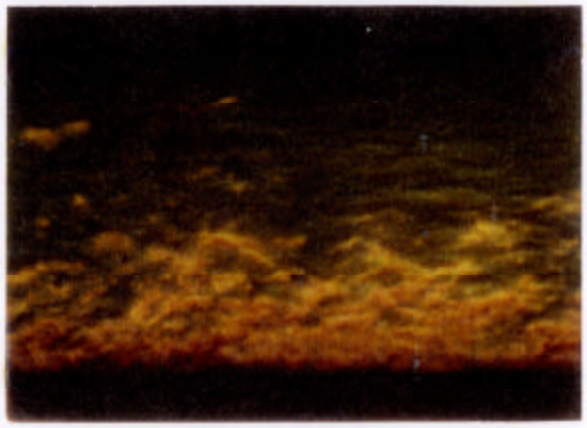

FIG. 49. HEATED FLOW FIELD OVER A FLAT PLATE IN SUPERCRITICAL $CO_2$ AT 1,100 psia AND 124.8°F. *

($V_o$ = 1.5 ft./sec., $T_w - T_o$ = 274.7°F.)

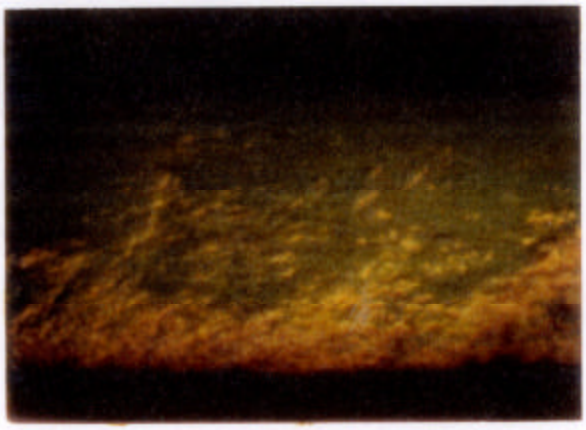

FIG. 50. HEATED FLOW FIELD OVER A FLAT PLATE IN SUBCRITICAL $CO_2$ AT 1,050 psia AND 75°F. *

($V_o$ = 1.5 ft./sec., $T_w - T_o$ = 9.8°F.)

---

* see p. 175

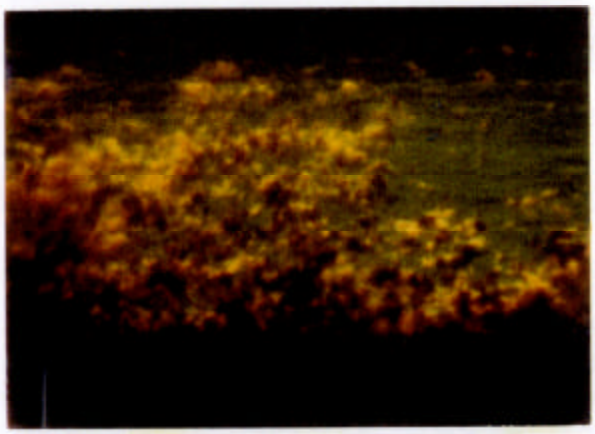

FIG. 51. HEATED FLOW FIELD OVER A FLAT PLATE IN SUBCRITICAL $CO_2$ AT 1,050 psia AND 75°F. *

($V_o$ = 1.5 ft./sec., $T_w - T_o$ = 83.2°F.)

* 7.5" from leading edge, 5 x enlarged.

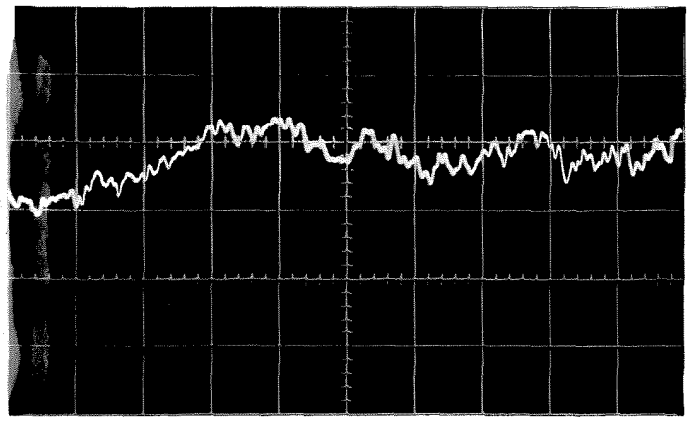

FIG. 52. OSCILLOSCOPE RECORD OF HOT WIRE CURRENT FLUCTUATIONS IN SUPERCRITICAL $CO_2$ AT 1,100 psia AND 75°F. *

(mean wire current 162 milliamps, $V_o = 1.5$ ft./sec., $T_w - T_o = 0°F.$)

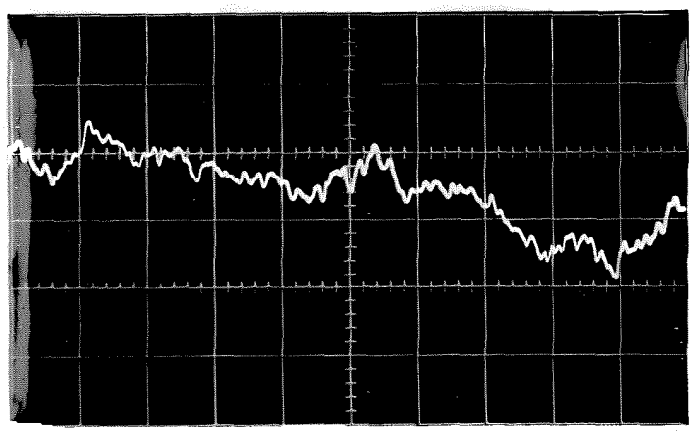

FIG. 53. OSCILLOSCOPE RECORD OF HOT WIRE CURRENT FLUCTUATIONS IN SUPERCRITICAL $CO_2$ AT 1,100 psia AND 75°F. *

(mean wire current 158 milliamps, $V_o = 1.5$ ft./sec., $T_w - T_o = 16.5°F.$)

---

* vertical scale, 1 cm. = 5 milliamps; horizontal scale, 1 cm. = 5 milliseconds.

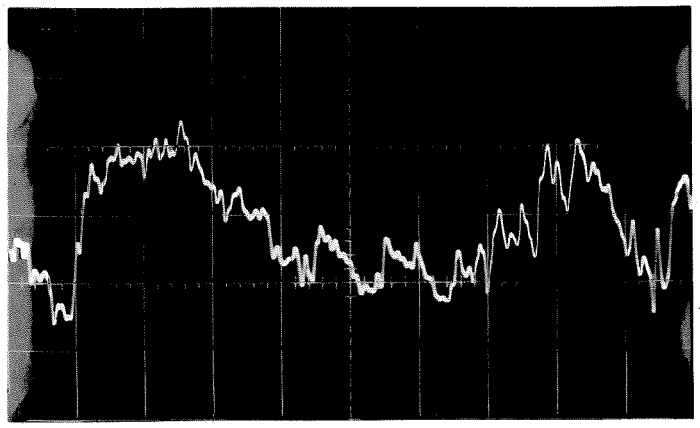

FIG. 54. OSCILLOSCOPE RECORD OF HOT WIRE CURRENT FLUCTUATIONS IN SUPERCRITICAL $CO_2$ AT 1,100 psia AND 75°F. *

(mean wire current 150 milliamps, $V_o$ = 1.5 ft./sec., $T_w - T_o$ = 136.0°F.)

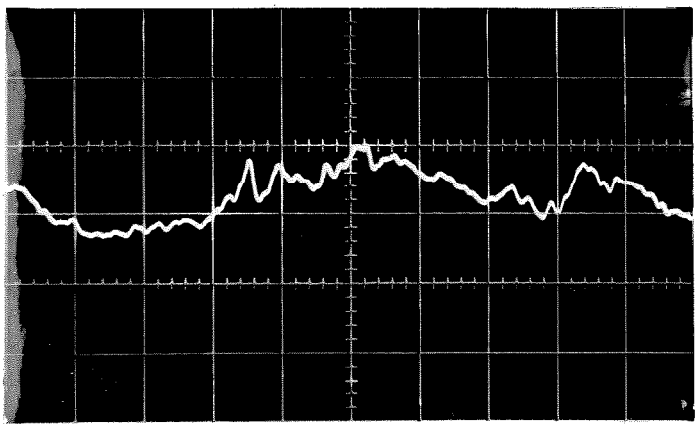

FIG. 55. OSCILLOSCOPE RECORD OF HOT WIRE CURRENT FLUCTUATIONS IN SUBCRITICAL $CO_2$ AT 1,050 psia AND 75°F. *

(mean wire current 143 milliamps, $V_o$ = 1.5 ft./sec., $T_w - T_o$ = 0°F.)

---

* see p. 176

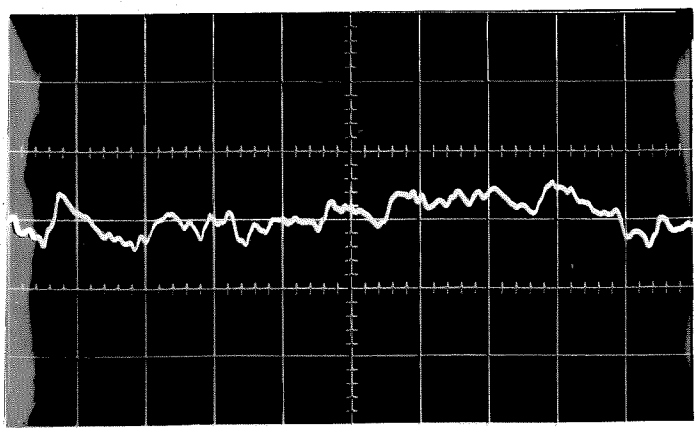

FIG. 56. OSCILLOSCOPE RECORD OF HOT WIRE CURRENT FLUCTUATIONS IN SUBCRITICAL $CO_2$ AT 1,050 psia AND 75°F. *

(mean wire current 136 milliamps, $V_o = 1.5$ ft./sec., $T_w - T_o = 8.3$°F.)

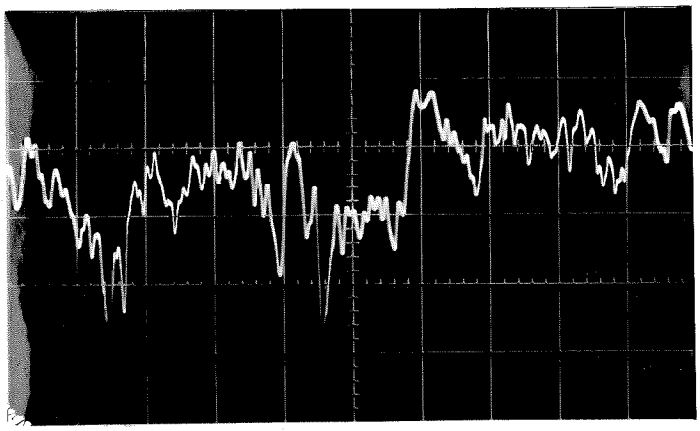

FIG. 57. OSCILLOSCOPE RECORD OF HOT WIRE CURRENT FLUCTUATIONS IN SUBCRITICAL $CO_2$ AT 1,050 psia AND 75°F. *

(mean wire current 140 milliamps, $V_o = 1.5$ ft./sec., $T_w - T_o = 195.8$°F.)

---

* see p. 176

# Appendix D

# OPTICAL PRINCIPLES OF SCHLIEREN SYSTEMS

# Appendix D

## OPTICAL PRINCIPLES OF SCHLIEREN SYSTEMS

### 1. General Considerations

Schlieren optical systems enable visualization of inhomogeneous flows by forming images of varying intensity on the film plane of the system. The intensity at any point on the film plane is proportional to the gradient in refractive index occurring in the conjugate point in the flow field. Since the refractive index is a simple function of density (or equivalently temperature) for most fluids, the flow streamlines and fluid temperature can be inferred from photographs taken with such systems.

A particularly simple type of schlieren system is shown in Figure 58. A point source of light is situated at the focal point $f_1$ of the lens $L_1$, producing a collimated beam of light which passes through a test section and is collected by a second lens $L_2$, which then forms an image of the source at its focal point $f_2$. If the light rays are undisturbed, an opaque knife-edge may be inserted at $f_2$ and adjusted so that all the light just passes below its edge and forms an image on the film plane.

If the flow at some point P is now heated, the light passing through this point will be deflected through some angle $\epsilon$ due to the

change in refractive index of the fluid which occurs. The deflected light no longer reaches the film plane, but is intercepted at the knife edge, thereby reducing the illumination as its conjugate point P . The angle $\epsilon$ can easily be shown to be proportional to the gradient in refractive index (or density), and length of disturbance path (93).

If the "point" source has the shape of a rectangle of width b and height h, and both lenses $L_1$ and $L_2$ have equal focal lengths f for simplicity, the illumination $I_o$ on the film in the absence of disturbances or knife edges is given as

$$I_o = \frac{Bbh}{(mf)^2} \quad ,$$

where B is the luminance of the source, and m is the magnification of an image at P on the film plane (94). When the knife edge is adjusted so that for no disturbances in the test section all but a height a of the image is cut off as shown in Figure 59, the general illumination on the film plane falls to

$$I = \frac{Bba}{(mf)^2} \quad .$$

If the light passing through the test section is deflected through an angle $\epsilon$ in the x-y plane, the corresponding image on

the film plane is reduced by an amount

$$\delta I = \frac{Bb\epsilon}{m^2 f} \quad .$$

Thus the contrast of this part of the film plane with respect to the background is given by

$$C = \frac{\delta I}{I} = \frac{f\epsilon}{a} \quad ,$$

and the sensitivity of the system by

$$S = \frac{dC}{d\epsilon} = \frac{f}{a} \quad .$$

The knife edge is usually adjusted so that $2a = h$, thus giving equal sensitivity for upward and downward deflections. The sensitivity of the system is then inversely proportional to the source height, and very small sources must be used for good sensitivity.

When the range of the system (defined as the maximum deflection of the source image $f_2\epsilon$ ) is larger than the height of the source h, the knife edge produces a non-linear response to density disturbances and is usually replaced by a graded filter (94).

2. Depth of Field Criteria

In conventional schlieren systems the light rays traversing the working section are not perfectly parallel, but are inclined at some angle with respect to each other owing to the finite size of source, as shown in Figure 60 (the size of the source is enlarged for clarity). The maximum inclination of the rays $\alpha$ is related to the source height $h$ and focal length $f$ by the expression

$$\alpha = \frac{h}{f} \quad .$$

A point $P$ in the image plane (the plane conjugate to the lens $L_2$ and the film plane) is illuminated by a cone of light subtending the angle $\alpha$ and forms a point image at $P'$ on the film plane. If the point is moved towards the lens $L_2$ it still is illuminated by a cone of light having the same angle $\alpha$, but its image is now moved to some new point $P'$ off the film plane as shown in Figure 61. The image of the point on the film plane is a finite sized disc rather than a perfect point. Small discs of light may not be distinguishable from points because of the resolution limitations of the film plane (or human eye). The largest disc which does not lead to appreciable blurring of the image is called the "circle of confusion", and occurs when $P$ is a distance $X_1$ away from the lens $L_2$. For a finished print, a circle of confusion approximately 0.25 mm. in diameter is

about the largest that most persons find tolerable for viewing at normal reading distance (59). In a similar manner, the point P can be moved a distance $X_2$ away from the lens $L_2$ before appreciable blurring occurs at the film plane, as is shown in Figure 62. The distance $X_2-X_1$ is called the "depth of field". From simple geometrical optics it can be shown that for X larger than f (the situation most commonly occuring in practice)

$$X_2 - X_1 = \frac{2c(X-f)}{\alpha f} \quad ,$$

where c is the diameter of the circle of confusion. Hence for given c, X and f, the depth of field is inversely proportional to the angle $\alpha$. Since normal schlieren systems have very small divergence angles $\alpha$ a considerable region of disturbances on either side of the image plane will appear in sharp focus at the film plane.

In optical systems such as cameras or the human eye, the angle $\alpha$ is determined by the lens aperture and object distance. For example, it is difficult to estimate relative positions of distant objects when one eye is covered, since the angle subtended by the eye is small and the depth of field large. Using both eyes, $\alpha$ becomes much larger and the depth of field is appreciably reduced. This is also the reason for the large depth of field obtained when a camera lens is stopped down to higher f/numbers.

3. Semi-Focusing Schlieren Arrangement

In a conventional schlieren system with fixed focal length lenses and test section geometry, the depth of field can only be reduced by increasing the divergence angle $\alpha$, which in turn can only be performed by increasing the source height h. However the description in Part 1 of this Appendix shows that increasing the source height decreases the sensitivity of the system, which is not desirable.

The semi-focusing schlieren system superimposes many conventional "point source" schlieren systems, each with its corresponding knife edge, so that the "parallel" beams from the separate point sources traverse the working section at an angle $\beta$ as shown in Figure 63. If the individual knife edge are initially set up in an identical fashion, the sensitivity of the system as a whole is equal to the sensitivity of an individual point source - cutoff combination, which can be made very large. However the light entering the lens $L_2$ can now be considered as being contained within a cone of angle $\beta$, where $\beta$ is given by

$$\beta = \frac{H}{f} \quad .$$

The quantity H is the maximum spacing between individual point sources, and is limited only by the geometry of the test section

and aperture of the lens $L_2$. Hence the depth of field for the entire system is inversely proportional to H, and can be reduced to an acceptable value without decreasing the sensitivity of the system.

It should be noted that each individual point source-cutoff combination still has a very large depth of field, and accordingly produces a sharp image of disturbances over a large portion of its optical path. However the images from the remaining individual schlieren systems will be superimposed onto this image, and only disturbances within the depth of field of the system as a whole can add up exactly to form a sharp image on the film plane. Thus the system "focuses" by blurring out regions outside the depth of field of the entire system.

The use of a semi-focusing system for studying flows near an opaque wall (boundary layer flows) is somewhat restricted because of reflections from the wall. For example with a horizontal flat plate, only horizontal light rays should pass through the working section in order to prevent spurious reflections off the plate from affecting the image. The source geometry for this case is restricted to either a horizontal row of point sources, or a thin horizontal slit (57).

Finally it should be mentioned that semi-focusing schlieren

systems are much more difficult to align than conventional systems, and great pains must be taken to insure that the source and cutoff plates are identical or else severe reduction in the quality of the image will occur. However in some instances these disadvantages may be compensated for by the ability to use optical components of reduced quality and price. A discussion of the merits of semi-focusing schlieren systems has been given by Fish and Parnham (96).

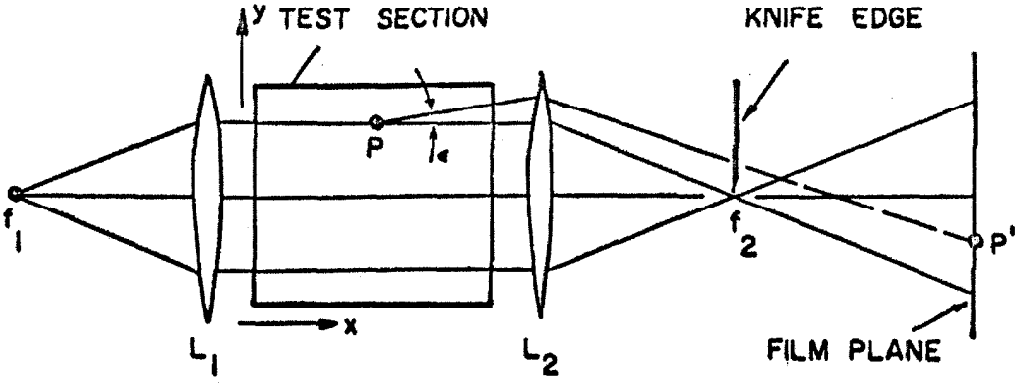


FIG. 58. CONVENTIONAL SCHLIEREN SYSTEM.

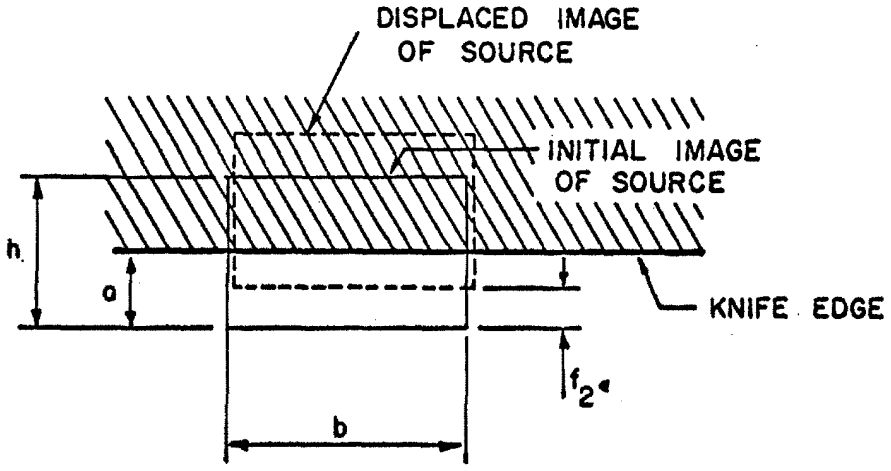


FIG. 59. OPERATION OF THE KNIFE EDGE.

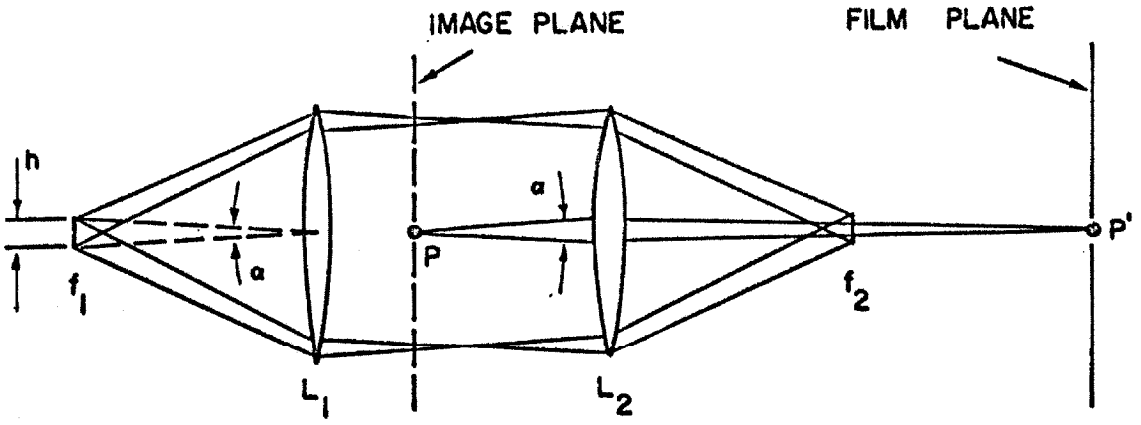


FIG. 60. THE REGION OF ILLUMINATION IN A CONVENTIONAL SCHLIEREN SYSTEM.

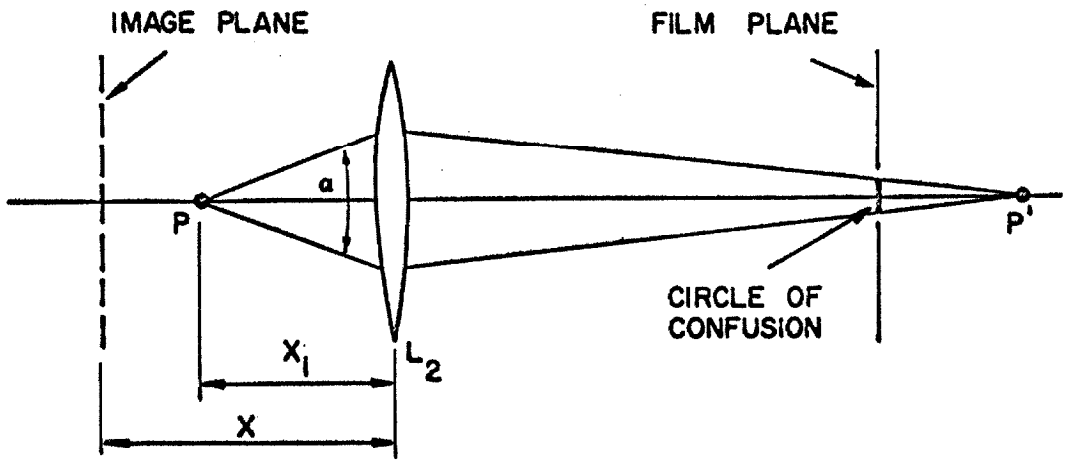


FIG. 61. IMAGE FORMATION FOR A POINT DISPLACED TOWARDS THE LENS.

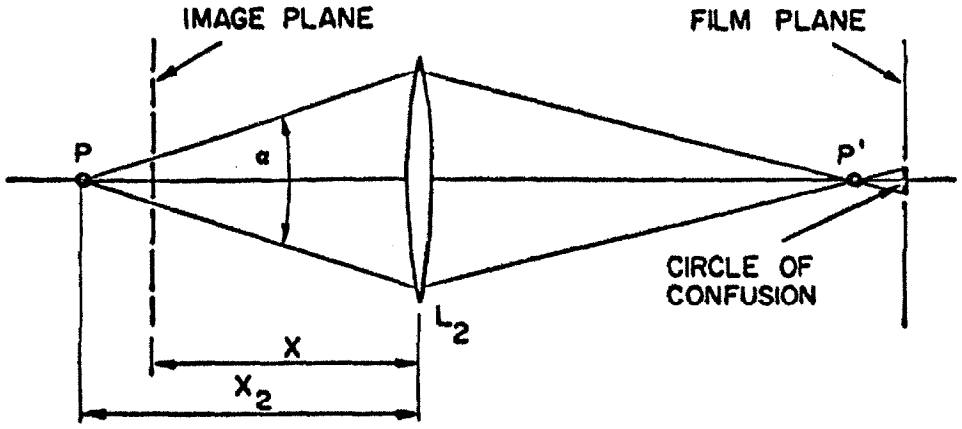


FIG. 62. IMAGE FORMATION FOR A POINT DISPLACED AWAY FROM THE LENS.

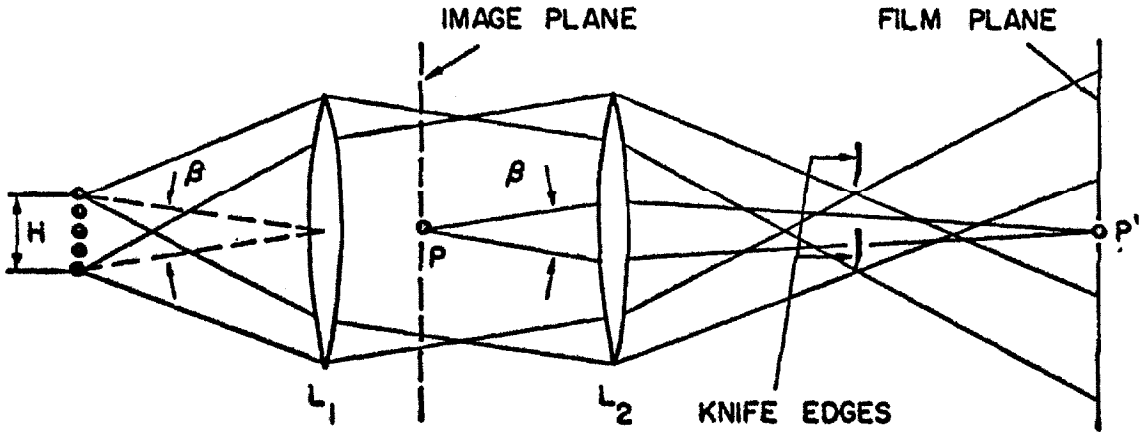


FIG. 63. SEMI-FOCUSING SCHLIEREN SYSTEM

# Appendix E

# INTERPRETATION OF HOT WIRE SIGNAL

## Appendix E

## INTERPRETATION OF HOT WIRE SIGNAL

The hot wire anemometer probe is a very small metallic cylinder in which an electrical current is dissipated, thereby raising the probe temperature above its environment. If the probe is situated in a moving fluid, fluctuations in flow velocity or temperature cause fluctuations in the probe temperature (or resistance) and heat transfer rate. When the temperature of the wire is held constant by appropriate means, the fluid velocity or temperature fluctuations must be accompanied by fluctuations in the current producing the heat dissipation within the probe.

For a great many situations, the heat transfer rate from a cylinder in a moving fluid can be expressed as

$$Nu = c_1 Re^n + c_2 \quad ,$$

where Nu is the dimensionless heat transfer rate (Nusselt number), Re the Reynolds number, and $c_1$, $c_2$, and $n$ are constants (97). Strictly speaking the quantities $c_1$, $c_2$, and $n$ are dependent on the thermodynamic state of the fluid as well as the flow velocity and probe current, but for purposes of discussion we will assume them constant within the range of operation envisaged for the probe. For

a hypothetical flow situation in which the fluid velocity and temperature can vary, but the fluid properties remain constant, the expression for heat transfer from the cylinder can be written as

$$i^2 = c_3 \Delta T (c_1 Re^n + c_2) \quad ,$$

where $i$ is the instantaneous probe current, $\Delta T$ is the temperature difference between the probe and the flowing fluid, and $c_3$ is a constant. When the probe temperature is fixed, the relationship between fluctuations in probe current, fluid temperature $T$, and fluid velocity $u$ can readily computed by logarithmic differentiation of both sides of the above expression so that

$$2 \frac{di}{i} = -\frac{dT}{\Delta T} + \frac{nc_1 Re^n}{c_1 Re^n + c_2} \frac{du}{u} \quad .$$

If it is assumed that the fluctuations in fluid velocity and temperature, and thereby probe current, are small compared with the mean values of these quantities, they may be expressed as

$$i = i_o + di \quad ,$$
$$u = u_o + du \quad ,$$
$$T = T_o + dT \quad ,$$

where the subscript $o$ denotes the mean value. Thus the equation governing the fluctuations in probe current may be written as

$$\frac{di}{i_o} = \frac{1}{2}\left[ - \frac{dT}{(\Delta T)_o} + n\left(1 - \frac{c_2}{Nu}\right)\frac{du}{u_o} \right].$$

If the fluid properties are also functions of temperature, the term $dT$ may be expected to have multiplicative factors which depend on the rate of change of the properties with temperature $T$. Nevertheless, this simple equation still serves to illustrate the interplay of temperature, velocity and probe current fluctuations.

For the range of operations encountered in the present study (probe Reynolds numbers from 50-150), the constants $n$ and $c_2$ can be approximated by those for constant property fluids given in (97), so that as an approximation

$$4\frac{di}{i_o} \quad -2\frac{dT}{(\Delta T)_o} + \frac{du}{u_o} \qquad \ldots(1)$$

The quantity $(\Delta T)_o$, called the "overheat" of the probe, may be set at any desired value by adjusting the hot wire set. Thus if sufficiently small overheats are used, the fluctuations in wire current depend largely on fluctuations in fluid temperature, and the probe operates as a thermometer. Conversely with sufficiently large overheats, temperature fluctuations become negligible and the probe functions as an anemometer.

In the present study, the hot wire probe was operated next to the heated flat plate at several plate temperatures in a liquid-like

supercritical fluid, and it might be expected that the response of the probe would be quite different for each particular plate temperature. For example, with no heat transfer from the plate, the fluctuations dT are zero, so that the probe current fluctuations become

$$4 \frac{di}{i_o} = \frac{du}{u_o}$$

The quantity most frequently measured is actually the root mean square of the current fluctuations, so that

$$\tau = \frac{\sqrt{\overline{(du)^2}}}{u_o} = 4 \frac{\sqrt{\overline{(di)^2}}}{i_o}$$

where $\tau$ is the "turbulence level" present in the flow.

If the plate is heated, temperature fluctuations appear and the fluid property variation may also be significant. However, for plate temperatures up to slightly below the pseudocritical, property variations may only be 10-15% of freestream values, and so will be neglected for simplicity. In order to obtain an estimate of the contributions to probe current fluctuations in this region of plate temperature, it is assumed that equation (1) is approximately correct. Since temperature and velocity profiles are intimately related, the temperature and velocity fluctuations are not independent quantities. Deissler (47) proposed that the relationship between

temperature and velocity in a variable property fluid was given by

$$\frac{1}{\beta}\left(1 - \frac{T}{T_w}\right) \approx \frac{u}{u^+} \quad ,$$

where the quantities $\beta$ and $u^+$ are the dimensionless heat transfer and velocity respectively, and are given in Deissler's paper. For Prandtl numbers from 1-10, this expression may be further approximated as

$$T_w - T \approx \left(\frac{T_w - T_o}{Pr}\right) \frac{u}{u_o}$$

so that

$$dT \approx -\frac{du}{u_o}\left(\frac{T_w - T_o}{Pr}\right).$$

Hence the fluctuations in probe current may be approximated by

$$4\frac{di}{i_o} \approx \frac{du}{u_o}\left[1 + \frac{2(T_w - T_o)}{Pr(\Delta T)_o}\right]. \qquad ..(2)$$

The temperature difference $T_w - T_o$ is about 15°F. when the plate is near the pseudocritical temperature. Thus owing to the large overheat (about 115°F.), the second term in the bracket of equation (2) should be much less than unity, and the fluctuations in probe current are largely due to fluctuations in velocity of the fluid. It should be stressed that although the arguments made

about temperature and velocity profile similarity are quite crude, and the expression (2) for the probe current fluctuations is by no means strictly correct, the overriding effect of the large overheat should still cause the probe to act as an anemometer for this region of plate temperatures.

When the surface temperature is increased above the pseudo-critical, the flow field becomes extremely complicated and contains "pockets" of hot fluid as discussed in Chapter VII. Both temperature and velocity fluctuations in the neighbourhood of the probe are large, and even a gross estimate of their relative magnitude is not possible. The "turbulence level" is given by

$$\tau = 4\,\frac{\sqrt{\overline{(di)^2}}}{i_o} = \sqrt{\left[\frac{\overline{(du)^2}}{u_o^2} + 4\frac{\overline{du\,dT}}{u_o(\Delta T)_o} + 4\frac{\overline{(dT)^2}}{(\Delta T)_o^2}\right]}\quad ,$$

so that the root mean square signal also includes the temperature fluctuation and velocity-temperature fluctuation correlation terms.

It should be noted that because of the relationship between velocity and temperature of the fluid, the fluctuations of these quantities should be largely in phase with each other when viewed on an oscilloscope trace. Consider for example the region where "pockets" of hot fluid are observed. These "pockets" rise through the fluid due to buoyancy effects, and can be considered to have

both a different velocity and temperature from their immediate surroundings. Upon striking the hot wire probe, they will produce both velocity and temperature fluctuations at the same instant, and will appear as a single fluctuation (of increased magnitude) on the oscilloscope trace.

# Appendix F

# CALCULATIONS AND ERROR ANALYSIS

# Appendix F

## CALCULATIONS AND ERROR ANALYSIS

### 1. Freestream Velocity

| | Measurement | Minimum Accuracy |
|---|---|---|
| Fluid density $\rho$ | $lb_m/ft.^3$ | 2.0% |
| Venturi throat dia. $d_t$ | 0.438 inches | 0.4% |
| Venturi entrance dia. $d_i$ | 0.875 inches | 0.2% |
| Pressure drop $\Delta h$ | inches of water | 2.0% |
| Discharge coefficient $C_d$ | 0.971 | 0.2% |
| Flow channel area $A_o$ | 0.0129 sq. ft. | 2.0% |

The mass flow rate through the venturi meter was computed from the formula

$$\dot{m} = \frac{C_d \pi d_t^2}{\sqrt{1-\left(\frac{d_t}{d_i}\right)^2}} \sqrt{\frac{\rho \Delta h}{8}} \quad ,$$

$$\text{or} \quad \dot{m} = 0.0192 \sqrt{\rho \Delta h} \quad lb_m/sec.,$$

where $\rho$ is the fluid density at the venturi in $lb_m/ft.^3$, and $\Delta h$ is in inches of water. The average velocity in the rectangular channel approaching the flat plate is given by

$$V_o = \frac{\dot{m}}{\rho_o A_o} \quad ft./sec.,$$

$$V_o = 1.49 \sqrt{\frac{\rho \Delta h}{\rho_o 2}} \text{ ft./sec.,}$$

where $\rho_o$ is the freestream fluid density in $lb_m/ft.^3$.

At $p_o = 1,100$ psia, $T_o = 75°F.$, with $\Delta h = 46$ inches of water,

$$V_o = 1.49\sqrt{\frac{46}{45}} = 1.50 \text{ ft./sec.}$$

The approximate error in $V_o$ may be computed by logarithmic differentiation of the combined expressions for $V_o$ and $\dot{m}$, and summing the individual error contributions which result. This results in a total error in $V_o$ of 7.1%, with 3% of the error due to uncertainties in the fluid density alone.

2. Pressure Measurements

The pressure tap was located at the downstream end cap of the apparatus, so that a slight pressure drop exists from the rectangular test section inlet to the pressure tap. Assuming no heat transfer, and that the carbon dioxide acts as an incompressible fluid, the pressure drop between the leading edge of the plate and the pressure tap is approximately given by

$$\Delta p = \frac{\rho V_o^2}{2} \Sigma K_i \quad ,$$

where $K_i$ are the head loss coefficients for the various portions of the rectangular channel and pressure vessel. Estimating the total head loss coefficients $\Sigma K_i$ as 10, at 1,100 psia and 75°F. with $V_o = 1.5$ ft./sec., the pressure drop is

$$\Delta p \approx \frac{(450)(1.5)^2}{(64.4)(144)} = 0.11 \text{ psi} \quad ,$$

and so can be neglected in the system pressure measurements.

Within the rectangular channel itself, boundary layer growth on the heated plate plus the slight inclination of the plate causes the freestream fluid velocity to change slightly along the plate. Assuming a fully turbulent boundary layer starts at the leading edge of the plate, the displacement thickness at the down-

stream end of the plate for $V_o$ = 1.5 ft./sec. at 1,100 psia and 75°F. is approximately $\delta^*$ = 0.025", so that the ratio of the downstream velocity to the entering freestream velocity is about 9/7.75, or about a 12% increase in freestream velocity. The experimental results indicate that the heat transfer coefficient depends only slightly on freestream velocity, so that the "blocking effect" should not produce any significant change in results. The actual pressure drop in the rectangular channel alone is approximately 0.02 psi, and can be neglected for present purposes.

The Heise bourdon tube gauge used for pressure measurements was accurate to within 1 psi in 1,000, so that the total error in pressure readings is largely due to the inaccuracy of the gauge. The maximum error in pressure measurement was thus approximately 0.1%.

3. Heat Transfer Rate Measurements

Heat transfer rates were computed from readings of current flow and voltage drop through the heated film. Two corrections were required to compute the local heat transfer rate at the back thermocouple location; a correction due to non-uniform power dissipation along the length of the film; a correction due to the heat conducted through the glass plate to the fluid flowing on the opposite side of the plate.

The first correction occurs because of the non-zero resistance of the conducting strips along the edge of the film. A straightforward computation gives the power dissipated per unit area at the back thermocouple as

$$Q = 0.97 \frac{W}{A} \quad ,$$

where W is the measured power input to the dissipating film and A is the film surface area. This correction has been included in all of the experimental results presented in Appendix C.

The second correction occurs because of the non-zero thermal conductivity of the glass plate, and the resultant conduction of heat through the plate to the side opposite the heated film. This correction becomes largest for large values of power dissipated in the heating film. For the case of the heated film

facing upwards the maximum percentage of heat transferred downwards was estimated at 4% of the heat generated in the film. For the heated film facing downwards, the conduction upwards through the glass plate became as large as 27% of the heat dissipated in the film at the highest dissipation rates. The experimental results in Appendix C are also corrected for both these effects.

The error in the heat transfer rate is determined from the sum of the errors in plate current, voltage drop, surface area, and non-uniformity of the heated film. With the meter accuracies stated in Chapter IV, and an error of 1.0% in the measured surface area, the estimated heat transfer rate error is 6.0% at the largest heat transfer rates.

4. Temperature Measurements

The thermocouples employed for temperature measurements in this study were calibrated against a ASTM precision thermometer, and the maximum error in temperature obtained from each thermocouple is estimated to be within 0.2°F. Thus the error in the freestream temperature is a maximum of approximately 0.35% for the lowest freestream temperatures investigated, and is somewhat less for higher freestream temperatures.

The temperatures of the heated surface were measured by thermocouples placed in small holes drilled through the glass plate as explained in Chapter IV. The actual temperature measured by the thermocouple may differ slightly from the temperature of the heated film, and although this difference could not be determined exactly it was estimated to be small for most of the experimental conditions encountered. The thermocouple head is actually located in an epoxy cement plug (fashioned to be smooth with the plate surface) and receives heat by conduction from the glass plate. The heat conducted away by the thermocouple wires was estimated to be quite small, so that the epoxy plug reaches a steady state temperature when the heat conduction from the glass plate equals the heat convected away by the fluid flowing over the upper surface of the plug.

A rough approximation of the difference in temperature between the electrical film and plate thermocouple can be made by assuming the glass plate is at a uniform temperature $T_w$, and the heat conducted to the plug comes from a distance of one plug diameter $d$ from the plug as shown in Figure 64. If the heat transfer coefficient at the top of the plug is $h_t$ and the glass has a thermal conductivity $k_g$, the temperature difference between the film and the thermocouple $T_w - T_t$ is approximately

$$T_w - T_t \approx (T_t - T_o) \frac{h_t d}{10 k_g} ,$$

where $T_t$ is the actual thermocouple temperature, and the length of the plug $l$ has been taken to be approximately equal to $d$. The quantity $h_t(T_t - T_o)$ is the heat transfer from the plug to the fluid, which must of course be less than the heat transfer from the electrical film to the fluid, so as a further approximation

$$T_w - T_t < \frac{Qd}{10 k_g} .$$

For the largest heat transfer rates used in the present study (temperature differences $T_t - T_o$ of about 400°F.), the difference in the film and thermocouple temperatures is less than

15°F. This results in a heat transfer coefficient correction of less than 4% when the heat transfer coefficient is computed from the thermocouple temperature (the actual heat transfer coefficients are 4% less than those presented here).

At lower heat transfer rates the temperature difference between the film and thermocouple becomes much less, although the heat transfer coefficient correction may increase. For example at the peak heat transfer coefficient shown in Figure 38, the temperature difference $T_w - T_t$ is about 1.0°F., but the temperature difference $T_t - T_o$ is only about 2-3°F., so that the heat transfer coefficient correction may be as large as 30-50%, and the results in Figure 38 may be 30-50% high.

Owing to the indeterminacy of an analysis such as above, no corrections to the experimental results presented in Appendix C could actually be made for the effect of the thermocouple plug. However, this correction in itself would not change any of the conclusions presented in Chapter VIII.

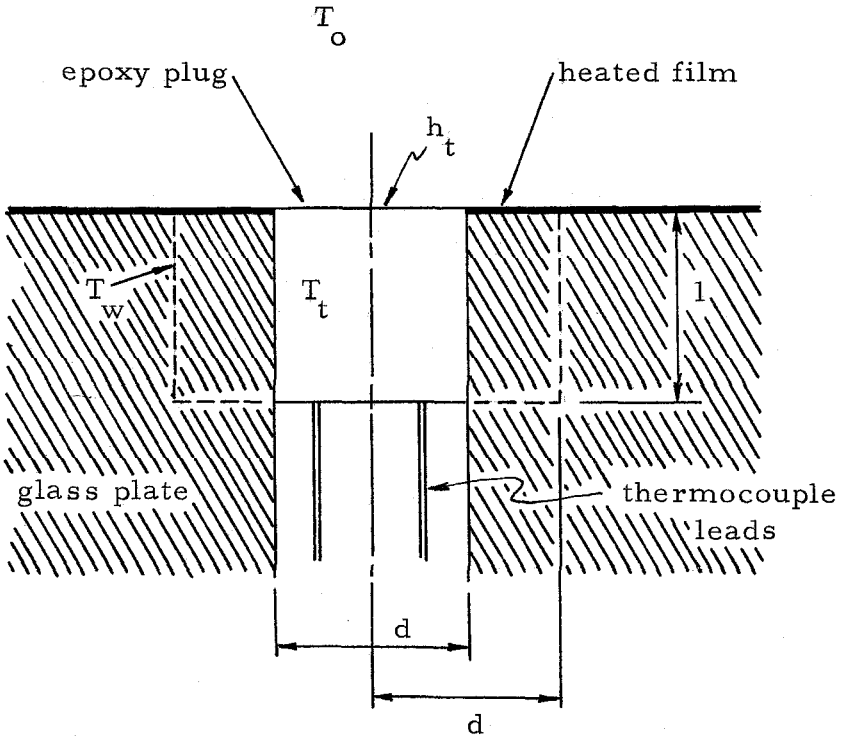


FIG. 64. THERMOCOUPLE PLUG ARRANGEMENT

| Fluid | Critical Pressure psia | Critical Temperature °F. |
|---|---|---|
| Carbon Dioxide | 1,071 | 87.8 |
| Water | 3,206 | 705 |
| Freon-114 | 473 | 294 |
| Hydrogen | 188 | -400 |
| Oxygen | 730 | -182 |

TABLE 1. THE CRITICAL STATE FOR VARIOUS FLUIDS

| | Constant Property Fluids | | Variable Property Fluids | | | |
|---|---|---|---|---|---|---|
| | | | Discontinuous Variation | | Smooth Variation | |
| | Non-viscous | Viscous | Non-viscous | Viscous | Non-viscous | Viscous |
| Zero Velocity | | | Rayleigh (65)<br>Taylor (66) | Harrison (67)<br>Bellman & Pennington (68) | Rayleigh (65)<br>Taylor (66) | Teng Fan (69)<br>Morton (70) |
| Zero Shear (discontinuous velocity profile) | | | Kelvin (71)<br>Helmholtz (72) | | | |
| Constant Shear (linear velocity profile) | Rayleigh (73) | von Mises (74)<br>Hopf (75) | Taylor (76)<br>Goldstein (77) | Feldmann (78)<br>Miles (79) | Case (80)<br>Plesset & Hsieh (81) | |
| Smoothly Varying Shear (curved velocity profile) | | Curle (82) | Tollmien (83)<br>Schlichting (84)<br>Lin (85) | | Drazin (86) | Lees & Lin (88)<br>Schlichting (87) |

TABLE 2. CLASSIFICATION OF HYDRODYNAMIC STABILITY PROBLEMS